

**NINEVAH UNIVERSITY**  
**COLLEGE OF ELECTRONICS ENGINEERING**  
**DEPARTMENT OF COMMUNICATION ENGINEERING**



**Design and Analysis of Frequency Reconfigurable  
Filters**

A Dissertation Submitted by

**Arqam Mohammed Shareef**

To the

Council of the College of Electronics Engineering

Ninevah University

**In Partial Fulfillment of the Requirements**

**For the Degree of Master of Sciences**

**In**

**Communication Engineering**

**Supervised by**

**Prof. Dr. Khalil Hassan Sayidmarie**

2022 A.C.

1444 A.H.

### ***Supervisor's Certificate***

I certify that the dissertation entitled “**Design and Analysis of Frequency Reconfigurable Filters**” was prepared by **Arqam Mohammed Shareef** under my supervision at the Department of Communication Engineering, Ninevah University, as a partial requirement for the Master of Science Degree in Communication Engineering.

Signature:

**Name: Prof. Dr. Khalil Hassan Sayidmarie**

Department of Communication Engineering

**Date:**

### ***Certificate of Linguistic Reviewer***

I certify that the linguistic reviewing of this dissertation was carried out by me and it is accepted linguistically and in expression.

Signature:

**Name:**

**Date: / / 2022**

### ***Certificate of the Head of Department***

I certify that this dissertation was carried out in the Department of Communication Engineering. I nominate it to be forwarded to discussion.

Signature:

**Name: Dr. Mahmood A. Al Zubaidy**

**Date: / / 2022**

### ***Certificate of the Head of Postgraduate Studies Committee***

According to the recommendations presented by the supervisor of this dissertation and the linguistic reviewer, I nominate this dissertation to be forwarded to discussion.

Signature:

**Name:**

**Date: / / 2022**

## *Committee Certification*

We the examining committee, certify that we have read this dissertation entitled “**Design and Analysis of Frequency Reconfigurable Filters**” and have examined the postgraduate student ‘**Arqam Mohammed Shareef**’ in its contents and that in our opinion; it meets the standards of a dissertation for the degree of Master of Science in Communication Engineering.

Signature:

Name: Prof. Dr. Jafar R. Mohammed

Head of committee

**Date: / /2022**

Signature:

Name: Dr. Mahmood A. Al Zubaidy

Member

**Date: / /2022**

Signature:

Name: Dr. Saad Wasmi Osman

Member

**Date: / /2022**

Signature:

Name: Prof. Dr. Khalil Hassan Sayidmarie

Member and Supervisor

**Date: / /2022**

The college council, in its ..... meeting on / /2022, has decided to award the degree of Master of Science in Communication Engineering to the candidate.

Signature:

Name: Khalid K. Mohammed

Dean of the College

**Date: / /2022**

Signature:

Name: Sedki B. Thanoon

Council registrar

**Date: / /2022**

**Some of the Obtained Results in this Dissertation has been Published in:**

Arqam M. Shareef, and Khalil H. Sayidmarie,"Compact Reconfigurable Band-Reject/All-Pass Microstrip Filter Using U-Shaped Slot", presented at the 4th International Conference on Advanced Science and Engineering, ICOASE2022, 21-22 Sept. 2022. IEEE will publish the proceeding of the conference.

# **ACKNOWLEDGEMENTS**

Thanks, and appreciation

I would like to express my appreciation and gratitude to my professor and supervisor, Prof Dr. Khalil Hassan Sayidmarie, who had a great role in supporting, following-up and guiding me with observations and instructions to present this dissertation in the best possible way.

Additionally, I would like to express my appreciation to the staff of the department of Communication Engineering, in particular the head of the department. I also must mention my respected academics professors who gave me lectures throughout my academic career, as well as those who have provided me with a lot of support, special thanks to the Deanship of Electronics College and I would also like to extend my deepest gratitude to the presidency of Ninevah University.

Special thanks to my wonderful parents for the support and encouragement during the whole period of my study. I simply couldn't have done this without their support and prays. I dedicate my success to them.

I also thank all my family members for their patience and for enduring the psychological and physical stress throughout the past years.

## ABSTRACT

With the widespread use of communication devices, companies are competing to provide better devices to the user, aiming to offer small sizes, lightweight, and at affordable prices. As the filter is one of the most important stages in these devices, many studies have focused on minimizing size and weight by reducing the number of filters by developing them into reconfigurable ones.

In this thesis, the compact band-reject filter employing the U-shaped slot that is etched on the microstrip line was thoroughly investigated aiming to develop it into a reconfigurable filter. The CST Studio EM software was used in the simulations. The slot parameters were found to control the resonance frequency and bandwidth. The developed filter provided two states of all-pass and band-rejection at 2.45 GHz by inserting a PIN diode switch at the center of the slot. The ON and OFF states of the PIN diode were represented by short and open circuits, and then the equivalent circuits for the two states were implemented. The distribution of the electric field around the U-slot was investigated and found useful for understanding how the filter works. To verify the proposed design a vector network analyzer was used to test the fabricated. The fabricated filter offered an insertion loss of 14 dB at the reject band and about 1dB for the all-pass state.

The idea of the U-shaped slot was developed into a few configurations including a meandered slot filter. Detailed investigations of the proposed designs are given. The results showed that the designs can offer bandwidth reconfiguration by simply switching a single PIN diode. The proposed designs are applicable to a wide range of applications requiring small size and reconfigurability.

## TABLE OF CONTENTS

SUBJECT		Page
ACKNOWLEDGMENTS		I
ABSTRACT		II
TABLE OF CONTENTS		III
LIST OF FIGURES		V
LIST OF TABLES		IX
LIST OF ABBREVIATIONS		X
LIST OF SUMBOLS		XI
<b>CHAPTER ONE</b>		
<b>INTRODUCTION</b>		
1.1	Overview	1
1.2	Literature Review	3
1.3	Aims of Dissertation	10
1.4	Dissertation Layout	11
<b>CHAPTER TWO</b>		
<b>BASICS OF MICROSTRIP LINES AND RECONFIGURBALE FILTERS</b>		
2.1	Introduction	12
2.2	Filter Parameters	13
2.3	Filter Realization with Microstrip Technology	15
2.4	Various Designs of Existing Filters	18
2.4.1	Closed and Open Rings	18
2.4.2	Coupled or Connected Stubs	21
2.4.3	Slots in the Ground Plane	23
2.4.4	Slots and Rings in the Microstrip Line	24
2.4.5	Stepped Impedance	26
2.4.6	Hair Pin, and Coupled Lines	27
2.5	Various Methods for Re-configuration of the Filter	29
2.5.1	Re-configuration Using Varactor Diodes	30
2.5.2	Re-configuration Using PIN Diodes	31
2.5.3	Re-configuration Using Liquid Crystals	33
2.5.4	Re-configuration Using MEM's	34
<b>CHAPTER THREE</b>		
<b>ANALYSIS AND DESIGN OF RECONFIGURABLE FILTER USING U-SHAPED SLOT</b>		
3.1	Introduction	37
3.2	The Band-Stop Filter Using U-Shaped Slot	37

<b>SUBJECT</b>		<b>Page</b>
3.2.1	Analysis and Development of the U-shaped Filter	42
3.3	The Reconfigurable U-Shaped Slot Filter	47
3.3.1	Distribution of the Electric Field in the Slot	49
3.4	Equivalent Circuit of the PIN Diode	51
3.5	Experimental Validation of The Proposed Filter	53
3.6	Comparison with Other Works	56
<b>CHAPTER FOUR</b>		
<b>DEVELOPMENT OF THE U-SLOT FILTER FOR BAND EXTENSION AND RECONFIGURATION</b>		
4.1	Introduction	58
4.2	A Bandwidth Reconfigurable Filter	58
4.3	The Meandered Slot Filter	64
4.3.1	Bandwidth Extension	64
4.4	Analysis of The Meandered Slot Reconfigurable Band-Reject Filter	70
4.4.1	Changing the Position of the Opening in the Slot	73
4.4.2	An Alternative Way to Increase the Bandwidth	77
<b>CHAPTER FIVE</b>		
<b>CONCLUSIONS AND FUTURE WORK</b>		
5.1	Conclusions	81
5.2	Future Work	83
<b>REFERENCES</b>		
REFERENCES		84
ABSTRACT IN ARABIC		1

## LIST OF FIGURES

Figure	Title	Page
<b>CHAPTER TWO</b>		
2.1	Photos of various designs of microstrip line filters	12
2.2	The scattering parameters of the two-port filter	13
2.3	Microstrip transmission line	16
2.4	(a)-Microstrip transmission configuration (b)- Effective dielectric constant	17
2.5	Frequency response of various types of filters	18
2.6	(a)-Photograph of the proposed open loop filter (b)-Geometry of the proposed filter. length $l = 17$ mm, width $w = 12$ mm, thickness $t = 0.5$ mm	19
2.7	The simulated and measured results for the bandstop filter	19
2.8	(a)-Photograph of proposed C-open-loop resonator, (b)-Layout of the proposed C-open-loop single BSF	20
2.9	Simulated and measured S-parameters of the proposed C-shaped open-loop resonator (BSF)	21
2.10	Photograph of the prototype bandstop filter using (a)-Open and (b)-Short stub-loaded resonators	21
2.11	Measured and simulated results of (a)-Open stub-loaded (b)- Short stub-loaded resonators	22
2.12	(a)- Photograph of the fabricated microstrip wideband bandstop Filter. (b)- Configuration of the designed filter	23
2.13	Simulated and measured responses of the filter	23
2.14	(a)-SRR, (b)-SCRR, (c)- Front view of CSSR in the ground Plane, (d)- Frequency response	24
2.15	(a)-Configuration of open square-slot band-stop filter, (b)-Simulated scattering parameters for the filter	25
2.16	(a)- Photograph of the proposed U-slot filter, (b)- Simulated and measured S-parameters	26
2.17	Photographs of a two-pole microstrip BPF using the SIR (a)-Type1, (b)-Type2 and (c)-Type3	27
2.18	Photograph of a fabricated multiband microstrip hairpin diplexer	28
2.19	Measured and simulated performances of the proposed diplexer (a)-Input return loss, insertion loss at port 2, 3 and (b)-Return losses and isolation losses at port 2,3	28

<b>Figure</b>	<b>TITLE</b>	<b>Page</b>
2.20	(a)-The design of the bandpass filter and (b)-Measured and simulated results of the fabricated bandpass filter	29
2.21	(a)-Structure of the prototype (b)-S-parameters variation with frequency	31
2.22	(a)- Picture of the reconfigurable BPF, (b)- Geometry of the BPF. (c)- Simulated and fabricated S <sub>21</sub> response of the BPF	32
2.23	(a)- The picture of the fabricated proposed filter, (b)- Measured S-parameter for BSF, (c)- Measured S-parameter for BPF	34
2.24	Schematic picture of a micromechanical (MEM) switch	35
2.25	(a)-The layout of inter digital filter, (b)-Simulated results without MEMS switches, (c)- With two state MEMS switch	36
<b>CHAPTER THREE</b>		
3.1	The geometry of the reconfigurable filter using a U-shaped slot etched on the microstrip line, (a)- Front view, (b)- Side view	39
3.2	The filter performance for various dimensions	40
3.3	The equivalent circuit representation of the U-shaped slot filter using parallel RLC resonant circuit	42
3.4	(a)-The geometry of the central part of the slot, (b)- Frequency response	43
3.5	(a)-The geometry of the L-shaped slot filter, (b)- Frequency response	44
3.6	(a)-The geometry of the Z-shaped slot filter, (b)- Frequency response	45
3.7	The distribution of the electric field around the slot at; (a)-f=1.5 GHz, (b)-f=2.4 GHz, and (c)-f=3.5 GHz	46
3.8	The S-parameters (— S <sub>11</sub> ), and (-- S <sub>21</sub> ) of the U-slot filter for various slot lengths (L <sub>2</sub> =20mm), (L <sub>2</sub> =18.2mm), (L <sub>2</sub> =15mm), (W <sub>3</sub> =0.5 mm, W <sub>4</sub> =1.8 mm)	47
3.9	The geometry of the reconfigurable U-shaped slot filter showing placement of the PIN diode	48
3.10	The simulated scattering parameters of the proposed filter, when the PIN diode is replaced by a short circuit	48

<b>Figure</b>	<b>TITLE</b>	<b>Page</b>
3.11	The simulated scattering parameters of the proposed filter, when the PIN diode is replaced by an open-circuit	49
3.12	The distribution of the simulated E-field around the U-slot at 2.42 GH, when (a)-PIN diode in “OFF” state, and (b)-PIN diode is in “ON” state	50
3.13	The equivalent circuits of the PIN diode for (a)-The “OFF” State, and (b)-The “ON” State	51
3.14	Simulated S-parameters of the proposed filter, when the PIN diode is represented by its equivalent circuit (a)- The transmission coefficient, (b)- The reflection coefficient	52
3.15	Variation of the transmission coefficient with frequency, for the two cases when the diode was represented by an ideal switch, and by an equivalent circuit. (a)- ON State “All-pass”, (b)- OFF State “Band”reject	53
3.16	Photograph of the fabricated prototypes. (a)- U-Slot reconfigurable filter in the band-reject state (b)- The same filter in the All-pass state	54
3.17	Measured and simulated reflection and transmission coefficients of the prototype filter, (PIN Diode is in “OFF” state)	55
3.18	Measured and simulated reflection and transmission coefficients of the prototype filter, (PIN diode is in the “ON” state)	56
<b>CHAPTER FOUR</b>		
4.1	(a)-Proposed filter with one opened slot, (b)-Variation of the scattering parameters with frequency	60
4.2	(a)-Proposed filter with two opened slots, (b)-Variation of the scattering parameters with frequency	61
4.3	(a)-Proposed filter when the PIN diode is switched from “ON” to “OFF” states, (b)-Variation of the scattering parameters with frequency	62
4.4	Variation of the scattering parameters with frequency for various lengths (L)	63
4.5	The development of the U-Shaped filter (a) into meandered slot filter (b)	64
4.6	Variation of the scattering parameters with the frequency of the meandered slot for various lengths L	65

<b>Figure</b>	<b>TITLE</b>	<b>Page</b>
4.7	(a)-meandered slot filter has unequal lengths, (b)- frequency response	67
4.8	(a)- The proposed filter geometry showing the PIN diode, (b)- frequency response for both states (ON and OFF) of the diode	69
4.9	(a)- Filter geometry in normal mode, (b)- frequency response	70
4.10	(a)- Filter geometry when adding short on the left side at the marked point, (b)- frequency response	71
4.11	(a)- Filter geometry when adding shorts on both sides at the marked points, (b)- frequency response	72
4.12	(a)- The geometry of the filter in the first case, (b)- frequency response	74
4.13	(a)- The geometry of the filter in the third case, (b)- frequency response	75
4.14	(a)- The geometry of the filter in the third case, (b)- frequency response	76
4.15	(a)- Filter with equal slots, (b)- Filter with unequal slots, (c)- Frequency responses of both cases	77
4.16	(a, b and c)-The geometry of the filter with the addition of vertical slits, (d)- Frequency response of the three cases	79
4.17	(a)- Filter geometry where slots are placed on the left side while the right side has one slot (b)- obtained results for one side and both sides slots	80

## LIST OF TABLES

Table	TITLE	Page
<b>CHAPTER THREE</b>		
3.1	The Filter Dimensions	40
3.2	The Performance of the Filter with Different Dimensions	41
3.3	Shows a Comparison of the Filter Parameters and Characteristics with Other Designs	57
<b>CHAPTER FOUR</b>		
4.1	Parameters and Characteristics of the Three Designed Filters	63
4.2	Characteristics of the Meandered-slot Filter for Various Values of (L)	66
4.3	The Filter Characteristics when the PIN Diode is in “ON” and “OFF” States	69
4.4	The Filter Characteristics for the Three States Shown in Fig. 4. (9,10, and 11)	73
4.5	The Filter Characteristics with Changing the Location of the Slot Opening	76
4.6	The Characteristics of the Filter by Changing the Number of Vertical Slots	78

## LIST OF ABBREVIATIONS

Abbreviation	Full Form
BPF	Band Pass Filter
BSF	Band Stop Filter
CSRR	Complementary Split-Ring Resonator
DC	Direct Current
DGS	Defected Ground Structures
EBG	Embed Bandgap
GHz	Giga Hertz
HFSS	High-Frequency simulation Software
HPF	High Pass Filter
IL	Insertion Loss
LHM	Left-Handed Materials
LM	Liquid Metal
LPF	Low Pass Filter
MEMS	Micro-Electro-Mechanical Systems
MHz	Mega Hertz
MLS	Meander Line Slot
MMR	Multiple-Mode Resonator
MSR	Microstrip Slot Resonator
OLR	Open Loop Resonator
PCB	<i>Printed Circuit Board</i>
RF	Radio Frequency
RL	Return Loss
RLC	Resistor (R), Inductor (L), and a Capacitor (C)
SIR	Stepped-Impedance Resonator
SL	Spur Line
SMD	Surface Mount Device
SRR	Split-Ring Resonator
USS	U-Shaped Slot
UWB	Ultra-Wideband
VNA	Vector Network Analyzer
VSWR	Voltage Standing Wave Ratio
WIMAX	Worldwide Interoperability for Microwave Access
WLAN	Wireless Local-Area Network

## LIST OF SYMBOLS

Symbol	Meaning
$a_1$	Incident Voltages at the Input Port
$a_2$	Incident Voltages at the Output Port
$b_1$	Reflected Voltages at the Input Port
$b_2$	Reflected Voltages at the Output Port
$h_2$	Copper Layer Thickness
$L_1$	Substrate Length
$L_2$	Slot Length for the Horizontal Part
$L_s$	Slot Length
$R_p$	Parallel Resistance
$R_s$	Series Resistance
$S_{11}$	The Voltage Reflection from the Input Port or Reflection Coefficient
$S_{12}$	The Reverse Voltage Gain
$S_{21}$	The Forward Voltage Gain, or the Transmission Coefficient
$S_{22}$	The Voltage Reflection Coefficient at the Output Port
$W_1$	Substrate Width
$W_2$	Microstrip Line Width
$W_3$	Slot Width
$W_4$	Middle Tongue Width
$Z_0$	Microstrip Line Impedance or Characteristic Impedance
$Z_L$	Input Impedance of the RLC Circuit
$\epsilon_{\text{eff}}$	Effective Dielectric Constant
$\epsilon_r$	Dielectric Constant
$f_r$	Resonance Frequency
BW	Bandwidth
C	Speed of Light Traveling Through a Vacuum
dB	Decibel
F	Frequency
h	Height
$h_1$	Substrate Thickness
$I_F$	Forward Current
mm	Millimeter (1 meter * $10^{-3}$ )
V	Volt
$\delta$	Loss Tangent
$\epsilon$	Permittivity
$\lambda$	Wave Length

Symbol	Name
$\lambda_e$	Effective Wavelength
$\lambda_o$	Wavelength in Air
$\lambda_r$	Resonance Wavelength
$\Gamma$	Reflection Coefficients
$\Omega$	Ohm

# CHAPTER ONE

## INTRODUCTION

### 1.1 Overview

The filter is one of the most important elements in communication systems, whether it is used in transmitters or receivers. It is used to sort and recognize certain frequencies among other countless unwanted frequencies. In transmitters, the filter is used to ensure the transmission is across the allocated frequency range. Similarly, it is used in receivers, where the filter ensures that unwanted frequencies do not pass through. Further, the filters can be classified, in terms of their functions, into four main and common types. Some type allows the lower frequencies to pass from the cut-off point and prevent the higher ones; they are called Low Pass Filters (LPF). Some others prevent low frequencies less than the cut-off frequency and allow high frequencies that are higher than the cut-off frequency; there are called High Pass Filters (HPF). Some filters allow the passage of a specific range of frequencies and prevent others from passing; they are called Band Pass Filter (BPF). Moreover, some filters reject a specific band of frequencies and allow other frequencies; they are called Band Stop Filter (BSF) or band-reject filters. As filters deliberately attenuate the unwanted signals, an attenuation level of (50%) or 3dB designates the boundary between pass and reject bands [1,2].

**Radio Frequency (RF)**, and microwave filters are the type that operates on the frequency range from 300 MHz to 30 GHz, which is the range used in most communication systems. Like other filters, they consist of two ports; one for applying a signal containing a group of frequencies, and the other to output the desired filtered signal. Microwave filters differ from their counterparts that operate at lower frequencies in that the wavelength factor of microwave frequencies enters the design consideration, and the ratio of the filter

dimensions to the wavelength becomes an important design factor. In these filters, sections of transmission lines in the form of microstrip lines are used instead of the discrete capacitors and inductors. Although using microstrip lines leads to more complex and difficult designs, it also provides advantages, like higher efficiency, which is difficult to achieve in low-frequency filters. [2,3]

In many applications, it is desired to change one or more of the filter characteristics, without replacing the filter, so that the system performs better in the changing environment. This process is called configurability; the process via which a specific change is made to the principle of the filter's operation, such as changing the filter function from (LPF) to (HPF), for example, or a change from (All Pass) to (Band Pass) or (All Pass) to (Band Reject). Further, the cut-off frequency can be changed between two or more frequencies. The filter bandwidth may be decreased or increased, depending on the requirements of the application [4].

The properties of RF and microwave filters can be changed in several ways. The most important of which is adding an electronic component such as a diode, or an electronic switch to cut or connect paths or parts of the filter in order to change the shape or length of the path. The switching of the diode is controlled by an external control signal. Thus, one or more of the filter properties is changed at will to reconfigure the filter to perform a different function without physically changing the filter [5].

## 1.2 Literature Review

J. Hong and M. J. Lancaster in 2001 presented in their book an extensive study about the design and operation of the microstrip bandpass filters using square microstrip open-loop resonator. The influences of various parameters of the open squares loop and the location of the squares in terms of proximity and distance between them, the width of the microstrip line, were investigated [6].

A. Boutejdar et al., in 2007, proposed new DGS hairpin resonators and investigated various geometrical modifications. Controlling the center frequency and improving the proposed BPF's characteristics. A second-order filter was presented with a quasi-elliptic response. Controlling the center frequency and preserving good passband matching were obtained by varying the length or the width of some elements in the investigated structure without changing the area of the filter [7]. In the same year, compact microstrip stop-band filters were designed and implemented by using the sub-wavelength resonators of left-handed metamaterials, namely CSRR [8]. A single CSSR element etched in the ground plane results in a very narrow stop-band, but placing these CSRR structures on a regular basis produces wide stop bands. One advantage of these elements is that, these CSRR can be placed very close together unlike other conventional filter elements that need longer spaces between them [8].

In 2008, B. Jitha, et al. presented a compact and simple microstrip band-reject filter using opened rectangular loops [9]. It was shown that the notching frequency can be electronically varied by placing a varactor diode in the opening of the ring, which is appealing for modern communication systems [9]. S. Fallahzadeh et al., in 2009, proposed a compact bandstop filter having high rejection level was designed using an opened rectangular loop. The transmission line model was adopted in this resonator, and the corresponding

resonant frequency was calculated [10]. A varactor-tuned dual-mode bandpass filter was presented in 2010 by W. Tang, et al. [11], which used a dual-mode microstrip open-loop resonator for tuning the passband frequency with a single dc-bias circuit while maintaining nearly constant absolute bandwidth [11].

In 2010, I. Llamas-Garro, et al. presented various methods for tuning microwave filters in a detailed study [12]. The research discussed how filters are made with various technologies such as active devices, MEMS, ferroelectric and ferromagnetic materials. The operating frequency range of the filters, as determined by the technology used in their manufacture, is an important consideration [12]. A band-stop filter based on a defected ground structure was proposed in 2011 by M. Naghshvarian-Jahromi, et al. Two semi-complementary split-ring resonators etched on the ground plane and two-line resonators etched out of the microstrip line produce the notch frequency. The filter has a completely flat and lossless passband and high rejection with sharp cutoffs in the reject-band [13]. In 2012, L. BalaSenthilMurugan, et al presented a modified L-shaped resonator bandstop filter designed for microwave applications. The variation of the width of the elements, and cascading them were used as two methods for tuning the filter's bandwidth and center frequency [14].

Also in 2012, L. Gao, et al. presented two new bandstop filters based on opened and shorted stub-loaded resonators. The odd-mode frequencies are suppressed by using a special feeding method, and the harmonics are used as the second stopbands. Two bandstop filters were designed and the design methodology was described [15]. In the same year, a novel CSRR based on the Koch fractal curve was proposed and applied to a bandpass filter. Simulations and measurements showed that using fractal geometries

significantly reduces structure size. The use of LHM and fractal structure allows for the creation of a good capability filter[16].

K. H. Sayidmarie and T. A. Najm in 2013 proposed and investigated three band-notching techniques that use parasitic elements, slots, and stubs. The added element in each of the three approaches was designed to resonate at the notch frequency. The added element disturbs the current distribution in the radiating patch at the notch band, resulting in reduced radiation. In a different approach, the added element results in a high reflection coefficient at the notch frequency. When compared to the other methods, the use of the four stubs provides the highest reflection coefficient. By varying the width of the slot or stub, the U-shape slot and the 4 stubs can control the width of the notch band [17]. Thus, the stubs and slot being frequency sensitive elements can be utilized in frequency reconfigurable devices.

The tuning and reconfigurable capability provide a variety of benefits in wireless applications. This tuning selectivity is achieved by using varactors, micromachines, and PIN diodes. PIN diodes were also used as switching elements. Because of its excellent selectivity and ease of analysis, the Chebyshev filter has received the most attention in research. Several methods have been introduced in a review on reconfigurable low pass bandstop filter in 2013 by B. H. Ahmad, et al. [18]. A microstrip bandstop filter using split-ring resonator for ultra-wideband applications was presented in [19]. The filter has a wide stopband response. A Larger number of rings produces a sharper cut-off, which improves stopband performance. A microstrip bandstop filter with an ultra-wideband of 6 GHz was designed using single and double split-ring resonators [19].

In 2015, W. Y. Sam, et al. presented a review of reconfigurable integrated filters and antennas [20], where advances and applications in reconfigurable filters and antennas were presented and discussed. The majority of the designs

used microstrip structure because it is simple to build, lightweight, low cost, and simple to integrate with planar structures. However, producing a wider and more flexible tuning range with low loss is currently a major challenge [20]. A microstrip configuration was introduced to realize relatively wide bandstop filters using L and T-shaped resonators [21].

In 2017, A. Boutejdar and S. D. Bennani presented compact cascaded BSF filters with multi-band properties using double and triple open C-loop resonators [22]. Both multi-band filters were designed of several open-loop ring resonators, which were vertically stacked. Using this technique, flexible and compact filter topologies and excellent results were achieved [22]. B. Belkadi, Z. Mahdjoub, and M. L. Seddiki proposed a novel type of compact microstrip filter using CSRR and SRR in tandem to achieve dual-band performance and compact size. The structure has negative refractive index double rejection filters. Simulation results showed that the filter's performance and selectivity are significantly good [23].

In 2017, L. S. Yahya et al. presented a low-profile dual-port antenna system for WLAN and WIMAX applications [24]. Each of the two antennas used U-shaped slot in its feed line to offer excellent isolation performance. To control the position of the notched bands and obtain deep nulls, the parametric study was used to tune the position, length, and width of the inserted slots [24].

In 2017, Y. Wu, et al. proposed a novel perturbation approach for implementing the independently reconfigurable dual-mode dual-band substrate integrated waveguide filter. Dual-frequency manipulation is accomplished in each cavity by inserting perturbation via-holes and varying the lengths of the slots. The control of the upper passband was made through the second variable, whereas the lower passband was independently varied by combining the two variables [25].

In 2017, M. S. Khan, et al. presented a good demonstration of the idea to achieve frequency and radiation pattern reconfigurability of microstrip patch antennas in [26]. The frequency was reconfigured by varying the effective length of the patch antenna through the use of diodes, while a single feed was used to excite two microstrip patches. The operation of the wave propagation and radiation mechanisms for both patches was accomplished by connecting the feed line in succession using two PIN diodes [26].

In 2018, B. Sahu, et al. proposed a compact LPF with a wide stopband of up to 30 GHz employing four non-uniform cascaded triple isosceles DGS [27]. The filter's wide stopband was achieved by using twelve attenuation poles corresponding to four DGS units without increasing the filter's overall size. F. C. Chen et al. suggested a tunable dual-band filter that can be reconfigured from bandpass to bandstop by varying the state of the PIN diodes [28]. The center frequency of the two bands can be independently varied by adjusting the biasing of the varactors in the two sets of the  $\frac{1}{2}$  wavelength resonators. The feeding lines were loaded with two varactors, allowing for a wide tuning range [28].

In 2018, L. S. Yahya, et al. proposed a compact triple stop-band filter using various defected microstrip structures, to reject unwanted narrowband interferences in UWB systems [29]. A meander line slot (MLS), a U-shaped slot (USS), and a spur line (SL) were etched on the microstrip line to obtain the triple band-reject property while providing a wide tuning property by varying the dimensions of the MLS, USS, and SL [29].

In 2018, E. G. Ouf et al. presented two passband filters having a controllable center frequency and bandwidth [30]. The filters embed bandgap (EBG)- multiple-mode resonators (MMR) and interdigital coupled lines to achieve high performance, while maintaining a compact size of  $14.0 \times 10.1$

mm<sup>2</sup>. The filter bandwidth can be changed by varying the lengths of the open-circuited stubs that are controlled by PIN diodes [30].

In 2018, a general overview of microwave filters and their design for various applications was published by R. Bhat et al. [31]. They show that the demand for new filter designs is increasing at an exponential rate. New designs that can meet the requirements are being introduced on a daily basis, depending on new applications in this field [31]. In the next year of 2019, a comprehensive review of the history and development of the reconfigurable microwave tuning filter was published [32]. The review presented modern designs of adjustable microwave filters, particularly with regard to wireless communications and frequency ranges for common applications such as mobile phones and Wi-Fi frequencies, in their research [32].

A quarter-wavelength open-circuited stub was used to design a microstrip line band-stop filter. When the width of the stub is made equal to that of the signal line, the result leads to a narrow bandwidth, which is unsuitable for bandstop applications. Two methods are possible for constructing a band-stop filter. The first is to connect a series resonating circuit to the transmission line, while the second is to connect a parallel resonating circuit to the transmission line in series. Each of the two methods produces a transmission zero at quarter-wavelength [33].

In 2019, H. T. Ziboon and J. K. Ali, proposed a design for a compact microstrip bandpass filter (BPF) based on Minkowski fractal (DGS) resonators [34]. It showed that as the iteration level increases, the filter structure becomes more compact. A comparison with other filters based on Peano and Hilbert Fractal geometries was performed. The results showed that the proposed filter has good performance characteristics, with a significant reduction in higher harmonics [34].

C. F. Chen has recently proposed a microstrip three-state switchable and tunable BPF Filter with a wide frequency range and a fractional tuning range

of (127%). The design concept was demonstrated and validated experimentally. The proposed switchable and tunable BPF has potential practical applications in RF front-end communication systems due to its extra-wide frequency tuning range, flexible frequency/bandwidth control, and compact size [35].

In 2020, M. A. Al-Atrakchii, et al. proposed a bandstop filter [36], in which the resonant element is a slot folded into the shape of the letter U and embedded into the microstrip line. Furthermore, folding the slot reduces its length to 1/4 of the effective wavelength. The designed prototype at the WLAN frequency of 2.45 GHz was investigated by CST microwave simulation and verified by measurements. The slot folding and its placement in the microstrip line provided very low radiation at the stopband [36].

In 2020, C. Asci, et al. presented a compact tunable band-reject filter composed of split-ring resonators and reed switches [37], to represent a magnetically-tunable quad-band filter. The filter uses magnetic reed switches, which control the split-ring resonators into ON and OFF states. The reed switches that are connected to different split-ring resonators are actuated by applying an external magnetic field [37]. Another reconfigurable band-reject filter with a wide and continuously adjustable stopband was presented by Z. Zhibin and B. Lei [38]. Dumbbell-shaped defected ground cells based on dual coupling slots were used in the design. Three pairs of stubs were perpendicularly placed onto the microstrip line to improve the transmission in the passband [38].

Also in 2020, A. Gupta, et al. suggested a wideband BSF filter having a very broad stop-band extending from 3.52 GHz to 12.38 GHz and a small size of 7.4 X15 mm<sup>2</sup> for C and X band applications. The proposed filter has a 20 dB fractional bandwidth of (110%) and a roll-off factor of 0.144 (ratio of 3 dB bandwidth to 20 dB bandwidth). The proposed filter has two types of

resonators, one quad mode and the other L-shaped[39]. Bandstop filters with single and dual stop-bands were implemented using coupled-mode microstrip slot resonators (MSRs) [40]. MSRs provided excellent filter response due to their compact size and ease of fabrication. The method of coupled-mode resonator theory was used to demonstrate the designs of MSRs. MSRs could be a viable alternative to complicated and arbitrary BSF design in order to achieve desired frequency response [40].

In 2022, D. K. Jhariya, et al. presented a compact UWB filter with reconfigurable band notch property [41]. The filter was built using a stepped impedance slot line resonator and two open-ended coupled microstrips. The WLAN rejection band is achieved by positioning the U-shaped DGS near the slot line resonator. In addition, two capacitors were placed at the active slot of the U-shaped DGS to achieve WiMAX band rejection [41].

### **1.3 Aims of the Dissertation**

The current study was designed to investigate reconfigurable filters and the filter parameters that control the reconfigurability in order to design a new filter with multiple resonance frequencies. It aims at:

1. Studying the means used to change the resonance frequency or bandwidth of the filter.
2. Using the PIN diode as a controlling element to change the filter properties.
3. Developing current designs of filters, and proposing designs for reconfigurable filters, analyzing their operation and assessing their performance.
4. Fabricating prototypes for the proposed filters and testing their performance.

## 1.4 Dissertation Layout

This work is divided into five chapters as follows:

- Chapter 1 includes an introduction and a review of the literature.
- Chapter 2 discuss the background, tools for implementing filter reconfiguration, techniques used in reconfigurable filters, and various types of reconfigurable filters.
- Chapter 3 describe the design of a proposed microstrip line filter that has two states: all pass and band stop. To switch between the two states, the filter employs a PIN diode as a switching element. This chapter also discusses the experimental results.
- Chapter 4 introduces and discusses two other types of filters. One of them discussed the mechanism of controlling the bandwidth using one PIN diode, and the other discussed the mechanism of moving from one band rejection frequency to three band rejection frequencies within the Wi-Fi range using one or more conductive elements.
- In chapter 5, the conclusion and recommendations for future work are presented.

# CHAPTER TWO

## BASICS OF MICROSTRIP LINES AND RECONFIGURABLE FILTERS

### 2.1 Introduction

Microstrip line filters are types of filters that operate at microwave frequencies and are often used in various communication devices. Regardless of their shapes, sizes, or designs of resonance circuits, all microstrip line filters share their small size, as well as the principle of operation. They usually use one or more resonant elements designed in a specific format to meet the filter specifications in terms of filter function, resonance frequency, transmission and reflection coefficient. Figure (2.1) shows images of various designs of microstrip filters. In this chapter, the basics of microstrip filters are briefly described. The chapter also presents briefly various designs of filters that were presented in the literature.

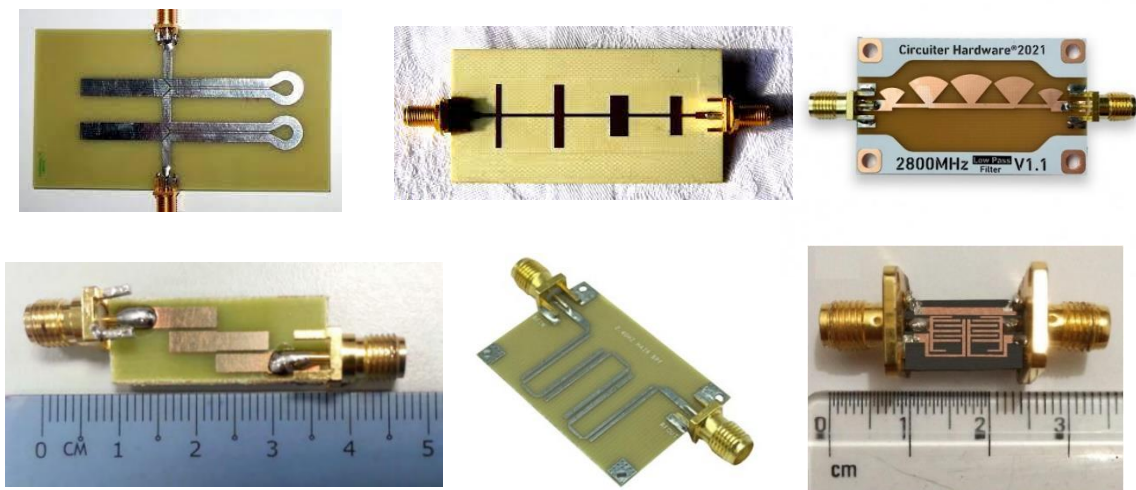


**Figure (2.1)** Photos of various designs of microstrip line filters.

## 2.2 Filter Parameters

The performance of the filter is described in terms of a few parameters, which are defined in the following:

### Scattering Parameters

A linear two-port network is shown in Fig. (2.2), where the test sinusoidal voltages,  $V_{s1}$  and  $V_{s2}$ , are applied at the input and output ports, respectively. It is assumed that the two voltage sources have the same series impedance  $R_o$ . This resistance is known as reference impedance. A standard value of 50 ohms is used for  $R_o$  [42]. So, in simple words, scattering parameters or S-parameters are used to describe the input-output relationships of N-Port circuits. At high frequencies, it is easier to describe the network in terms of waves rather than voltages or currents, and this explains why the S-parameters power waves are used. For two-port networks, the S-parameters are defined as illustrated in Fig. (2.2). The relations between the S-parameters and the waves at input and output are given in the following equations [43].

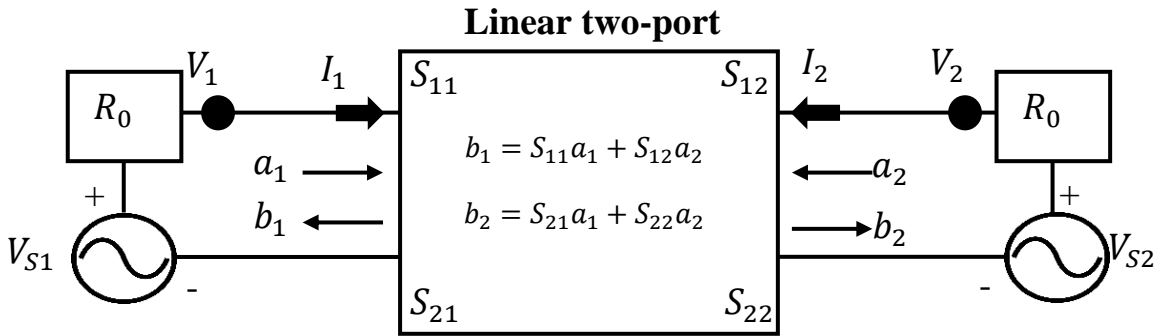


**Figure (2.2)** The scattering parameters of the two-port filter.

$$s_{11} = \frac{b_1}{a_1} \text{ at } a_2=0, s_{12} = \frac{b_1}{a_2} \text{ at } a_1=0, s_{21} = \frac{b_2}{a_1} \text{ at } a_2=0, s_{22} = \frac{b_2}{a_2} \text{ at } a_1=0 \quad (2.1)$$

$a_1, b_1$  : The incident and reflected voltages at the input port respectively.

$a_2, b_2$  : The incident and reflected voltages at the output port respectively.

$S_{11}$ : The voltage reflection coefficient at the input port.

$S_{12}$ : The reverse voltage gain.

$S_{21}$ : The forward voltage gain, or the transmission coefficient.

$S_{22}$ : The voltage reflection coefficient at the output port.

The S-parameter matrix is usually used to determine reflection and transmission coefficients at both sides of a two-port network. These concepts are also used in finding the gain, return loss, **Voltage Standing Wave Ratio (VSWR)**, and insertion loss.

**Reflection Coefficients ( $\Gamma$ ):** This is a parameter that describes how much of an electromagnetic wave is reflected by at an impedance discontinuity in the transmission medium or along a transmission line. It is a very useful quantity when assessing VSWR or checking the matching between a source supplying a certain load [44].

$$\Gamma = \frac{V_{reflected}}{V_{incident}} = \sqrt{\frac{P_{reflected}}{P_{incident}}} \quad (2.2)$$

**VSWR:** This is the abbreviation of **Voltage Standing Wave Ratio**, which expresses the efficiency by which an RF power is transmitted from a power source, through a feed line, into a load. It calculates the efficiency of power transmission from a source to a load via a transmission line. The minimum value of VSWR is unity, which is an ideal condition in which the load absorbs (100%) of the power from the source. However, VSWR is rarely found to be unity in practical applications, and systems are designed to keep the VSWR as close to unity as possible. A value of  $< 2$  has been widely adopted, and this corresponds to a reflection coefficient value of -10 dB. The VSWR is related to the reflection coefficient by the following [44]:

$$\text{VSWR} = \frac{1+|\Gamma|}{1-|\Gamma|} = \frac{1+|S_{11}|}{1-|S_{11}|} \quad (2.3)$$

**Return Loss (RL):** It is a measure of how close the actual input/output impedance of the network is to the nominal system impedance value [45].

$$RL_{in}(dB) = 10 \log_{10} \left| \frac{1}{S_{11}^2} \right| = -20 \log_{10} |S_{11}| \quad (2.4)$$

$$RL_{out}(dB) = -20 \log_{10} |S_{22}| \quad (2.5)$$

**Insertion Loss (IL):** it shows how much the filter attenuates a signal at a given frequency. The insertion loss is calculated by the ratio of the signal level at the input to that at the output of the filter. The ability of the filter to attenuate unwanted noise or certain frequencies is called its insertion loss. The value of the insertion loss usually varies with frequency and often changes by several orders of magnitude over the frequency range of the filter; thus, insertion loss is conveniently expressed in decibels (dB) units [45]:

$$IL(dB) = 20 \log_{10} \frac{\text{Input Signal Amplitude}}{\text{output Signal Amplitude}} \quad (2.6)$$

### 2.3 Filter Realization with Microstrip Technology

A microstrip line is a type of electrical transmission line that is commonly used at RF and higher frequencies and is made using printed circuit board (PCB) technology. The most common planar component in radio frequency (RF) applications is the microstrip transmission line shown in Fig. (2.3). Microstrip lines have a lower power handling capacity and higher losses than waveguides due to the fact that it is not enclosed by metals as waveguides, and have non-perfect substrates. Due to their lightweight, low cost, and compact size, microstrip filters are popular components in emerging wireless communication devices.

## Microstrip Line Impedance ( $Z_0$ )

The microstrip line impedance or characteristic impedance of a microstrip line is a function of the strip width  $W$ , to the substrate thickness  $h$ , and the relative permittivity of the substrate material. Among the several methods for finding the characteristic impedance of a microstrip line, the field equation method was used mostly to obtain an accurate value of the characteristic impedance. Alternatively, the characteristic-impedance of the microstrip line can be found from the well-known equation by making some changes, and this method is called a comparative, or an indirect, method [45].

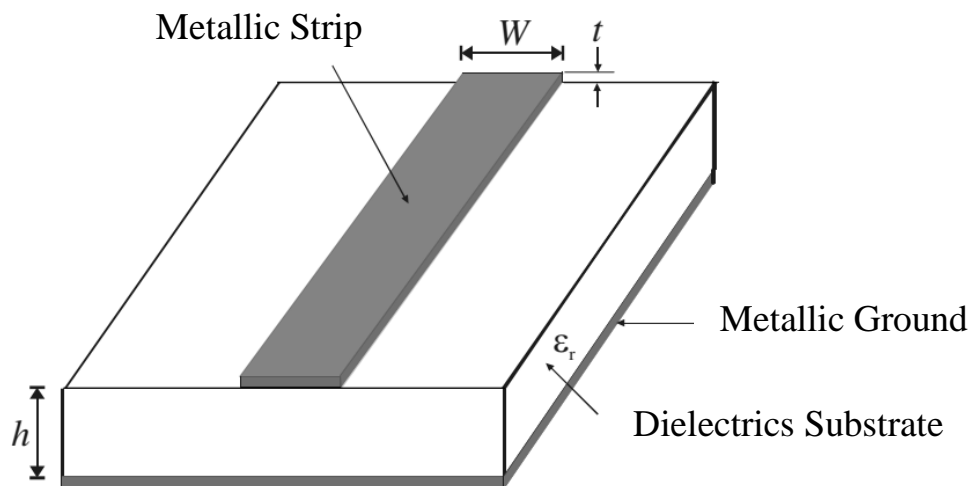


**Figure (2.3)** Microstrip transmission line [43].

**Dielectric constant ( $\epsilon_r$ ):** The dielectric constant, also known as the relative permittivity, describes how easily a material can become polarized when an electric field is applied to it. The ratio of “the permittivity of a substance to the permittivity of space or vacuum” is known as relative permittivity. The relative permittivity of the substrate material is an important factor in the filter design.

**Effective Dielectric Constant ( $\epsilon_{eff}$ )** is defined as the dielectric constant of an effective uniform dielectric material enclosing the strip line so that the line

shown in Fig. (2.4.b) has identical electrical characteristics, particularly propagation constant, as the actual line of Fig. (2.4.a) [46]. Thus, due to the electric field fringing to the surrounding air, the effective dielectric constant is always smaller than that of the substrate. The following relations show the characteristic impedance and effective relative dielectric constant [46].

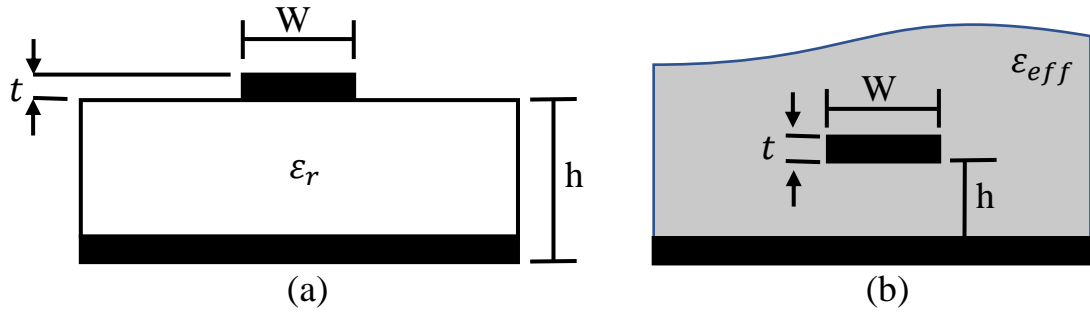


**Figure (2.4)** (a)-Microstrip transmission configuration (b)- effective dielectric constant [46].

if  $\left(\frac{W}{h}\right) < 1$ :

$$Z_0 = \frac{60}{\sqrt{\epsilon_r}} \ln\left(8 \left(\frac{h}{W}\right) + 0.25 \left(\frac{W}{h}\right)\right) \quad (2.7)$$

$$\epsilon_{eff} = \frac{\epsilon_r + 1}{2} + \frac{\epsilon_r - 1}{2} \left[ \frac{1}{\sqrt{1 + 12 \left(\frac{h}{W}\right)}} + 0.04 \left(1 - \left(\frac{W}{h}\right)\right)^2 \right] \quad (2.8)$$

if  $\left(\frac{W}{h}\right) > 1$ :

$$Z_0 = \frac{120\pi}{\sqrt{\epsilon_r} \left[ \frac{W}{h} + 1.393 + \frac{2}{3} \ln\left(\frac{W}{h} + 1.444\right) \right]} \quad (2.9)$$

$$\epsilon_{eff} = \frac{\epsilon_r + 1}{2} + \left[ \frac{\epsilon_r - 1}{2 * \sqrt{1 + 12 \left(\frac{h}{W}\right)}} \right] \quad (2.10)$$

## 2.4 Various Designs of Existing Filters

The filters can be categorized by their frequency response into four basic categories shown in Fig. (2.5) according to their frequency response. Therefore, each time filter should have one or more resonant element that should be connected in a certain way to achieve the wanted property. Another categorization is based on the layout of the filter and how the input and output ports are coupled. To achieve a specific frequency response, the input/output coupling should be through some frequency-dependent mechanism. This is usually achieved via some resonant element or elements.

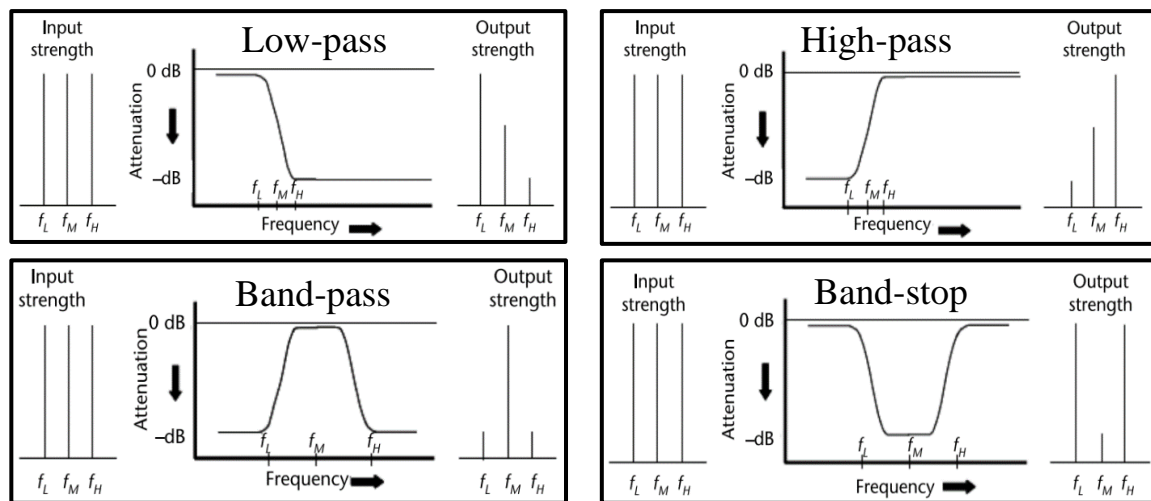


**Figure (2.5)** Frequency response of basic types of filters [47].

### 2.4.1 Closed and Open Rings

In this type of microstrip filters, the resonant element has the shape of a square or circular ring, which is simultaneously coupled to the input and output ports. This concept has been employed in many published designs. A microstrip band-reject filter using an open-loop rectangular resonator that is coupled to a microstrip line was proposed by B. Jitha et al. in 2007, as shown in Fig. (2.6). A rectangular loop of the dimensions shown in Fig. (2.6) was

built on RT Duroid substrate having  $\epsilon_r = 3.2$  and thickness 1.6 mm. The mitered  $50\Omega$  transmission line was bent closely around the resonating loop [9]. Fig. (2.7) shows the obtained results, the reflection and transmission coefficients are -2 dB and -25 dB respectively, which indicate a band-reject property at 1.72 GHz and a -10 dB bandwidth of 70 MHz.

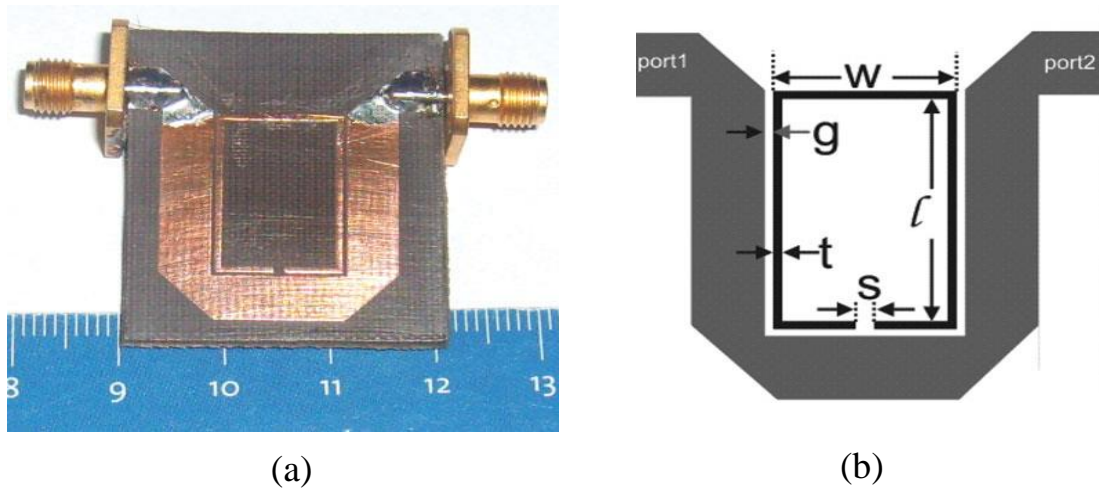


**Figure (2.6)** (a)-Photograph of the proposed open loop filter. (b)-Geometry of the proposed filter. length  $l = 17$  mm, width  $w = 12$  mm, thickness  $t = 0.5$  mm [9].

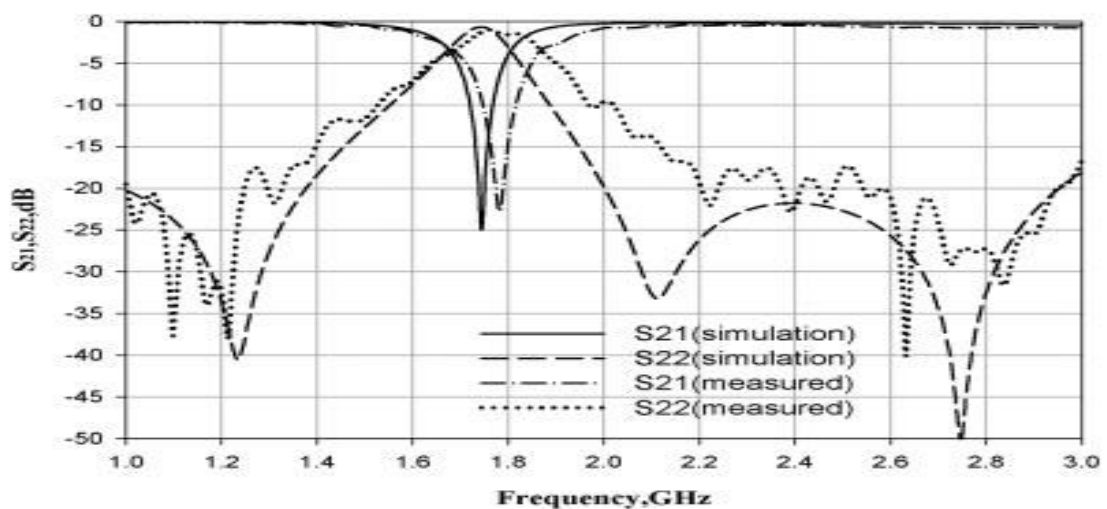


**Figure (2.7)** The simulated and measured results for the bandstop filter [9].

Open-loop ring resonators and the overlapping technique were used in [22], to design a BSF structure that is shown in Fig. (2.8). The first is a straight forward BSF with a single C-open-loop resonator. To reduce the size and improve the performance, a new compact multi-band microstrip BSF using a multi-reject band resonator was proposed. The idea was to place several open-loop ring resonators on top of each other, to achieve small size, and satisfactory results [22]. The building block of the proposed BSF is the C-shaped open-loop resonator, which employs a single microstrip that is connected directly to the two feed Lines. The BSF filter has a 5.6 GHz center frequency, less than -30 dB transmission coefficient and about -1 dB reflection coefficient at the reject band [22]. Fig. (2.9) shows the simulated and measured results of a single-layer filter which indicate band-reject properties.

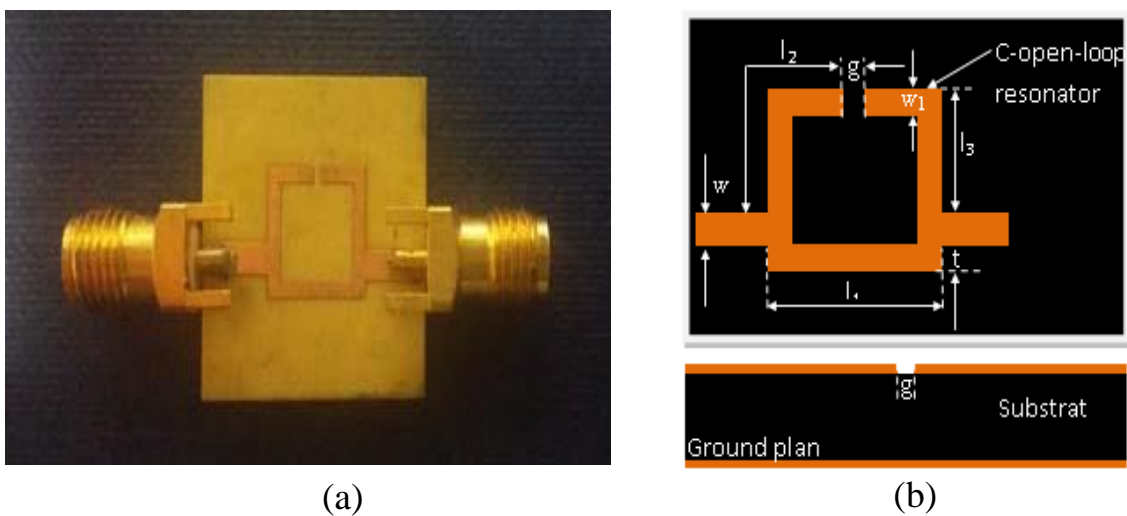


**Figure (2.8)** (a)-Photograph of proposed C-open-loop resonator, (b)-Layout of the proposed C-open-loop single BSF [22].

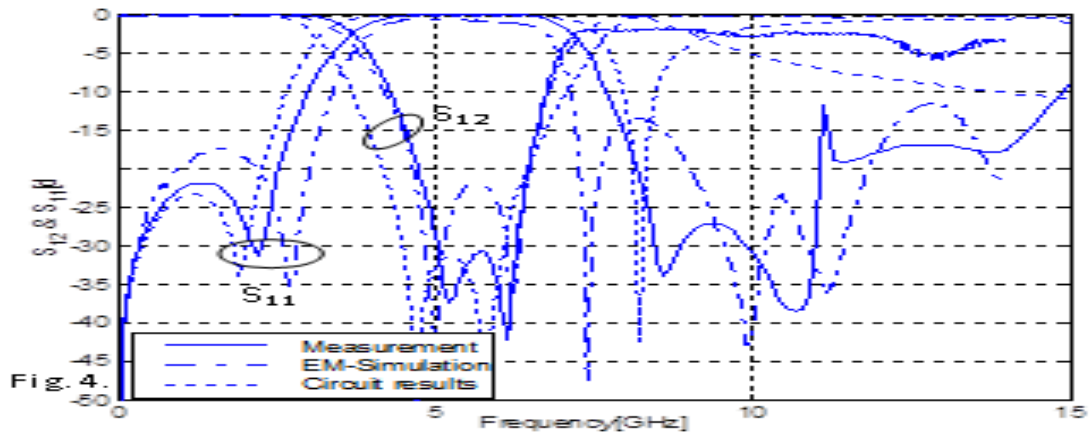


**Figure (2.9)** Simulated and measured S-parameters of the proposed C-shaped open-loop resonator (BSF) [22].

### 2.4.2 Coupled or Connected Stubs

This group of filters uses resonant elements in the form of stubs that are either coupled or connected to the microstrip line. This concept has been employed in many published designs. Two dual-band bandstop filters using open and short stub-loaded resonators were proposed by Gao, Li et al. in 2012, as shown in Fig. (2.10). The method of even- and odd-mode analysis was used to determine the frequency of the two bands. Because of the symmetrical feed, the odd-mode frequencies were considerably reduced, while the harmonic was

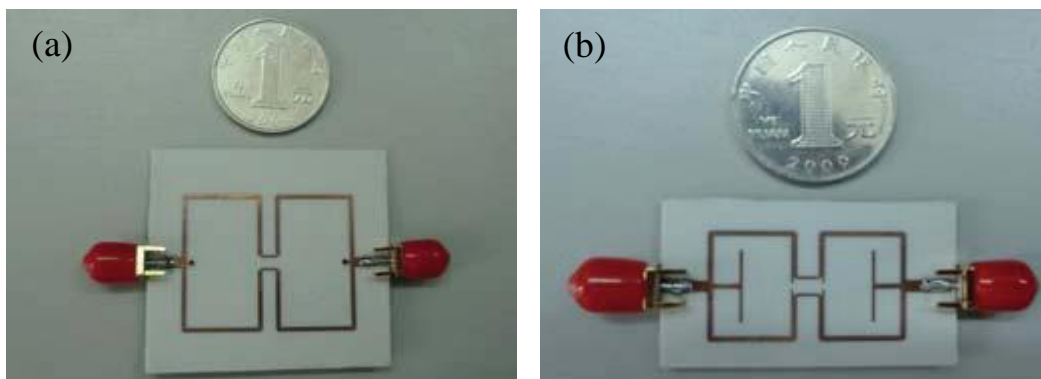


**Figure (2.10)** Photograph of the prototype bandstop filter using (a)-Open and (b)-Short stub-loaded resonators [15].

utilized as the second stopband. The filters were folded into loops to improve the effect of loading between the resonators and the microstrip line [15].

Figure (2.11.a) compares the measured with the simulated results of open stub-loaded resonators. The rejection level in the stopbands is about 20 dB and 16 dB, while the 3 dB bandwidths are (4.8%) and (5%), respectively. The insertion loss is smaller than 1dB, and the return loss is larger than 15 dB, in all the passbands. Fig. (2.11.b) shows the measured and simulated results for the short stub-loaded resonators BSF. The first stopband is located at 1.16 GHz, and has a rejection of 29 dB, and a (50%) 3 dB bandwidth. The second stopband appears at 3.5 GHz, which is about three times the frequency of the first stopband. It achieved a rejection of 28 dB and (14.3%) relative bandwidth [15].

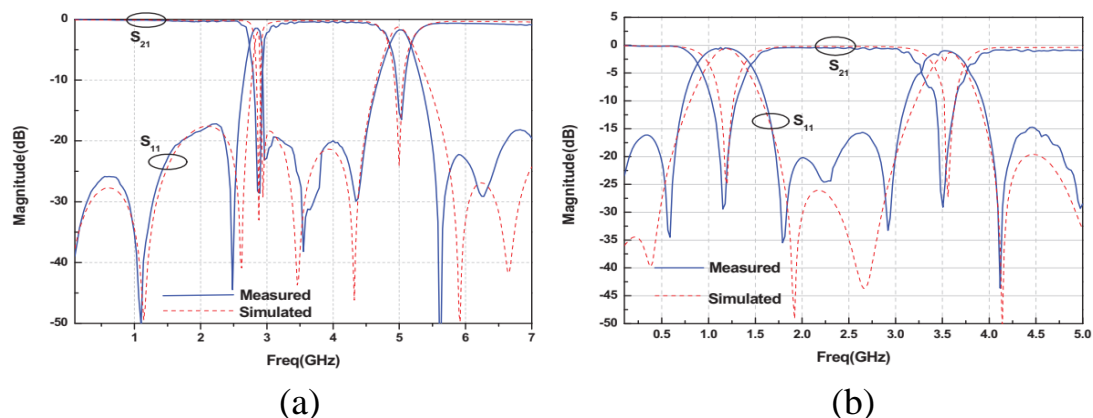


**Figure (2.11)** Measured and simulated results of (a)-Open stub-loaded (b)- Short stub-loaded resonators [15].

Two wide bandstop filters based on the microstrip transmission line, and loaded with a T-shaped and two L-shaped resonators was introduced by M. Esmaili et al. in 2016, as shown in Fig. (2.12). The investigation showed that the filter has two transmission zeros in the stopband and three reflection zeros in the lower and upper passbands. The used method is suitable for designing wide-band bandstop filter designs employing parallel-coupled line sections,

especially when tight coupling values cannot be obtained due to manufacturing limitations. [21]

Figure (2.13) compares the obtained simulated and measured results. The measured attenuation at the stopband is  $> 16$  dB, and the return loss in the lower passband is better than 12 dB, while that in the upper passband is better than 10 dB [21].

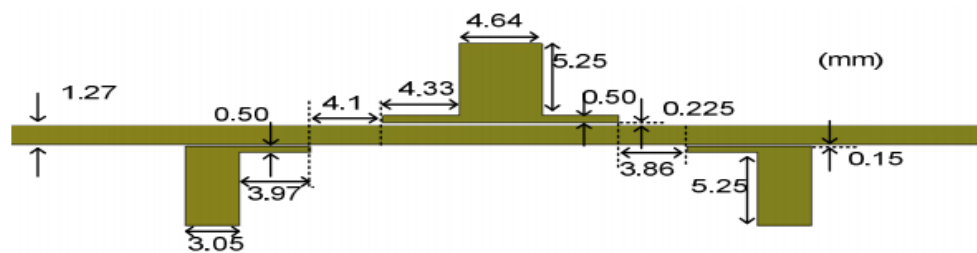


**Figure (2.12)** Configuration of the designed filter [21].

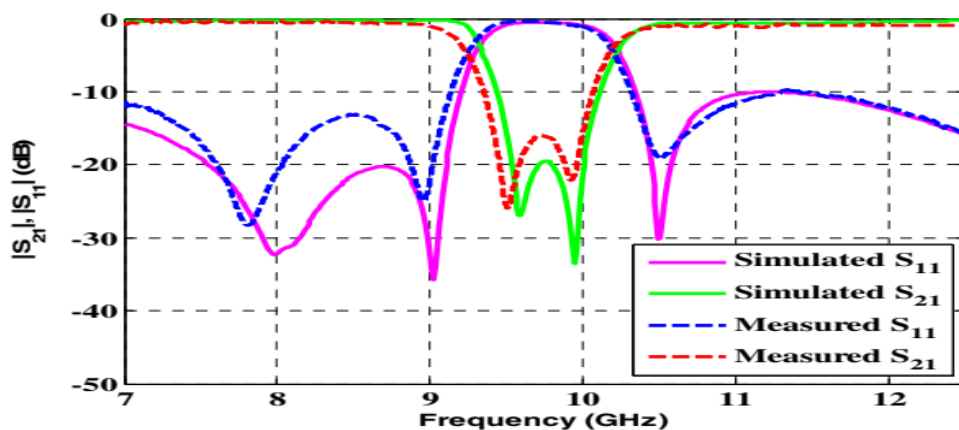


**Figure (2.13)** Simulated and measured responses of the filter [21].

### 2.4.3 Slots in the Ground Plane

These types of filters use slots of various shapes implemented in the ground plane to achieve the filtering properties. The use of **Split Ring Resonators (SRRs)** and **Complementary Split Ring Resonators (CSRRs)** was presented by R. S. Kshetrimayum et al. in 2007 in his design of the filter shown in Fig. (2.14) [8]. The size of the filter is much smaller than the operational

wavelength. Both of the SRR and CSRR resonate at the same frequency, as have the same dimensions. For applications like harmonic suppression of a bandpass filter, one can build the bandpass filter on one side of the substrate and etch CSRR rings on the other side, to achieve more degrees of freedom for designing the filter [8]. A CSRR structure is designed to resonate at 8.3 GHz of the X-band microwave frequency region, the filter has a transmission coefficient about 18 dB and a reflection coefficient of about 2 dB. The CSRR structure is placed in the ground plane exactly below the center of a microstrip line, and FR4 dielectric substrate of  $\epsilon_r=4.4$  and height ( $h$ ) 1.6mm, Fig. (2.14).

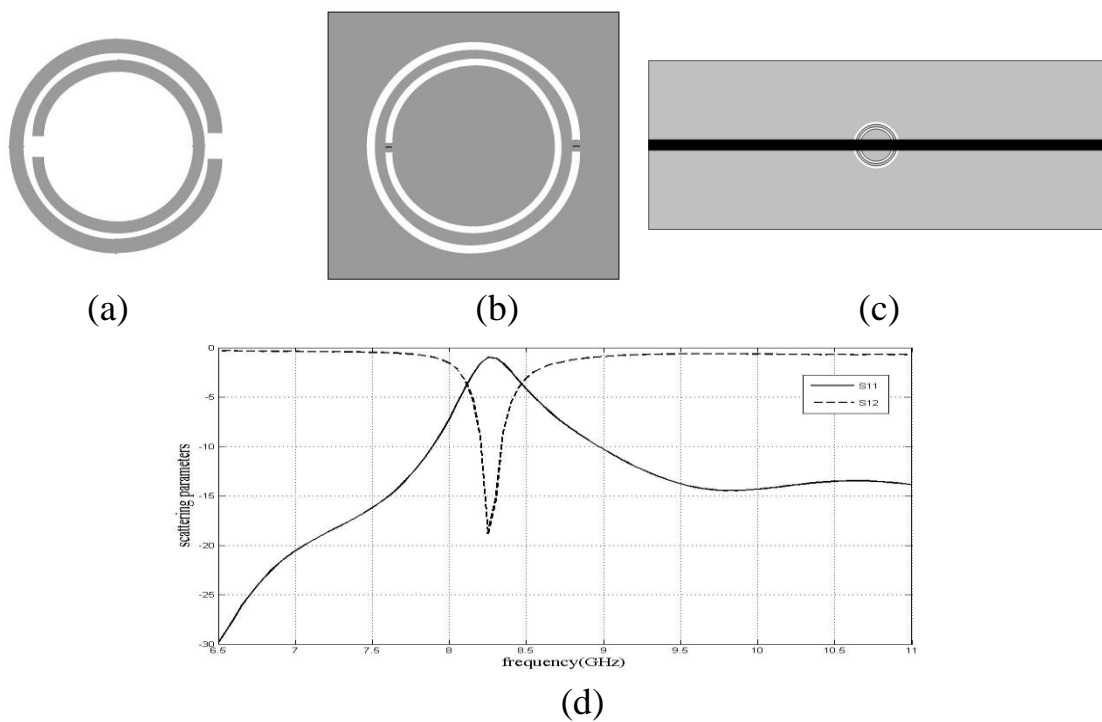


**Figure (2.14)** (a)-SRR, (b)-CSRR, (c)- Front view of CSSR in the ground plane, (d)- Frequency response [8].

#### 2.4.4 Slots and Rings in the Microstrip Line

As explained in the aforementioned section, the ring or open-rings slots were placed on the ground plane. Alternatively, the complementary open ring may be placed in the microstrip line itself. A bandstop filter having a square split-ring etched in the microstrip line was proposed by S. Fallahzadeh et al.

2009, as shown in Fig. (2.15) [10]. For the shown dimensions in Fig. (2.15.a), is  $L1 = 10$  mm,  $L2 = 9.6$  mm,  $c = 0.4$  mm,  $g = 0.4$  mm,  $w1 = 0.27$  mm and  $w2 = 0.2$  mm, and RT/Duroid 5880 substrate having a thickness of 0.508 mm and relative permittivity of 2.2, the obtained results are shown in Fig. (2.15.b). The filter shows the band-reject property of 30 dB at the 7 GHz frequency [10].

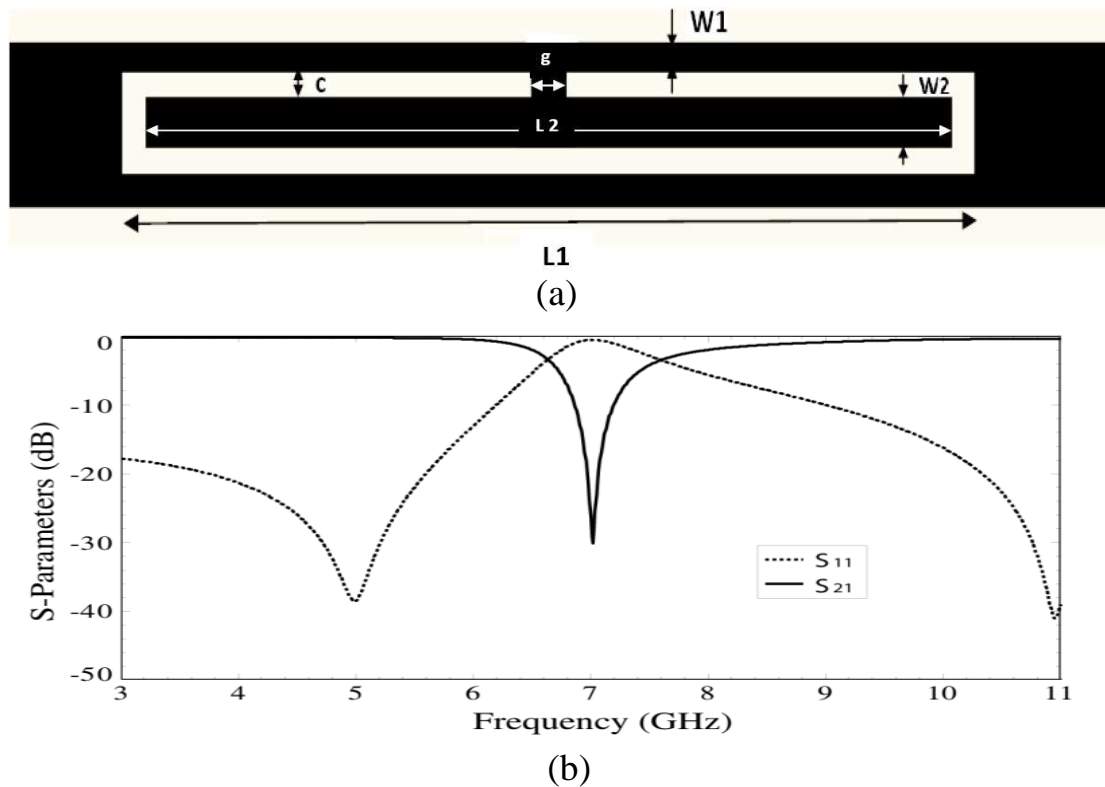


**Figure (2.15)** (a)-Configuration of open square-slot bandstop filter, (b)-Simulated scattering parameters for the filter [10].

A U-slot etched on a microstrip line was recently proposed as a high performance and compact-size bandstop filter by Mamoon A. Al-Atrakchii et al. 2020, as shown in Fig. (2.16) [36]. The resonant element is a slot, which is folded into the shape of the letter U. The slot is narrow enough and can be embedded into the microstrip line. Moreover, the folding reduces the length to 1/4 the effective wavelength, which is a considerable reduction in size compared to other filters that use resonating elements such as rings or short-circuited and open-circuited stubs that are connected to the main microstrip

line. In that paper, the FR4 substrate with a dielectric constant of  $\epsilon_r = 4.4$  and 0.025 loss tangent was used. The slot was designed to obtain resonance at 2.45 GHz [36].

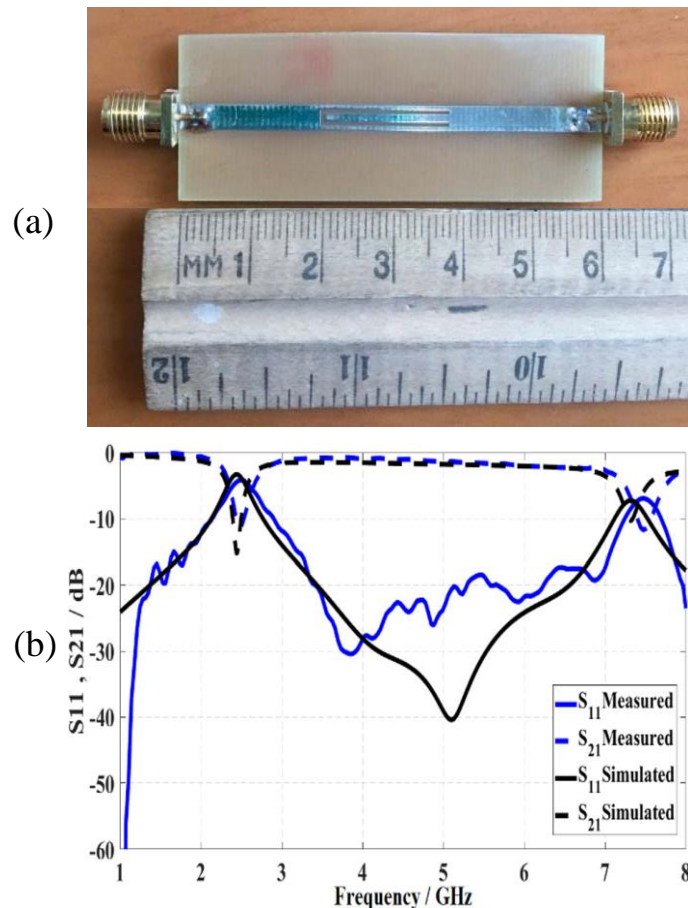


**Figure (2.16)** (a)- Photograph of the proposed U-slot filter, (b)- Simulated and measured S-parameters [36].

### 2.4.5 Stepped Impedance

In this group filters the input port is connected to the output by a microstrip line with different impedances. One example is the bandpass filter proposed by R. Phromlounsri et al. in 2010 [48]. The filter shown in Fig. (2.17) uses the stepped-impedance resonator (SIR) technique, where a quarter wavelength coupler that is connected to the stepped-impedance at the end of the lines. Each port has a step impedance feed line to tune the impedance of the filter to the characteristic impedance  $Z_0$  of the line. This resonator offers a reduction

in the second and third harmonics spurious response. Experimental tests of such design for 0.9 GHz bandpass, showed insertion loss and return loss of 1.86 dB and less than 20.1dB respectively [48]. The suppression at  $2f_0$ , and  $3f_0$  are about 64.1dB, and 52.3 dB for type I. Similar performance was found for the other two types of the filter [48].

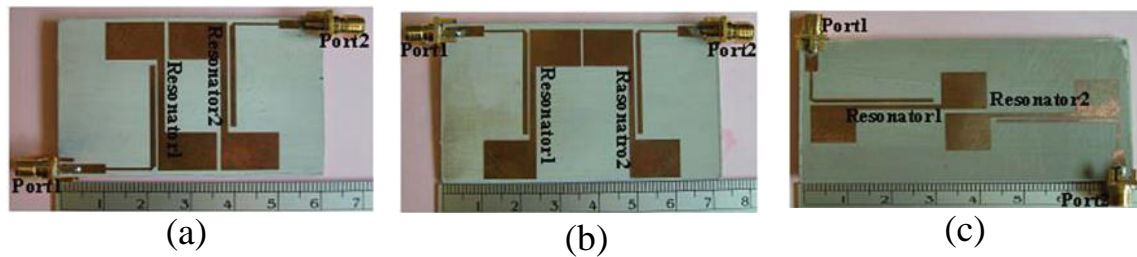


**Figure (2.17)** Photographs of a two-pole microstrip BPF using the SIR (a)-Type1, (b)-Type2 and (c)-Type3 [48].

#### 2.4.6 Hair Pin, and Coupled Lines

The resonators in the filters can have the form of coupled transmission line sections. In some designs these sections are folded to have a shape similar to the hairpin, thus it was called so. As one example, a microstrip hairpin filter and diplexer were presented by Sarayut Srisathit et al. in 2005. The proposed design is shown in Fig. (2.18), which operates at 0.9 GHz/1.8 GHz frequency with about 20 dB transmission coefficient and 0.5 dB reflection coefficient at the rejection bands. [49]. The design has high isolation performance between the 0.9 GHz and the 1.8 GHz ports as can be seen in the experimental in Fig. (2.19).

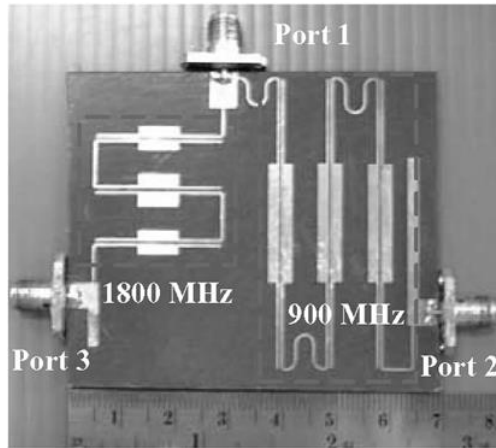


**Figure (2.18)** Photograph of a fabricated multiband microstrip hairpin diplexer [49].

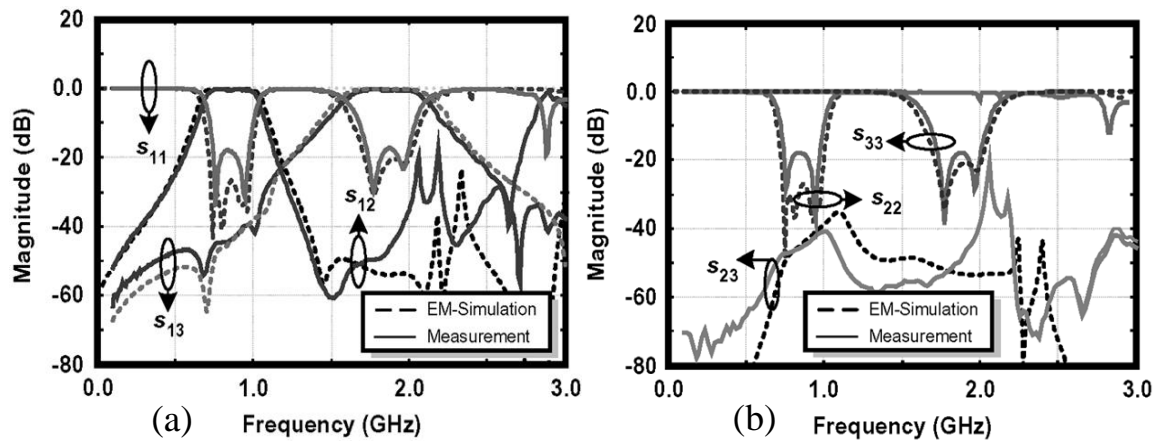


**Figure (2.19)** Measured and simulated performances of the proposed diplexer (a)-input return loss, insertion loss at Port 2, 3 and (b)-return losses and isolation losses at Port 2, 3 [49].

A wideband bandpass filter composed of a coupled line cross-shaped resonator structure was recently presented by Dong-Sheng La et al. in 2020, as shown in Fig. (2.20) [50]. To increase the coupling and improve the filter's performance, the parallel coupled-line feed type was replaced by three coupled microstrip lines. The HFSS simulation showed that the bandwidth can be varied by changing either the lengths of the short-circuited coupled line or the open-circuited coupled line [50].

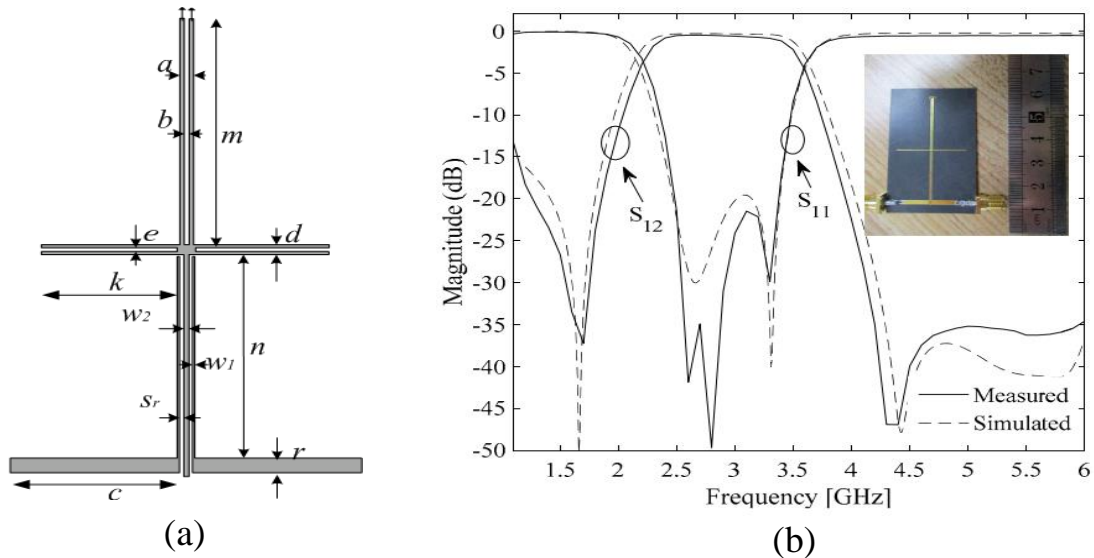


**Figure (2.20)** (a)-The design of the bandpass filter and (b)-Measured and simulated results of the fabricated bandpass filter [50].

### 2.5 Various Methods for Re-configuration of the Filter

The development of modern wireless devices requires multi-band filters, and filters where the filter properties can be changed to be more suitable to the changing environment. Such required changes can be a shift in the filtration band, or changing the bandwidth of the filter. The property or the type of the filter may be desired to be changed, such as switching the property from a band-notch to all-pass, or from band-pass filter to band-stop filter. Instead of switching from one filter to another, the system can perform better if some of the filter characteristics can be varied by some electronic elements. In other words, the filter in question can be reconfigured from one state to other as required by the system. Thus, there has been much interest in the field of reconfigurable filters for use in many wireless communications systems. In the following subsections, various examples of reconfigurable filters are discussed.

### 2.5.1 Re-configuration Using Varactor Diodes

A varactor diode is a semiconductor device in which the junction capacitance varies with the reverse voltage applied to the diode. Since there is no DC current passing in the diode, due to its reverse biasing, the losses in this nonlinear element will be minimal. The capacitance of the depletion layer varies with the applied reverse biasing. Varactor diodes are made of Gallium Arsenide because it has a higher maximum operating frequency (up to 1000 GHz) and can operate at low temperatures.

Several reconfigurable BPFs using varactor diodes have been introduced in recent years [32, 51]. A reconfigurable microstrip BPF using a varactor diode was proposed by W Tang et al. in 2010 to obtain a constant impedance bandwidth. The reconfigurable properties were achieved by tuning the resonance frequencies of the odd and even modes, where there is no mutual coupling between these two modes. Fig. (2.21) shows the built prototype of the proposed tunable BPF along with the obtained performance. A good roll-off skirt on the lower edge of the band, an insertion loss of  $< 2.2$  dB, and a return loss of  $>10$  dB can be seen from the obtained results. A tuning rate of (40%) for the 0.60 GHz to 1.0 GHz range was achieved by applying a reverse bias voltage between 2.2 V and 22.0 V across the varactor diode. The impedance bandwidth for all configurations was preserved at 91 MHz [11].

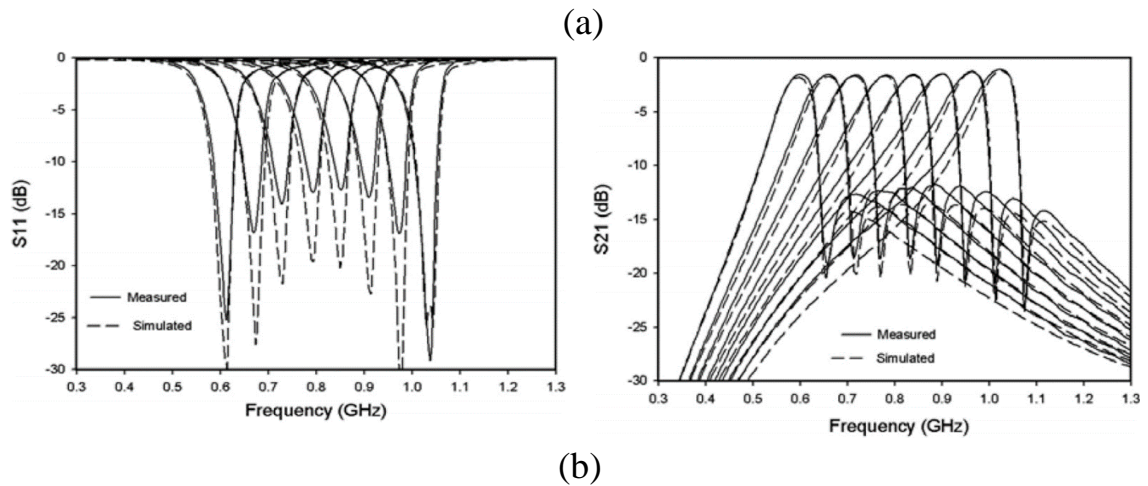
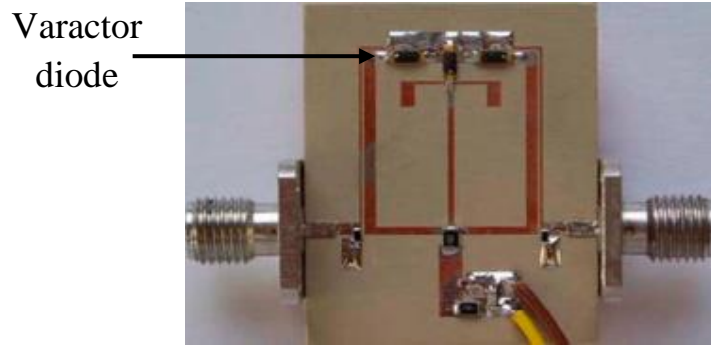


**Figure (2.21)** (a)-Structure of the prototype (b)-S-parameters variation with frequency [11].

## 2.5.2 Re-configuration Using PIN Diodes

The PIN diode consists of heavily doped P and N layers that are separated by an intrinsic or un-doped layer. The intrinsic layer exhibits high resistance to the passing current. The PIN diode works as an ordinary diode for frequencies up to 100 MHz, and it is used in the switching of microwaves. However, above 100 MHz it ceases to operate as a rectifier and behaves as a switch or resistance, while in reverse bias it can act as a capacitor.

In 2022, Ambati Navya et al. proposed a reconfigurable BPF that was built from polimide, having a relative permittivity of 3.5, a loss tangent of 0.0008, and a thickness of 0.1 mm [52]. The reconfigurable BPF has dimensions of 10 x 9.2 mm and is depicted in Fig. (2.22). This design

incorporates a concentric square loop and an H-shaped resonator, as well as three 1/4 wavelength transmission lines. The concentric square loop resonates at the wanted frequency, while the H-shaped resonator produces the transmission zeroes. A PIN diode is placed at the position of maximum current distribution, so that the filter can be reconfigured between the two frequency bands, such as KU and K [52]. Fig. (2.22.c) shows the simulated and measured  $S_{21}$  response of the filter under diode ON and OFF states. This BPF resonates at 12 GHz and 18 GHz, and at those frequencies, the  $S_{21}$  response of the filter is less than 3 dB, 0.3 dB for simulated and 0.9 dB for measured during diode ON, and 0.4 dB for simulated and 0.6 dB for measured during diode OFF [52]. It should be noted here that the simulated and measured values of  $S_{21}$  are both negative, (as listed in the insert), but the vertical scale shows positive values.

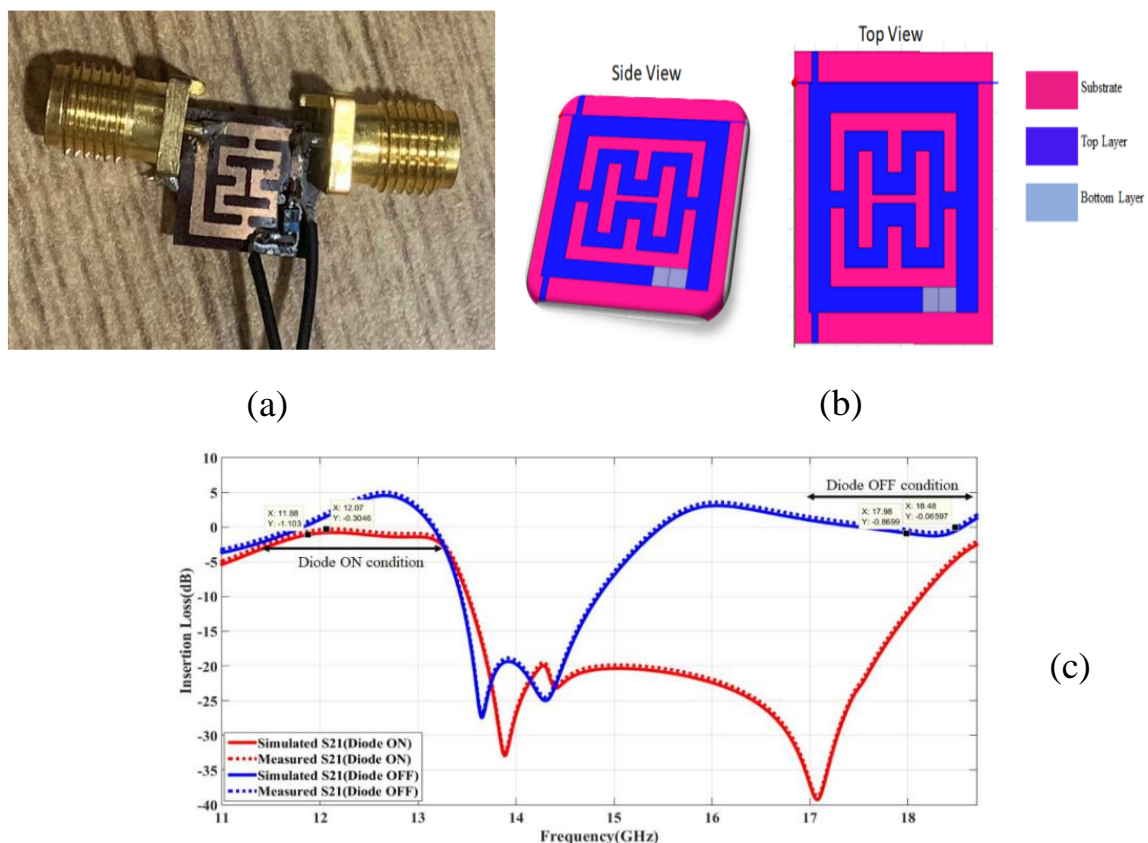


**Figure (2.22)** (a)- Picture of the reconfigurable BPF, (b)- Geometry of the BPF, (c)- Simulated and fabricated  $S_{21}$  response of the BPF [52].

### 2.5.3 Re-configuration Using Liquid Crystals (LM)

A Liquid Metal switch or (LM) flowing by micropumps or an electrochemically controlled capillary method can offer regions on variable conductivity in the layout of the filter or RF device. They have been used to implement reconfigurability in filter designs. The movement of LM over a large physical dimension enhances the reconfigurable state of the antenna or filters, without the need of other nonlinear solid-state devices [53].

In 2019, Eiyong Park et al. proposed a switchable band-pass/band-stop filter using liquid metal (LM) alloy as a fluidic switch as shown in Fig. (2.23). When the fluidic switch is applied to the short stub using a micro-pump, the filter acts as a bandpass filter (BPF) with the short-circuited stubs. When the fluidic switch is applied to the open-circuited stub, the filter acts as the bandstop filter (BSF) with the open stubs. The BPF state is characterized by a 2.5 GHz center frequency and 1 dB bandwidth between 1.75 and 3.07 GHz. The insertion loss is about 0.5 dB. At the BSF state, a stop band extending from 2.4 GHz to 2.65 GHz with the 15 dB attenuation was achieved [54].

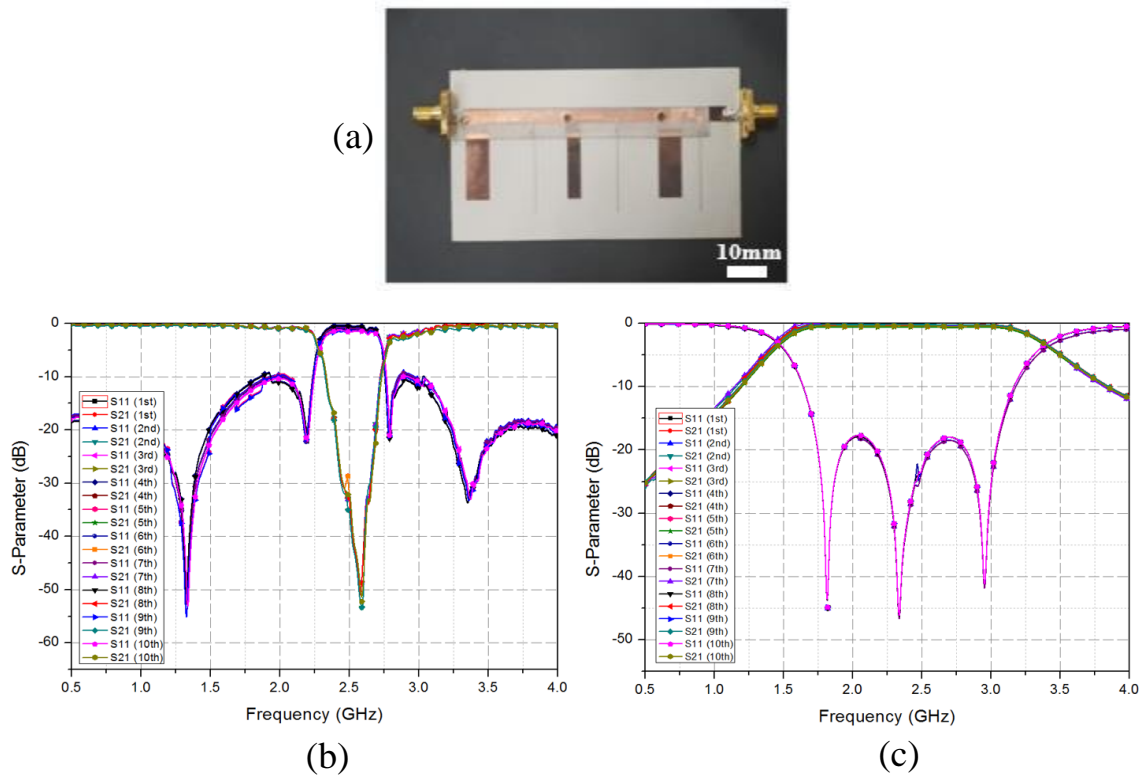


**Figure (2.23)** (a)- The picture of the fabricated proposed filter, (b)- Measured S-parameter for BSF, (c)- Measured S-parameter for BPF, [54].

### 2.5.4 Re-configuration Using MEM's

The RF Micro-electro-mechanical-systems or MEMS switches are small switches that have low power consumption and are fabricated using conventional MEMS production. The mechanical components of the switch are only microns in size, Fig. (2.24) [55-56].

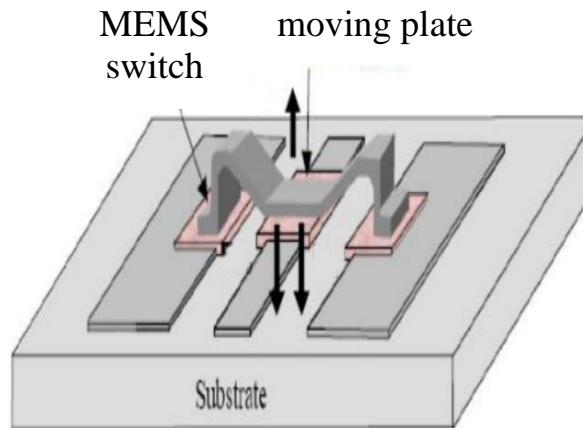


**Figure (2.24)** Schematic picture of a micromechanical (MEM) switch [56].

The bandwidth tunable RF filter was presented by A. H. M. Zahirul Alam et al. in 2009, using RF MEMS, as shown in Fig. (2.25). The bandwidth tunability is obtained by using capacitive MEMS switches that can be tuned across the frequencies from 3.6 GHz to 4.4 GHz. The obtained performance depends on the geometry, location, and types of the MEMS switches [57]. The filter geometry is shown in Fig. (2.25.a). The design parameters are  $f_0 = 4$  GHz and bandwidth = 0.8 GHz, and five resonators are assembled on an alumina substrate, that is backed by a copper ground plane, while the feed is a microstrip line [57].

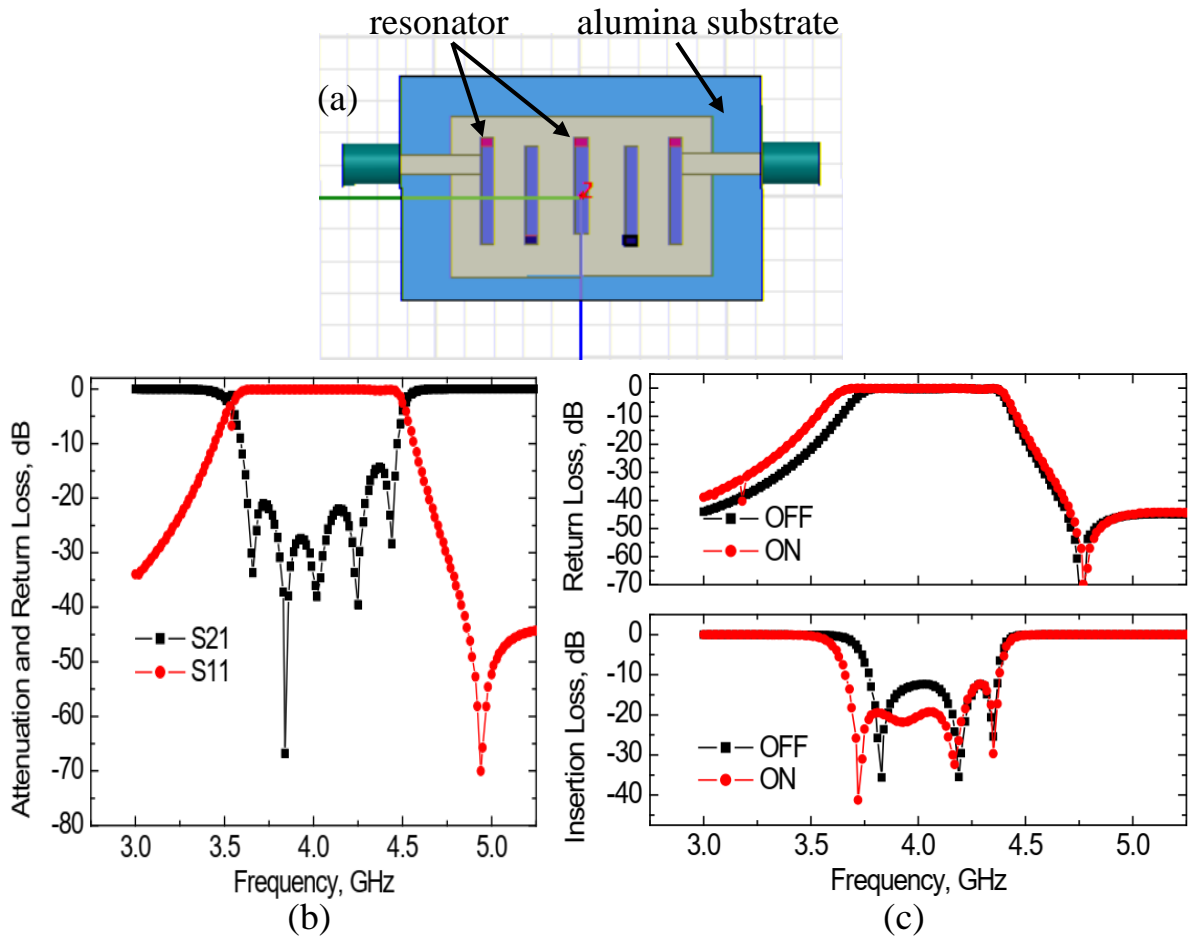


**Figure (2.25)** (a)-The layout of inter-digital filter, (b)-Simulated results without MEMS switches, (c)- with two state MEMS switch [57].

# CHAPTER THREE

## ANALYSIS AND DESIGN OF RECONFIGURABLE FILTER USING U-SHAPED SLOT

### 3.1 Introduction

In this chapter, the analysis and design of a reconfigurable filter using a U-shaped slot are presented. The principle of operation of a band-reject filter that employs a U-shaped slot will be explained. An approach of how to change the role of this filter from blocking a specific frequency band to passing all frequencies in a simplified and feasible way using only one PIN diode is demonstrated. The influence of changing some of the filter parameters on the performance of the filter is presented too.

The simulation software (CST Microwave Studio) was used to simulate the proposed filter. Through it, it is possible to design the microstrip line filter and investigate its performance, such as working frequency, resonance frequency, transmission or reflection coefficients. The software has the capability to determine the (electric or magnetic) field distribution across the filter, which was found very important in understanding the operation of the filter.

### 3.2 The Band-Stop Filter Using U-Shaped Slot

The filter has a simple and compact design, it comprises a slot in the shape of the English language letter (U) engraved on the microstrip line shown in Fig. (3.1), with FR4 (Flame Retardant) substrate that has a dielectric constant of 4.4, 0.025 loss tangent, and thickness  $h_1=1.6$  mm, while a copper layer is used for the microstrip line and the ground plane. The substrate dimensions are 40 mm \* 20 mm \* 1.6 mm. The microstrip line width has to be determined

such that the line impedance is 50 Ohm, and the relation Eq. (3.1) was employed for this purpose [46]:

$$Z = \frac{120\pi}{\sqrt{\varepsilon_r} \left[ \frac{W_2}{h_1} + 1.393 + 0.667 \ln \left( \frac{W_2}{h_1} + 1.444 \right) \right]} \quad (3.1) \quad \frac{W_2}{h_1} > 1$$

$\varepsilon_r$  : is the relative dielectric constant of the substrate.

$\frac{W_2}{h_1}$  : is the ratio of substrate height  $h_1$  to the line width  $W_2$ .

The width  $W_2$  of the microstrip line was found to be 3.05 mm to get an input impedance of  $Z = 50 \Omega$  based on the Eq (3.1). It is also consistent for all subsequent designs presented in this dissertation. The slot that is engraved in the microstrip line consists of three rectangular segments connected to each other to form one slot folded into the shape of the letter U. The total length  $L_s$  of these rectangular segments was carefully calculated to be resonant at the required frequency according to the slot length Eq. (3.2):

$$L_s = 2L_2 + W_4 \quad (3.2)$$

where ( $W_4$ ) is the slot width. The effective dielectric constant  $\varepsilon_{eff}$  is given by [46]:

$$\varepsilon_{eff} = \frac{\varepsilon_r + 1}{2} + \frac{\varepsilon_r - 1}{2} \left( 1 + 12 \frac{h_1}{W_2} \right)^{-0.5} \quad (3.3)$$

and for the used substrate, it was found to be 3.26.

The resonance of the slot happens when the slot length is equal to half the effective wavelength as shown in Eq. (3.4) [24,36].

$$f_r = \frac{NC}{2 L_s \sqrt{\varepsilon_{eff}}} \quad (3.4)$$

$N$ : An integer number representing multiples of resonant frequency.

$C$ : The speed of light in vacuum =  $3 \times 10^8$  m/s.

Using Eqs. (3.2, 3.3), and (3.4), a slot length  $L_2$  and width  $W_4$  were chosen to get a resonant frequency at 2.45 GHz. At any operating frequency, the effective wavelength can be calculated using the effective dielectric constant given by Eq. (3.3) to get

$$\lambda_e = \frac{\lambda_0}{\sqrt{\epsilon_{eff}}} = \frac{C}{f_r \sqrt{\epsilon_{eff}}} \quad (3.5)$$

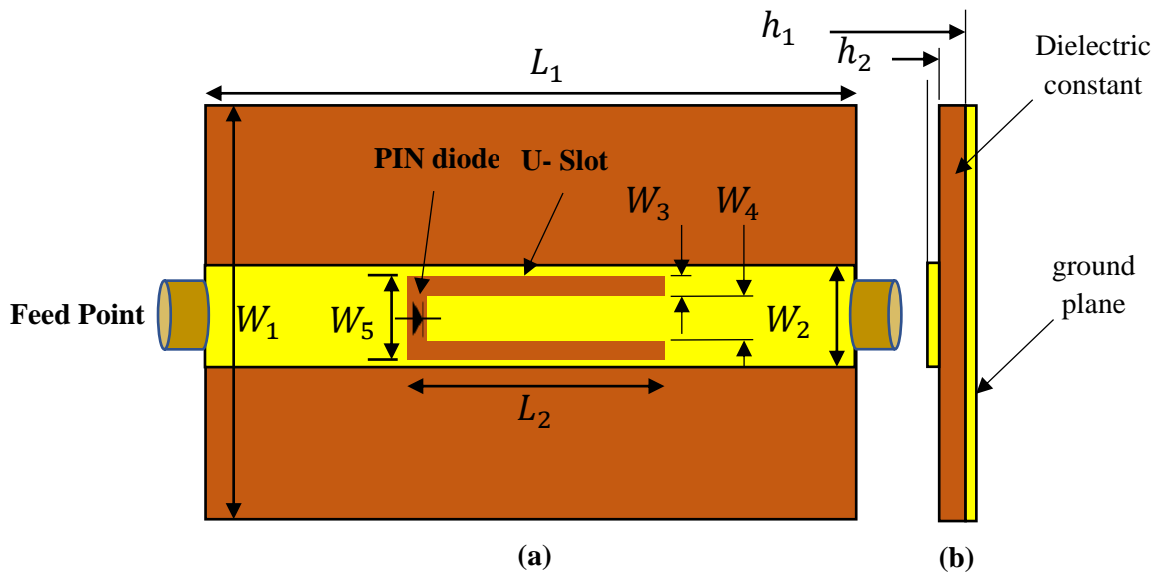


**Figure (3.1)** The geometry of the reconfigurable filter using a U-shaped slot etched on the microstrip line, (a)- “front view”, (b)- “side view”.

The performance of the filter was improved by finding the proper values of the U-shaped dimensions  $W_3$  or  $W_4$ , considering that changing  $L_2$  contributes to changing the resonance frequency according to Eq. (3.4). That will lead to a lower value of  $S_{21}$  at the resonance frequency (reject-band). Through the CST simulation software, the filter performance was checked and manipulated with several parameters as  $W_3, W_4$  and  $W_5$ , after several attempts, the best performance was reached for the values  $W_3 = 0.5 \text{ mm}$ ,  $W_4 = 1.8 \text{ mm}$  and  $W_5 = 2.8 \text{ mm}$ , and the filter parameters are listed in Table 3.1.

Parameter	$L_1$	$L_2$	$h_1$	$h_2$	$W_1$	$W_2$	$W_3$	$W_4$	$W_5$
Value <sub>mm</sub>	40	18.2	1.6	0.035	20	3.05	0.5	1.8	2.8

Figure (3.2) shows the filter frequency response for various sets of dimensions, where it can be seen that the best performance regarding  $S_{21}$  has been obtained for the design A. As shown in Fig. (3.2), and Table (3.2), this design is better than that achieved by [36] by 7.4 dB in the value of  $S_{21}$ , and it also offers a slightly larger bandwidth. These improvements can be attributed to the use of a wider slot (1.8 mm in design ‘A’) as compared to 1 mm in [36]. It can also be seen from Fig. (3.2) and Table (3.2) that wider slot values lead to slightly lower resonance frequency, as it is indicated by Eqs. (3.2) and (3.4).

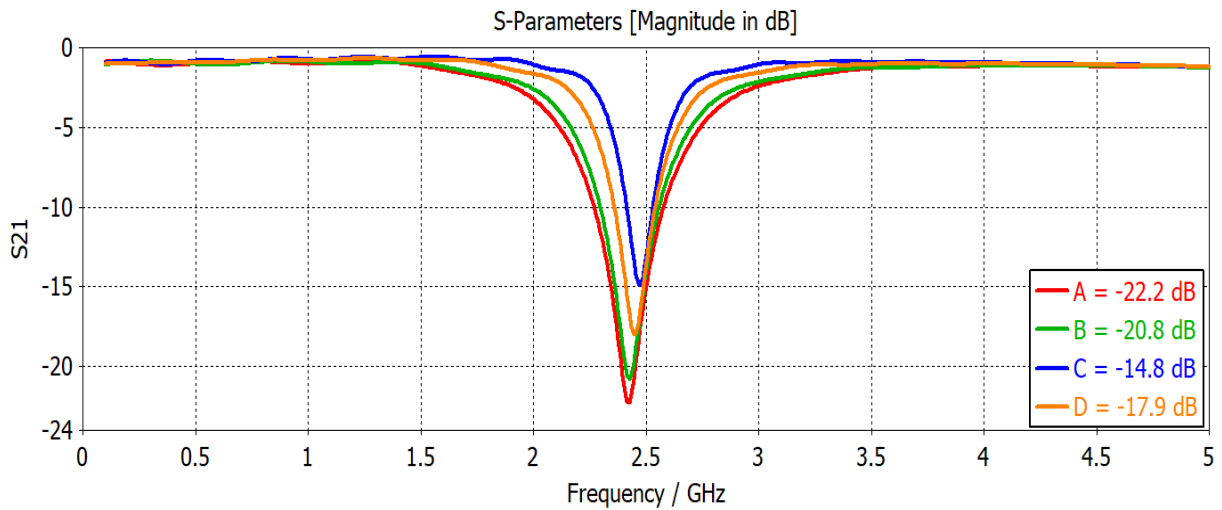


**Figure (3.2)** The filter performance for various dimensions.

<b>Table (3.2)</b> The Performance of the Filter with Different Dimensions ( $L_2=18.2_{mm}$ fixed).						
Design	$W_{3_{mm}}$	$W_{4_{mm}}$	$W_{5_{mm}}$	$S_{21}$ dB	Frequency GHz	Reference
A	0.5	1.8	2.8	-22.2	2.42	
B	0.9	1	2.8	-20.8	2.42	
C	0.5	1	2	-14.8	2.47	[36]
D	0.7	1	2.4	-17.9	2.44	

The frequency response of the filter can be explained using an equivalent circuit of a parallel RLC circuit that is connected in series with the microstrip line, as depicted in Fig. (3.3), Thus the reflection coefficient at the input of the filter can be written as:

$$\Gamma=S_{11}=[Z_L(\omega)-Z_0]/[Z_L(\omega)+Z_0] \quad (3.6)$$

Where  $Z_0$  is the characteristic impedance of the microstrip line (without the slot), which was set to 50 Ohm by setting the width of the line.  $Z_L(\omega)$  is the input impedance of the RLC circuit, which is given by:

$$Z_L(\omega)=\frac{j\omega L}{(1-\omega^2 LC+j\omega L/R)} \quad (3.7)$$

When the RLC circuit resonates at  $\omega = \omega_0$ , then its high impedance forms a mismatch that is exhibited by an increased reflection coefficient  $S_{11}$  and a reduction in the transmission factor  $S_{21}$ . The resonance frequency is given by  $\omega_0=1/\sqrt{LC}$ , and then  $Z_L(\omega_0) = R$ . Thus, at resonance (band-reject frequency), the impedance of the RLC circuit will equal R, and the reflection coefficient will be:

$$\Gamma(\omega_0)=S_{11}(\omega_0)=\frac{R-Z_0}{Z_L+Z_0}=\frac{R-50}{R+50} \quad (3.8)$$

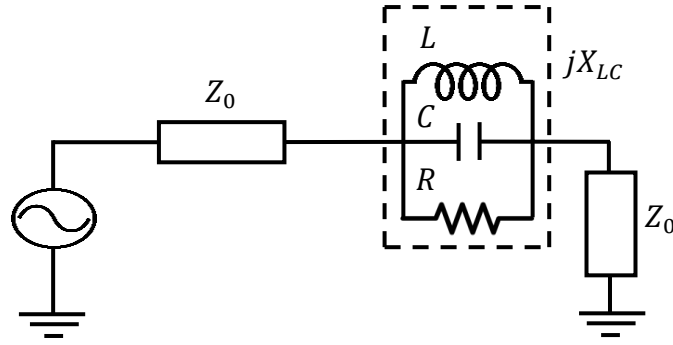


**Figure (3.3)** The equivalent circuit representation of the U-shaped slot filter using parallel RLC resonant circuit.

### 3.2.1 Analysis and Development of the U-shaped Filter

To obtain more insight into the operation of the U-shaped filter, the various sections of the slot are investigated in this section. The U-shaped slot has three sections namely, the central part, and the two side parts or legs. The frequency response of the central part (see Fig. (3.4.a)) was determined and it is shown in Fig. (3.4.b). The response shows all-pass property with a slightly decreasing transmission coefficient ( $S_{21}$ ) as the frequency is increased, which is related to the loss in the substrate. There is no resonance in the shown range of frequency, as the estimated resonance frequency by Eq. (3.4), for this length equal to approximately (2.6 mm) of the slot will be about 31 GHz.

$$f_r = \frac{3 \cdot 10^8}{2 \cdot 2.6 \cdot 10^{-3} \cdot \sqrt{3.26}} = 31.95 \text{ GHz}$$

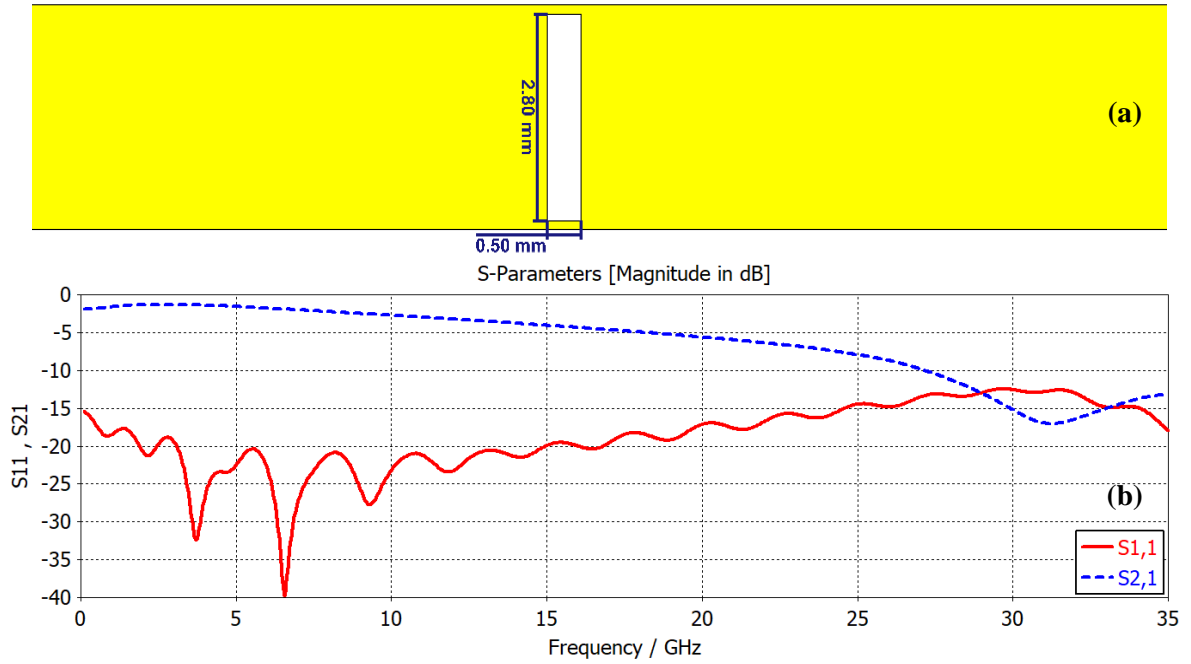


**Figure (3.4)** (a)-The geometry of the central part of the slot, (b)-frequency response.

In the next simulation, the central part was added to one of the side parts to get an L-Shaped slot as shown in Fig. (3.5.a), which has resulted in the frequency response shown in Fig. (3.5.b). The band-reject property appears at the frequency of 7.139 GHz. The calculated length of the L-shaped slot in terms of the equivalent wavelength at this frequency using Eq (3.4) is:

$$f_r = \frac{c}{2 L_s \sqrt{\epsilon_{eff}}} = \frac{3 \cdot 10^8}{2 (9.5 + 2.3) \cdot 10^{-3} \cdot \sqrt{3.26}} = 7.04 \text{ GHz}$$

This is a result very close to the frequency in Fig. (3.5.b). The effective wavelength  $\lambda_e$  at this frequency is:

$$\lambda_e = c / f_r * \sqrt{\epsilon_{eff}} = 23.6 \text{ mm}$$

Thus, the length of the filter ( $10 + 2.8 - 0.5 = 12.3$  mm) is equal to  $0.521 \lambda_e$  which is very close to the 0.5 value expected by Eq. (3.4).

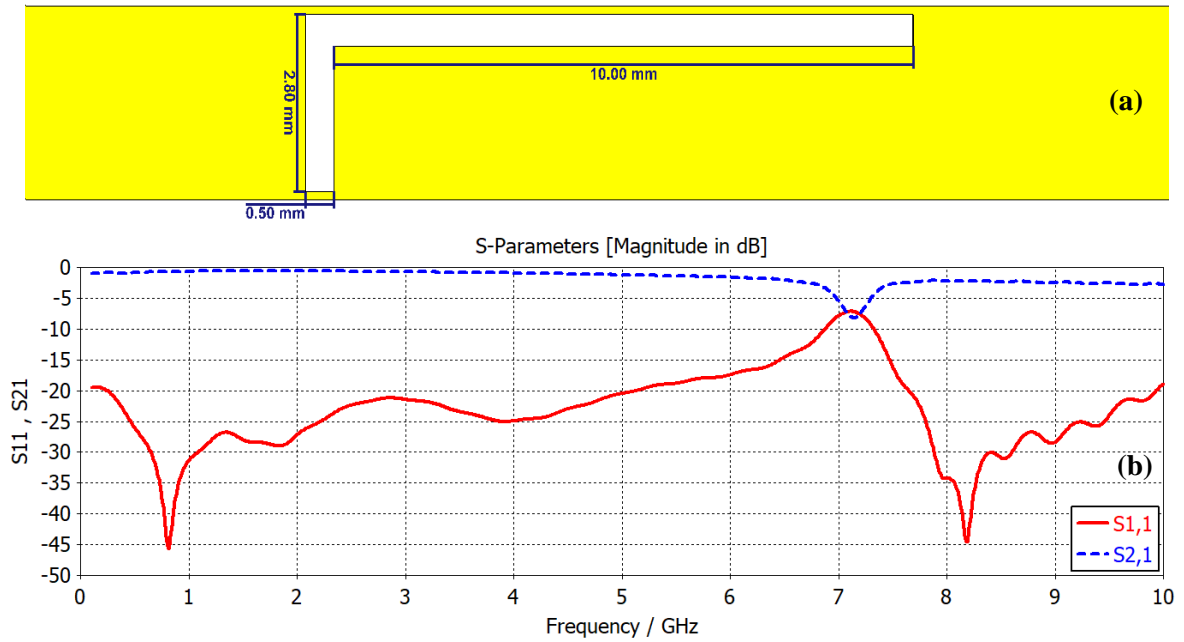


**Figure (3.5)** The geometry of the L-Shaped slot filter (a), and its frequency response (b).

In the next simulation, the two side parts of the slot were connected in a way to form a shape similar to the letter Z, as shown in Fig. (3.6.a). The obtained frequency response is shown in Fig. (3.6.b), which clearly shows the band-reject characteristics at the frequency of 4.08 GHz. At this frequency, the total length of the slot is  $0.53 \lambda_e$ , which confirms the relation between slot length and multiple halves of the effective wavelength at the band-reject frequency.

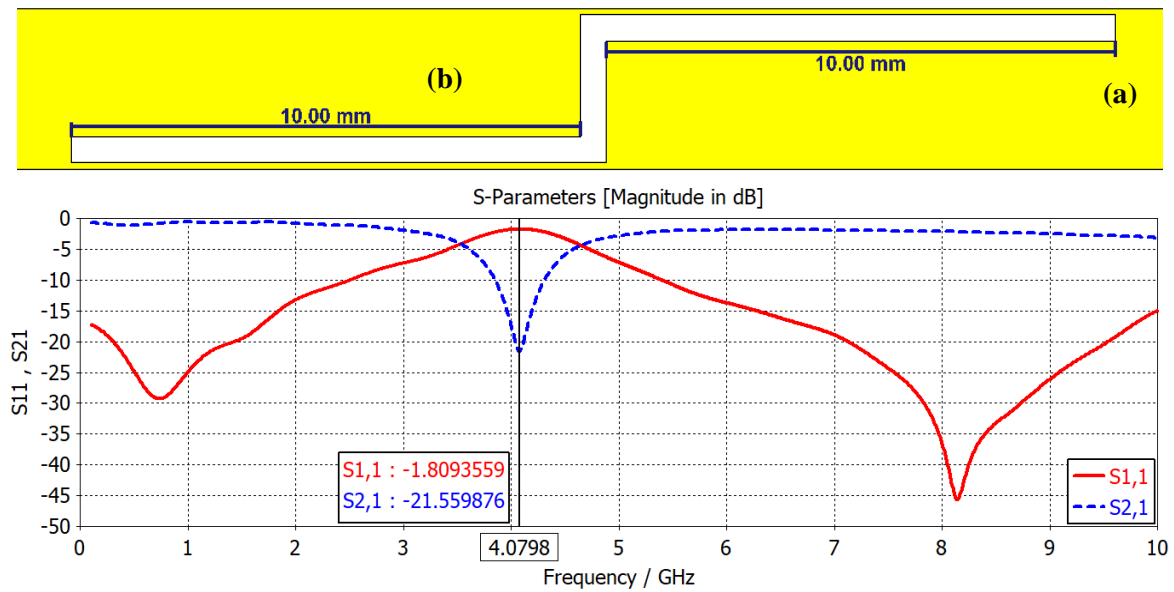


**Figure (3.6)** The geometry of the Z-Shaped slot filter (a), and its frequency response (b).

In the last simulation, the three parts of the slot were arranged into the U-shape, and the used dimensions were those used in Table (3.1). The filter behavior was examined by exploring the electric field distribution along the microstrip line and across the slot at the band-reject frequency, as well as two frequencies below and above the resonance frequency. The results obtained from the simulations are shown in Fig. (3.7). In these simulations, the input signal was applied at the left port (port-1) and a matched load was assumed at the right port (port-2). The colors indicate the strength of the electric field in units of Volt/m and dB scale. It can be seen that at the band-reject frequency there is a high concentration of the electric field at the central part of the slot, which prevents the propagation of the signal to the other port leading to very low transmission coefficient. However, away from the band-reject frequency (at 1.5 GHz, and 3.5 GHz) the electric field along the filter is much more uniform, and there is an appreciable field at the out port of the filter indicating good transmission through the filter.

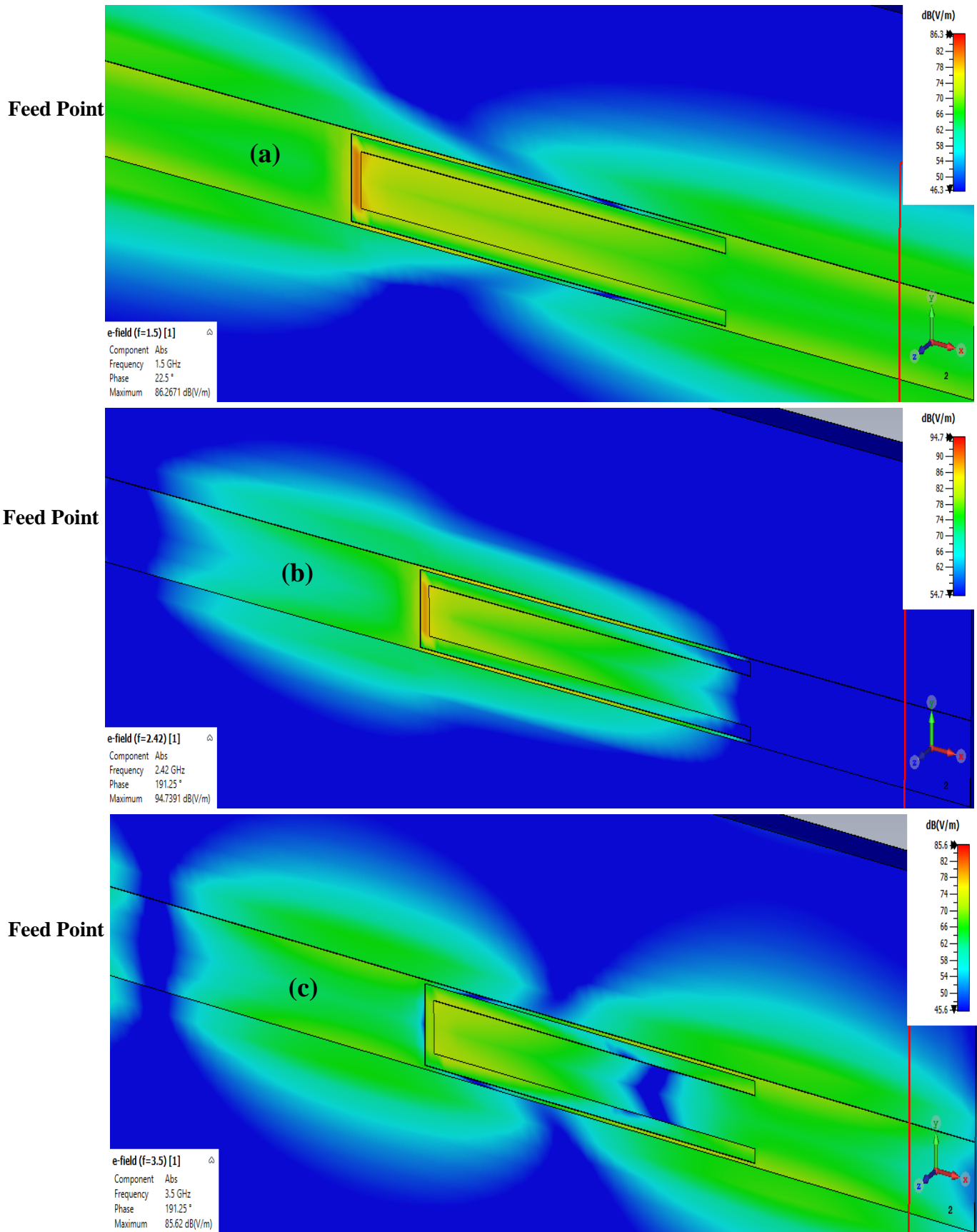


**Figure (3.7)** The distribution of the electric field around the U-Slot at; (a)  $f=1.5$  GHz, (b)  $f=2.4$  GHz, and (c)  $f=3.5$  GHz.

The next investigation of the U-Shaped slot filter shows the effect of the slot length on the band-reject frequency. The calculated scattering parameters  $S_{11}$  and  $S_{21}$  are displayed as a function of the frequency for various lengths ( $L_2$ ) of the slot, as shown in Fig. (3.8). It is evident that as the slot length ( $L_s = L_2 + W_4$ ) increases the frequency of the reject band decreases, as expected from Eqs. (3.2) and (3.4). The filter offers a band-rejection of 22 dB. At  $L_2 = 18.2$  mm, the maximum rejection occurs at a frequency of 2.42 GHz, at which the equivalent wavelength according to Eq. (3.5) is 68.65 mm, and thus the slot length is equal to  $0.54 \lambda_e$ . The figure also shows that the band-reject feature is seen again at 7.3 GHz frequency, which is about 3 times ( $N=3$ ) the resonant frequency (2.42 GHz) of the first band. In this case, the length of the slot is 1.5 the guided wavelength, as expected by Eq. (3.4).

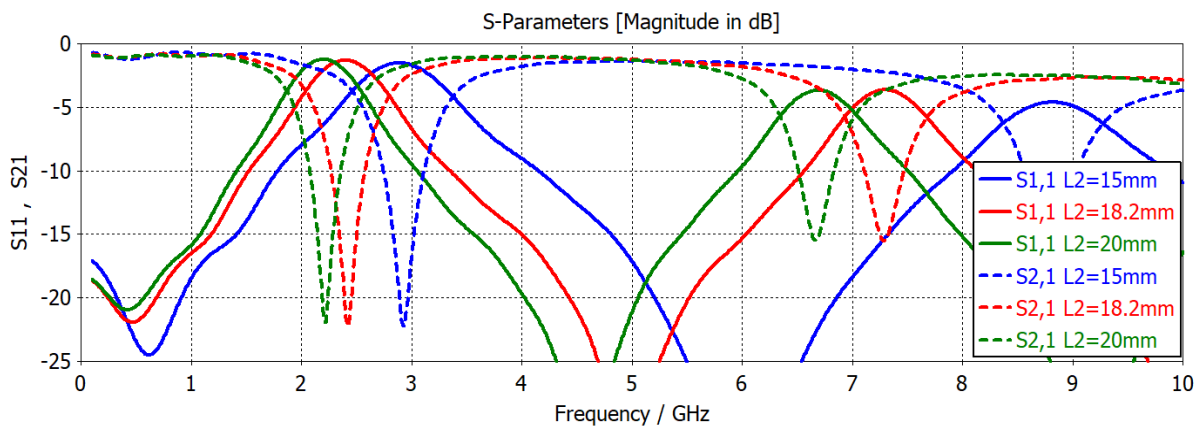


**Figure (3.8)** The S-parameters (—  $S_{11}$ ), and (---  $S_{21}$ ) of the U-slot filter for various slot lengths ( $L_2=20$ mm), ( $L_2=18.2$ mm), ( $L_2=15$ mm), ( $W_3=0.5$  mm,  $W_4 = 1.8$  mm).

### 3.3 The Reconfigurable U-Shaped Slot Filter

To achieve configurability for the filter, a PIN diode is added at the center of the U-Slot filter, and it is connected between both sides of the slot as shown in Fig. (3.9). The diode can be switched between the “ON” and “OFF” states

where it behaves as short circuit and open circuit respectively. When the PIN diode is in the “ON” state, the PIN diode behaves as a short-circuit, short-circuiting the slot at its center, or effectively dividing the U-Shaped slot into two parallel slots. The filter response is shown in Fig. (3.10). The filter shows good matching ( $S_{11} < -30$  dB) for the frequency range from 1 GHz to 4.7 GHz, while the transmission coefficient is approaching unity ( $S_{21} = -0.5$  dB) indicating full transmission of the microwave signal to the output port. The filter behavior is like an all-pass filter.

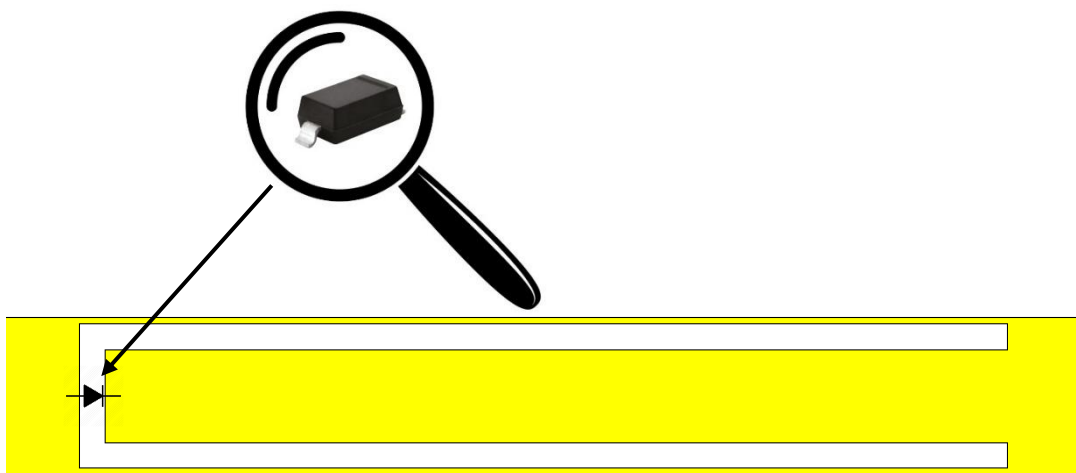


**Figure (3.9)** The geometry of the reconfigurable U-Shaped slot filter showing placement of the PIN diode.

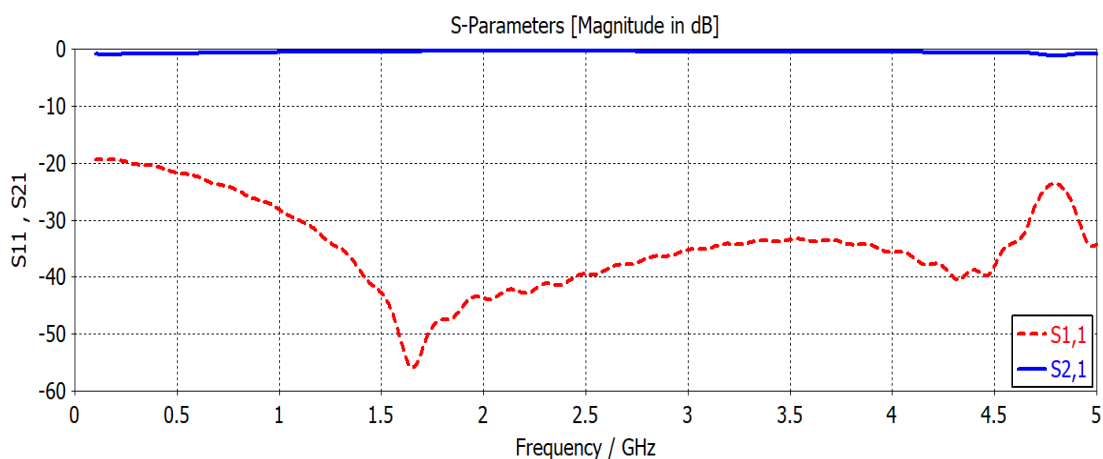


**Figure (3.10)** The simulated scattering parameters of the proposed filter, when the PIN diode is replaced by a short circuit.

The other state of the reconfigurable filter is when the diode is in the “OFF” state, which is represented here by an open-circuit. The obtained results are shown in Fig. (3.11). It is evident that the filter shows a band-reject property, with an insertion loss approaching -21.4 dB, and a reflection coefficient of -1.2 dB at the center frequency of 2.42 GHz.

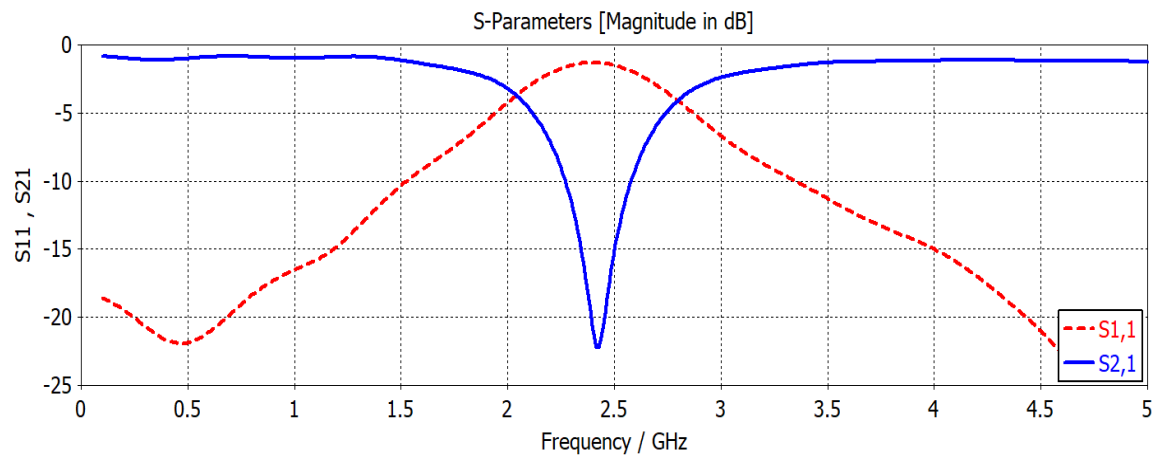


**Figure (3.11)** The simulated scattering parameters of the proposed filter, when the PIN diode is replaced by an open-circuit.

### 3.3.1 Distribution of the Electric Field in the Slot

For a better understanding of the U-shaped slot effect on the characteristics of the microstrip line, the distribution of the E-field around the slot was investigated. Fig. (3.12) shows the obtained electric field distribution at the frequency of the reject band (2.42 GHz), when the PIN diode is in the “OFF” and “ON” states. When the PIN diode is in the “OFF” state, the E-field vector inside the slot has a maximum value at the center of the slot and declines to very small values at both ends of the slot, thus representing a spatial variation of  $\frac{1}{2}$  the effective wavelength. The electric field vectors in the two legs of the slot are in opposite directions, due to the folding of the slot. The maximum value of the electric field is 54623 V/m, which is located at the center of the slot, Such a value of the electric field may seem large, but it is 54.623 V/mm.

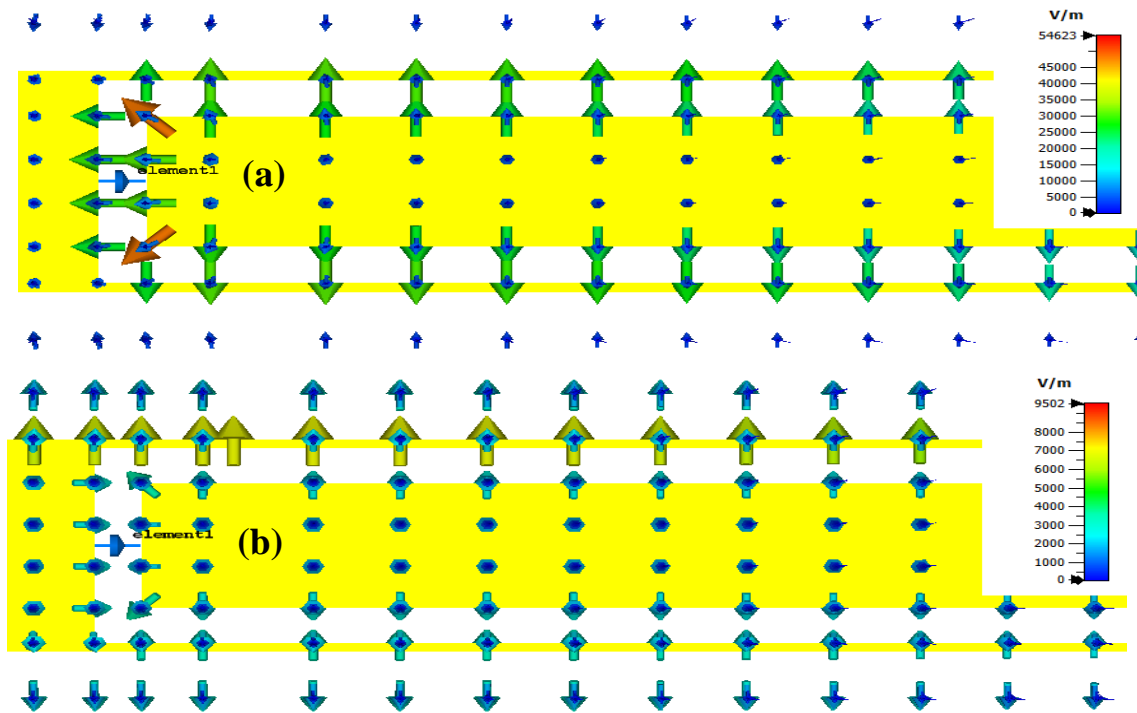


**Figure (3.12)** The distribution of the simulated E-field around the U-slot at 2.42 GHz, when (a) PIN diode in “OFF” state, and (b) PIN diode is in “ON” state.

When the PIN diode is driven into the “ON” state, the slot is then divided into two parts. As can be seen in Fig. (3.12.b), there is no resonance in each of the two parts of the slot at the frequency of 2.4 GHz. This is evident from the very low values of the electric field along the two parts of the slot, where the maximum field, in this case, is 9502 V/m, which is only (17%) of that found when the PIN diode is in the “OFF” state. As the central part is now connected to the rest of the microstrip line then transmission through the microstrip line occurs with minimal attenuation, as can be seen from Fig. (3.10), where  $S_{11} = -30$  dB, and  $S_{21} = 0.5$  dB along a wide range of frequencies.

### 3.4 Equivalent Circuit of the PIN Diode

In the examination and comparison operations that took place in the previous steps for the cases (ON and OFF), the diode in (ON state) was represented by a short circuit. Since the PIN diode has internal components such as a resistor, capacitor, and inductance, taking them into account gives more accurate results for the simulation process. The equivalent circuit of the diode can be represented in Fig (3.13) by [58]:

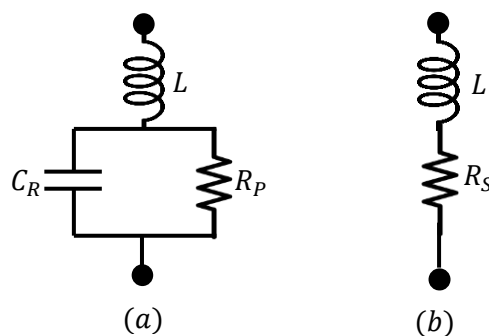


**Figure (3.13)** The equivalent circuits of the PIN diode for; (a)-the “OFF” state, and (b)-the “ON” state [58].

From the datasheet of the diode (RS-BAP51L) [59], the following parameters ( $R_s=1.5 \Omega$  at  $I_F = 10 \text{ mA}$  in the forward bias state,  $R_p=10 \text{ k}\Omega$  representing the net dissipative resistance of the diode in the reverse bias state, and  $C_R=0.3 \text{ pF}$  at  $V_R = 0 \text{ V}$  in the reverse bias state, and  $L=0.6 \text{ nH}$ ) were used in the simulation program. The (CST Microwave Studio) program provides the feature of using the diode as an equivalent circuit of lumped elements. The diode parameters such as resistance, capacitance and inductance with the design to be applied, whether it is parallel such as Fig. (3.13.a) for the off state, or serial such as Fig. (3.13.b) for the ON state were supplied to program suite. Fig. (3.14) shows the simulation results for the reflection and transmission coefficients for the two states of “ON” and “OFF”. The results in Fig. (3.14.a) show that the transmission coefficient varies between -0.5 dB and -21.4 dB at

the two states of “ON” and “OFF” respectively. The results of Fig. (3.14.b) shows that the reflection coefficient  $S_{11}$  varies between  $< -40$  dB and  $-1.5$  dB at the two states of “ON” and “OFF” respectively. the transmission coefficient  $S_{21}$  varies between  $-21$  dB and  $-2$  dB for the the “ON” and “OFF” states, respectively.

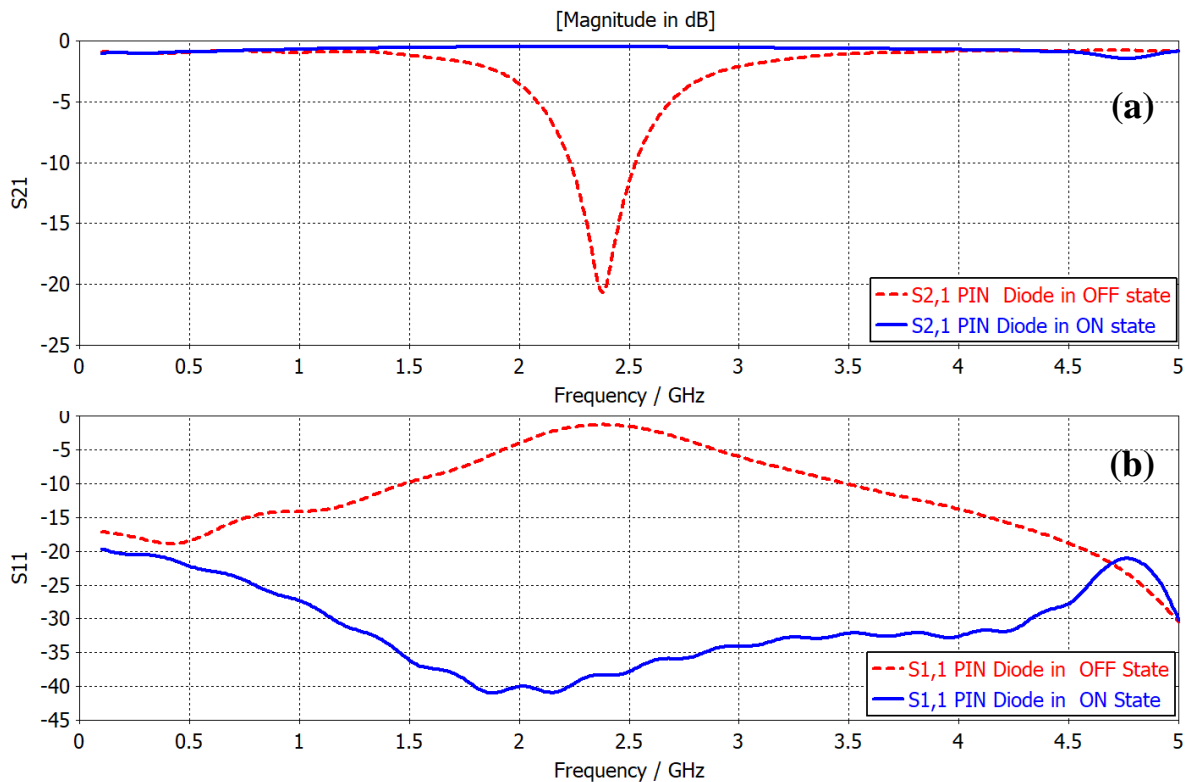


**Figure (3.14)** Simulated S-Parameters of the proposed filter, when the PIN diode is represented by its equivalent circuit.  
(a)- The transmission coefficient, (b)- The reflection coefficient.

Figure (3.15) shows a comparison between the obtained results when using the real diode represented by the equivalent circuit according to Fig. (3.13), and the ideal diode represented by the (open, short) cases. The comparison shows that the performance is very close in the case of (All-pass) as seen in Fig. (3.15.a), while there is a very small difference in the resonance frequency in the case of (band-reject), see Fig. (3.15.b). The reason for that can be attributed to the fact that the “open-circuit” representation ignores the

capacitance. However, the equivalent circuit takes the capacitor into consideration, and thus the added capacitance affects the value of the resonance frequency.

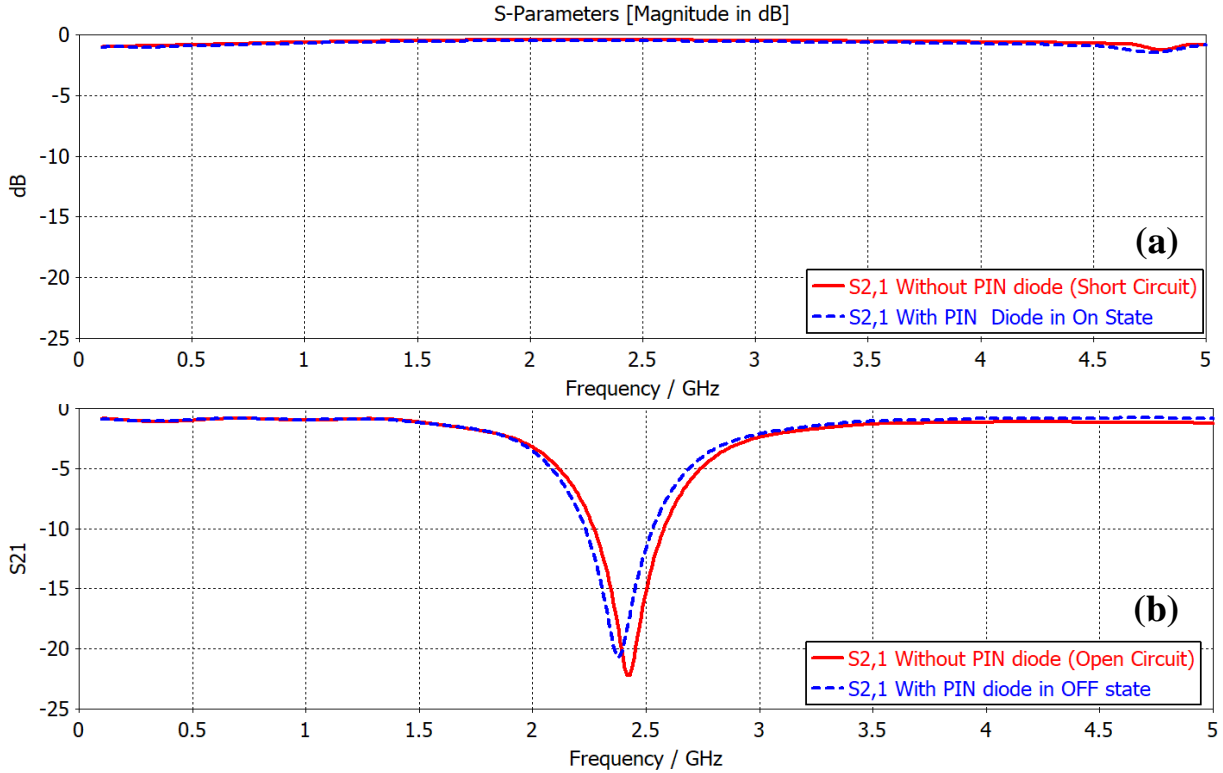


**Figure (3.15)** Variation of the transmission coefficient with frequency, for the two cases when the diode was represented by an ideal switch, and by an equivalent circuit. (a)- ON state “All-pass”, (b)- OFF state “Band reject”.

### 3.5 Experimental Validation of The Proposed Filter

In order to verify the proposed design, two microstrip filters were fabricated, Using FR4 substrate as shown in Fig. (3.16). The prototypes were; a U-Shaped slot reconfigurable filter in the band-reject state and U-Shaped slot reconfigurable filter in the all-pass state. For the experimental realization of the PIN diode, a shorting strip at the center of the slot was soldered. A vector network analyzer (VNA) made by Rohde and Schwarz (Model ZVL13) was used to test the filters by measuring the scattering parameters of the two

prototypes. The acquired data from the VNA were represented by (201) data points in magnitude and phase at evenly distributed frequencies in the selected frequency range. The data were then transported to MATLAB code for plotting the frequency response of the S-parameters.

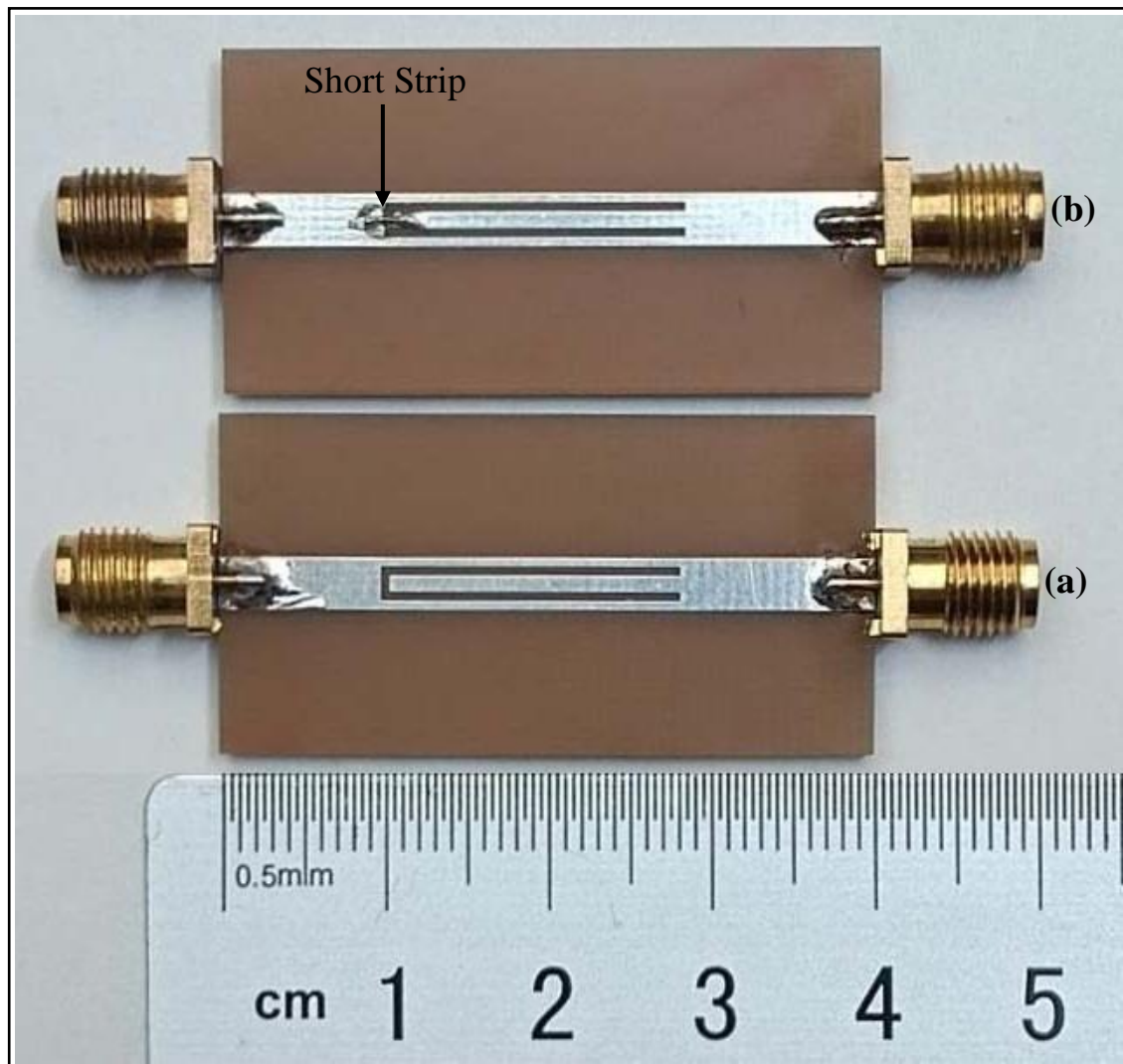


**Figure (3.16)** Photograph of the fabricated prototypes.

- (a)- U-slot reconfigurable filter in the band-reject state,
- (b)- the same filter in the all-pass state.

Figure (3.17), shows the measured results for the transmission coefficient  $S_{21}$  of the proposed filter compared with the simulation results when the PIN diode is in the “OFF” state. This case was implemented practically by an “open

circuit” (without the diode). The response shows a band-reject property insertion loss of 14 dB, and about 24 dB for the simulation results. The simulated results for the reflection coefficient show a value of -3.6 dB, thus complementing the band-reject properties.

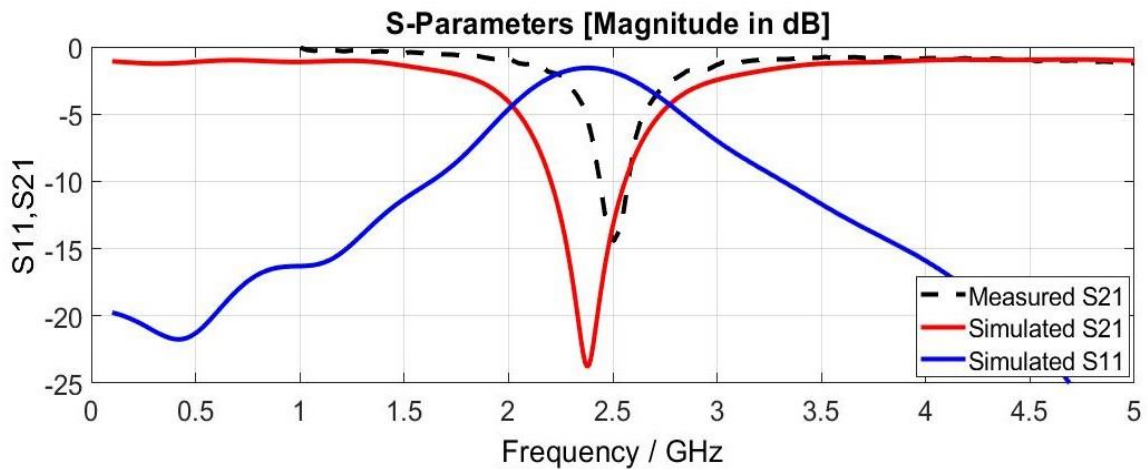


**Figure (3.17)** Measured and simulated reflection and transmission coefficients of the prototype filter, (PIN diode is in “OFF” state).

Figure (3.18) compares the measured and simulated results for the transmission coefficient  $S_{21}$  of the proposed filter when the PIN diode is in the “ON” state. This state was implemented by connecting a strip “short circuit” in place of the PIN diode. It can be seen that the filter shows a high transmission coefficient of about -1 dB indicating all-pass behavior for a wide range of frequencies. Fig. (3.18) also shows a very good matching ( $S_{11}$  better than -40 dB) for the passband.

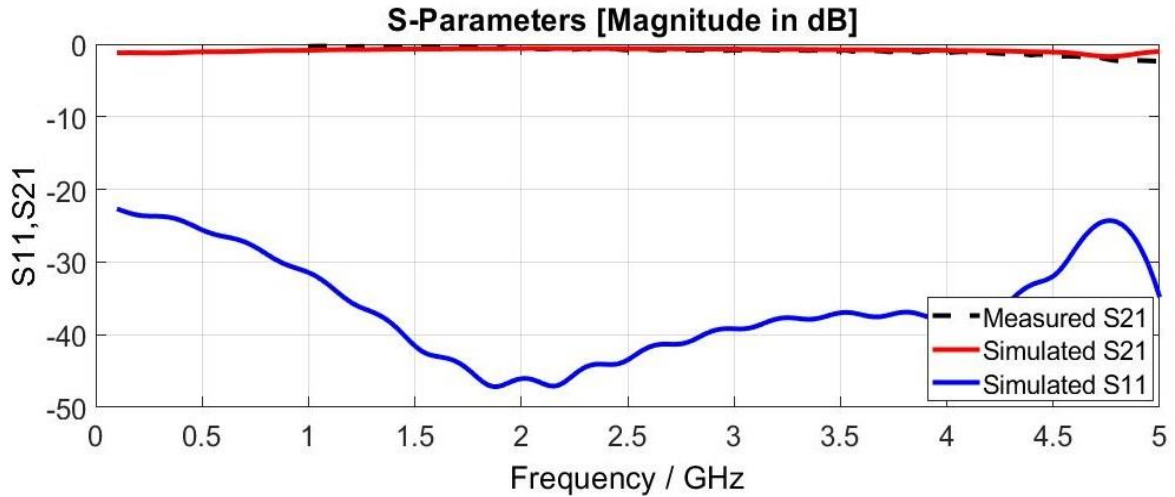


**Figure (3.18)** Measured and simulated reflection and transmission coefficients of the prototype filter, (PIN diode is in the “ON” state).

### 3.6 Comparison with Other Works

Table (3.3) shows a comparison of the filter parameters and characteristics with other designs for reconfigurable filters that operate at similar or near frequencies. The filter dimensions were also given in terms of the guided wavelength  $\lambda_e$  at the center frequency to make a fair comparison of size. Regarding the size of the filters in terms of  $\lambda_e$ , the proposed filter stands at 3rd place after those presented in [60] and [63] among the listed designs. The designs presented in [8,13,19,23,27], and [64] have placed the slots (U-shaped, V-shaped, and rings) in the ground plane, where any leakage from the slots will interfere with circuits at the other side of the ground plane. In the proposed design and in [36], the two sides of the ground plane are isolated as there is no opening or defects in the ground plane. The high rejection values of the filters in [63] and [62] are results of using two, and four cascaded resonators respectively, while in [36] and this work a single resonator was used. As compared to the filter in [36], the proposed filter has a smaller size, and yet it offers configurability between band-reject and all-pass states. Moreover, as shown in section (3.2), the proposed filter has achieved a band rejection of -22.2 dB compared to -15 dB that was achieved in [36]. While few

filters in the Table show better rejection, the proposed filter is compact and of easier design.

**Table (3.3)** A Comparison Between the Filter Parameters and Characteristics with Other Designs.

Ref	Band Freq. GHz	Dimensions mm	$\epsilon_r/\tan\delta$	Dimensions $\lambda_e * \lambda_e$	$S_{11}$ dB	$S_{21}$ dB	Resonant element	Re-configurability
[63]	3.52 5.2	17*17 17*17	4.3/0.025	0.36 * 0.36 0.53 * 0.53		-43 -28	2 <sup>nd</sup> order	Band switching from 3.52 GHz to 5.2 GHz
[64]	2.37	90*60	4.3/_	1.28*0.85		-17	1 <sup>st</sup> order	Tunable bandstop using varactor diode
[60]	1.3	50*25	3.05/_	0.33*0.16	-2	-15	1 <sup>st</sup> order	Tunable bandstop using varactor diode
[54]	2.5	79.4*45	2/_	0.86*0.49	-3	-52	2 <sup>nd</sup> order	BSF to BPF Using Liquid metal alloy switch
[61]	3.5	63*20	4.7/_	1.38*0.44	-2	-20	2 <sup>nd</sup> order	Bandstop To All-pass
[62]	26.4 26.4	44*30 33*30	2.2/_	4.4 * 3 3.3 * 3	-2.4	-39.4	2 <sup>nd</sup> order	Bandstop to all-pass using PIN diode
[36]	2.45	60*20	4.4/0.025	0.9*0.3	-3.34	-13.5	1 <sup>st</sup> order	Stopband Non Reconfigurable
<b>This work</b>	2.45	40*20	4.4/0.025	0.6*0.3	-3	-13	1 <sup>st</sup> order	Bandstop to All-pass

# **CHAPTER FOUR**

## **DEVELOPMENT OF THE U-SLOT FILTER**

### **FOR BAND EXTENSION AND**

### **RECONFIGURATION**

#### **4.1 Introduction**

In the previous chapter, the choice was concentrated on changing the nature of filtration, where a band-reject filter was reconfigured to be an all-pass filter. The switching was implemented by using one PIN diode. In this chapter, other construction will be proposed and investigated. These are:

1. The proposed configuration with one/two opened slots. Here the U-Shaped slot is divided into two slots, where each one can have an opening at one of its ends.
2. The meandered slot, where the U-Shaped slot is unfolded, and meandered to improve the performance. Openings at the slot ends are deployed to initiate the configurability.
3. Few ideas are presented aiming to extend the bandwidth of the filter.

#### **4.2 A Bandwidth Reconfigurable Filter**

In chapter 3, the proposed reconfigurable filter offered a switching between band-reject and all-pass states. There are applications where it is needed to change the bandwidth of the filter so as to the band of the desired signal. This section presents a reconfigurable filter whose bandwidth can be changed between two values. The main shape of the filter is developed from the U-Shaped slot by splitting the folded slot into two parallel slots, and then placing an opening at the end of one of the resulting slots, as shown in Fig. (4.1.a).

This design was simulated using the dimensions shown in Fig. (4.1.a), using FR4 substrate, and the obtained response is shown in Fig. (4.1.b). The filter shows a band-reject property and has a -17.7 dB transmission coefficient, and a 1.5 dB reflection coefficient at a resonant frequency of 2.4 GHz. The -10 dB bandwidth is 0.14 GHz (5.8%). Recalling Eq. (3.3), it can be shown that the effective dielectric constant is 3.26, and thus the effective wavelength is 69.2mm at the frequency of 2.4 GHz. The open slot operates as a  $\frac{1}{4}$  wavelength resonator, as the length of the open slot 17.7 mm is equal to  $0.25 \lambda_e$  at the rejection frequency of 2.4 GHz. For the wave inside the open slot, the right side of the slot behaves as a short-circuit, while the open-circuit condition is realized at the frequency where the length equals  $\frac{1}{4}$  wavelength.

The other feature that is noticed in Fig. (4.1) is that the band-reject property is repeated at the frequency of 7.2 GHz, which is almost three times that at the lower band of 2.43GHz. This is attributed to the 3<sup>rd</sup> order resonance of the slot, where the slot length of 18 mm is equal to 1.5 the effective wavelength at the upper band, where  $\lambda_e = 23$  mm. The performance of the upper band as regards to the values of the reflection and transmission coefficients are lower than those of the lower band. It can also be noticed from Fig. (4.1.b) that there is a wide pass-band in between the two reject bands.

Now, if the other slot is opened at one of its ends, and its length is slightly different from the other slot, then the resulting two resonance frequencies, will lead to a band-rejection of a wider band. This idea was realized in the design shown in Fig. (4.2.a), which was simulated, and gave the frequency response shown in Fig. (4.2.b). It can be seen from the figure that this filter has a -10 dB bandwidth of 0.57 GHz, as compared to the former one Fig. (4.1.b) which has a 0.14 GHz bandwidth. The reflection coefficient at the midband is lower than -2.1 dB, and the transmission coefficient is from -12.7 to -20 dB.

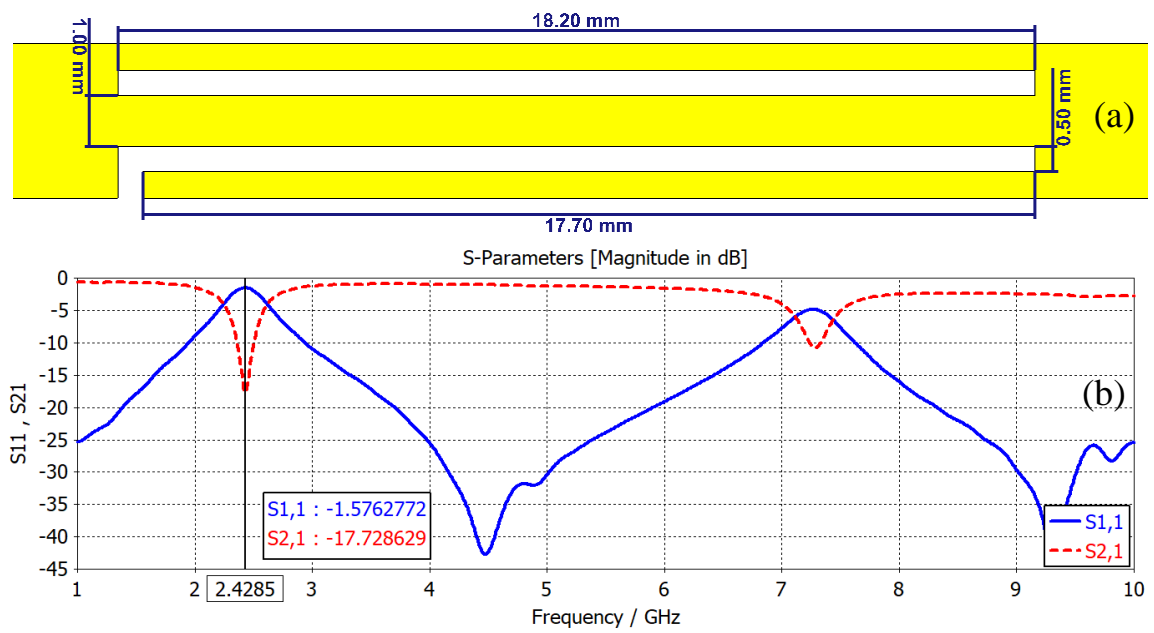


**Figure (4.1)** (a)-proposed filter with one opened slot, (b)-Variation of the scattering parameters with frequency

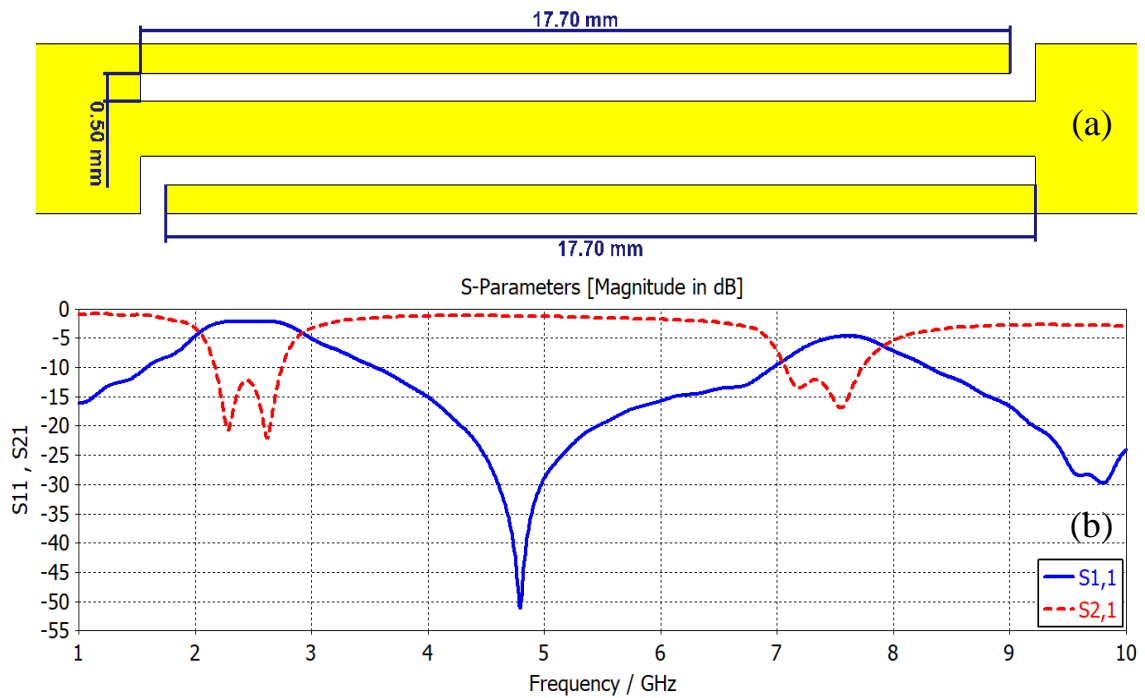


**Figure (4.2)** (a)-proposed filter with two opened slots, (b)-Variation of the scattering parameters with frequency

The idea of controlling the bandwidth by inserting a diode in one of the slots at the opening of the slot is presented in Fig. (4.2.a). When the diode is switched into the ON state, the filter will behave as a one-open slot as in Fig. (4.1.a), and the frequency response will appear as shown in Fig. (4.1.b). However, when the diode is placed in the OFF state, the filter will behave as shown in Fig. (4.2.a), and the frequency response will appear as shown in Fig. (4.2.b), Fig. (4.3) shows that the proposed reconfigurable filter can switch the bandwidth from 140 MHz to 570 MHz by simple control of one PIN diode.

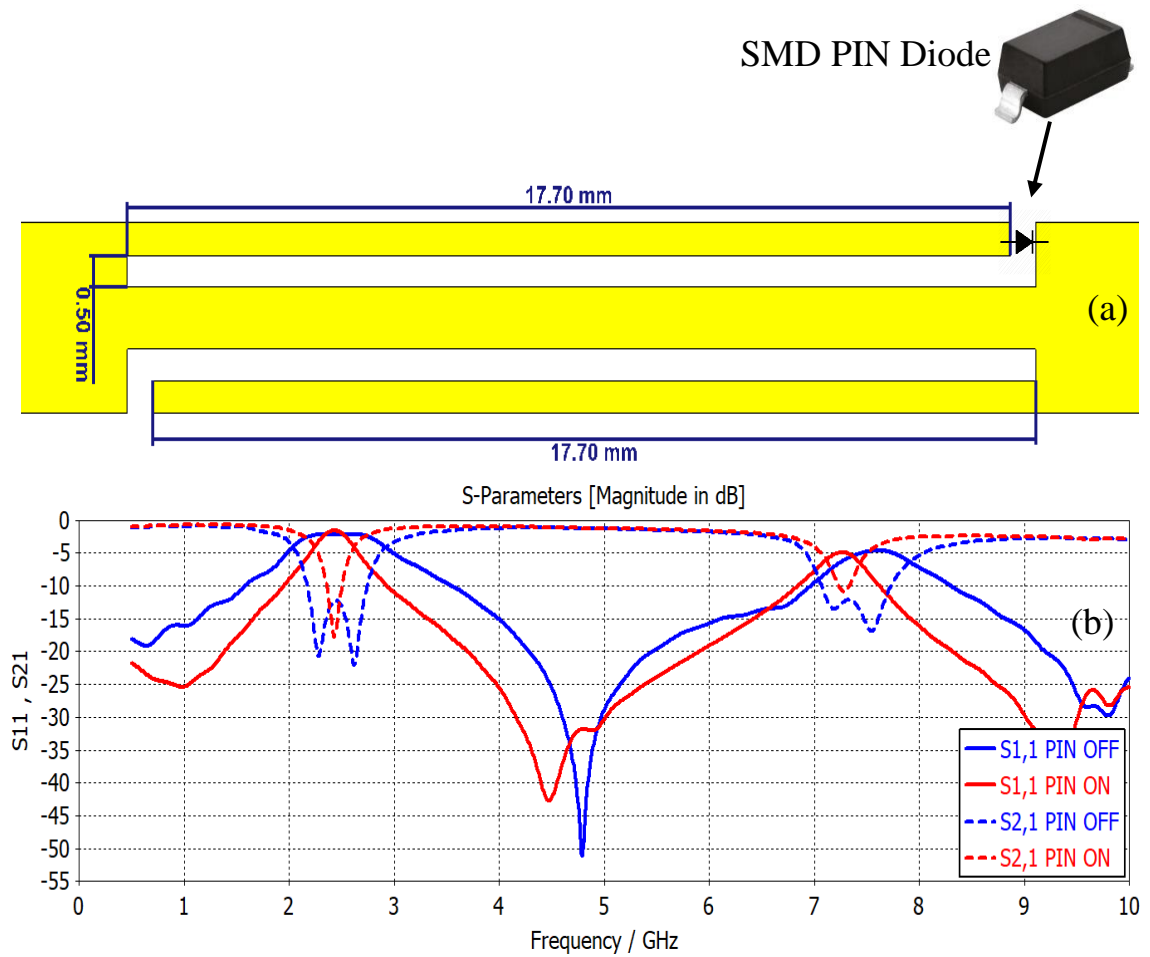


**Figure (4.3)** (a)-proposed filter when the PIN diode is switched from “ON” to “OFF” states, (b)-Variation of the scattering parameters with frequency

For the purpose of understanding the effect of the open slot length on the resonant frequency and bandwidth, Fig. (4.4) shows a comparison of the frequency response for three design cases in which the length of the open slot ( $L$ ) was changed, while Table (4.1) shows all details for each case.

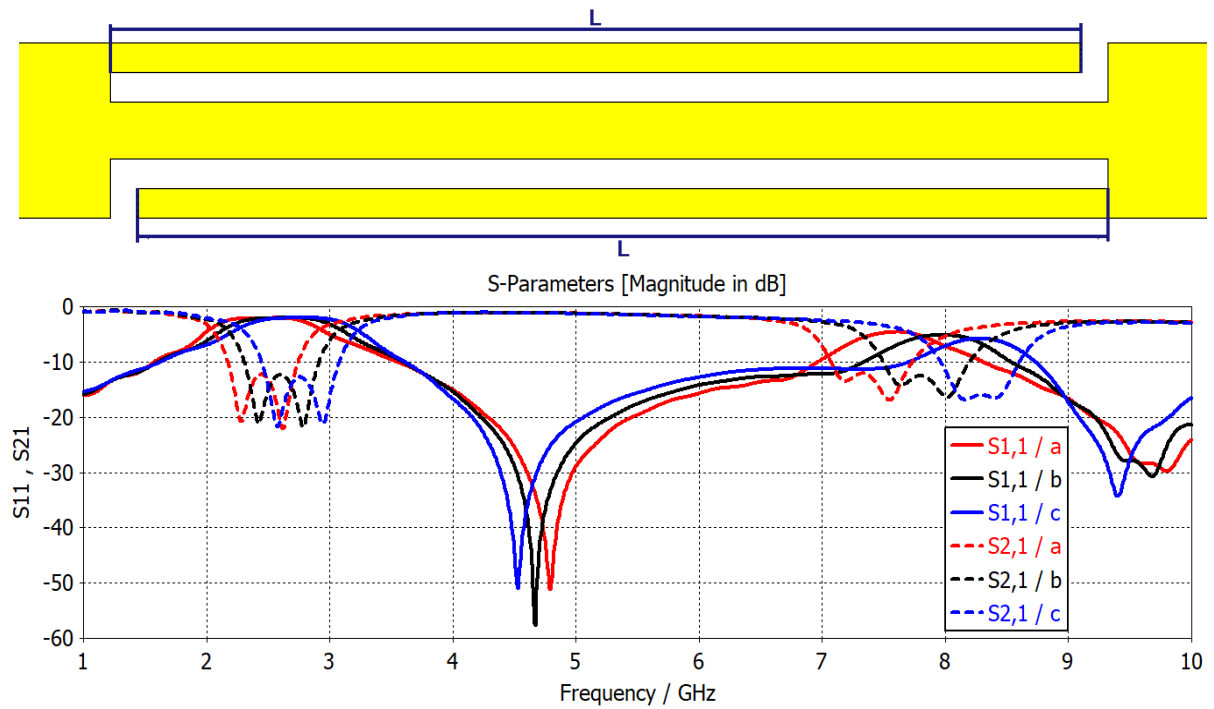


**Figure (4.4)** Variation of the scattering parameters with frequency for various lengths (L)

<b>Table (4.1)</b> Parameters and Characteristics of the Three Designed Filters					
Design	$L_{mm}$	Center Frequency in GHz	$\lambda_{emm}$	Bandwidth in GHz	$\frac{Slot\ length}{\lambda_e}$
a	17.7	2.44	68	0.57	0.26
b	16.7	2.60	63	0.6	0.265
c	15.7	2.75	60	0.63	0.261

### 4.3 The Meandered Slot Filter

In this section, the U-shaped reconfigurable filter that was proposed and presented in chapter 3 is further developed, by meandering the slot along the microstrip line. This change in the construction is illustrated in Fig. (4.5.b), where the sides (legs) of the U-Shaped slot were diverted to be on both sides of a central part. In this new arrangement, there are two openings in the slot, and thus can give more degree of freedom to obtain various designs as it is shown in the following sections. The main idea in the proposed designs in the following sections is to change the dimensions of various parts of the meandered slot or to place the PIN diode at certain positions to achieve the desired performance.

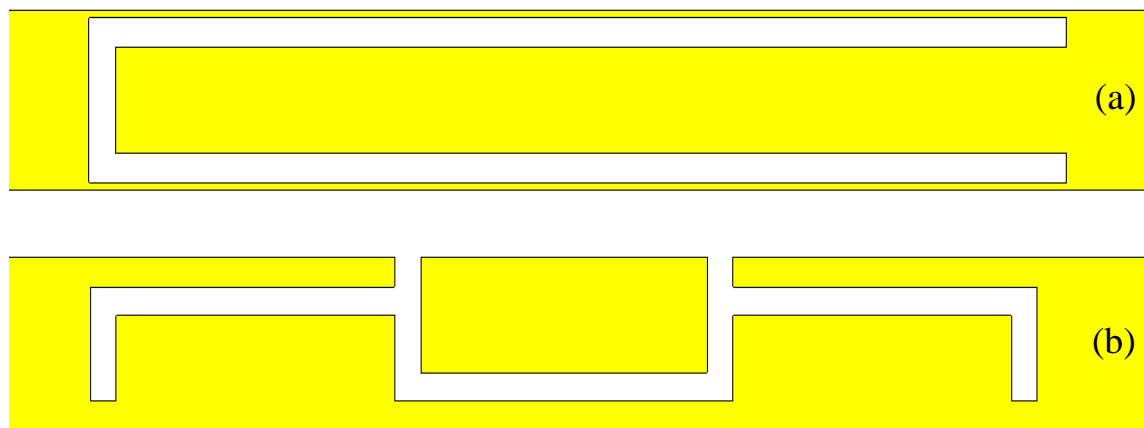


**Figure (4.5)** The development of the U-Shaped filter (a) into meandered slot filter (b)

#### 4.3.1 Bandwidth Extension

One design for the general shape, which is shown in Fig. (4.5.b), is the one with the dimensions that is shown in Fig. (4.6.a). The variation of the scattering parameters  $S_{11}$  and  $S_{21}$  with the frequency is shown in Fig. (4.6.b) for various values of the side portions of the meandered slot (L-slot). It can be seen that for each value of the length of the L-slot, the filter shows a band-

reject property (large  $S_{11}$  value and small  $S_{21}$  value) at a certain frequency. The frequency of the rejection decreases as the length of the L-slot is increased.

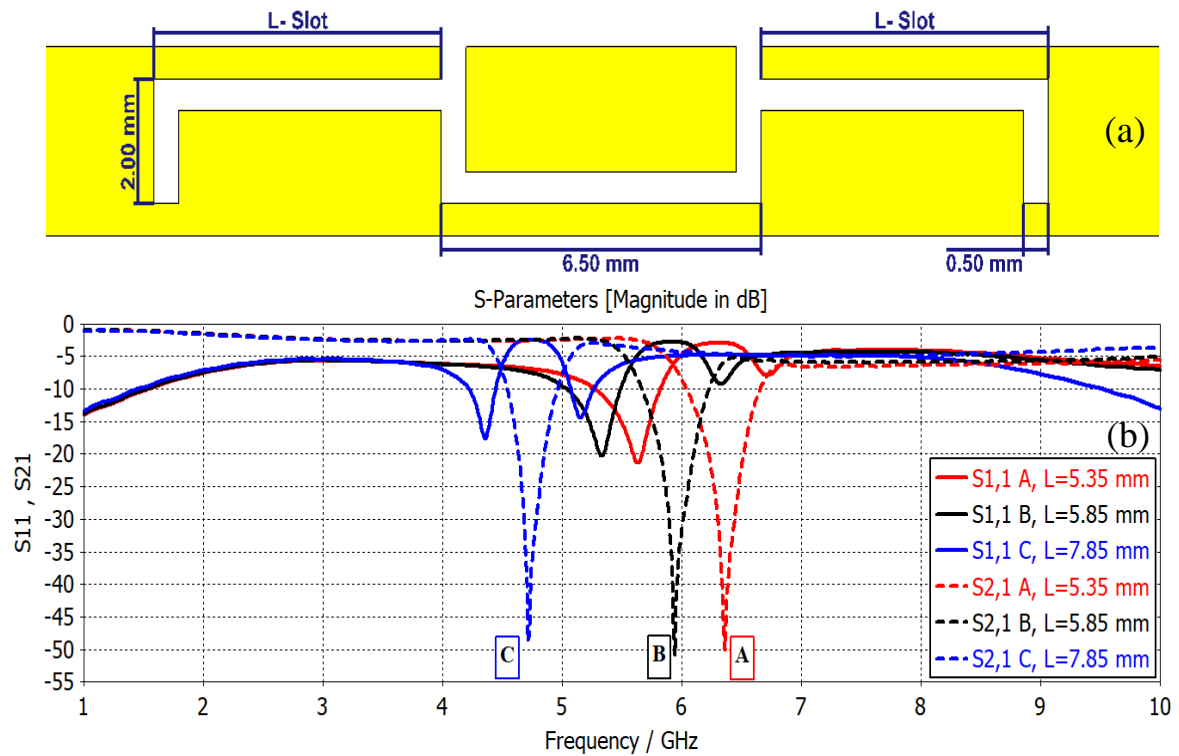


**Figure (4.6)** Variation of the scattering parameters with the frequency of the meandered slot for various lengths  $L$

The length of each of the left and right slots is almost equal to  $0.25\lambda_e$  (error in the estimation is  $<2.4\%$ ). This means that each slot is behaving like an open-ended quarter-wavelength transmission line resonator. Thus, the notch frequency (band-reject frequency) can be chosen by setting the slot length to the proper value.

The length of the slot "Ls" should be set to:

$$LS = \frac{C}{4 f_r \sqrt{\epsilon_e}} = \frac{\lambda_r}{4\sqrt{\epsilon_e}} = \frac{\lambda_e}{4} . \quad , \left( \lambda_r = \frac{C}{f_r} , \lambda_e = \frac{\lambda_r}{\sqrt{\epsilon_e}} \right) .$$

Table (4.2) shows the characteristics of the filter for various values of the L-slot length when the central section is kept at a length of 10 mm.

<b>Table (4.2)</b> Characteristics of the Meandered-slot Filter for Various Values of L, (Length of the center slot $\approx 10$ mm)						
Case	$L_{mm}$	Left slot (mm)	Right slot (mm)	Frequency (GHz)	$\lambda_e$ (mm)	$\frac{Slot\ length}{\lambda_e}$
A	5.35	$5.35+2-1 = 6.35$	$5.35+2-1 = 6.35$	6.356	26.4	0.24
B	5.85	$5.85+2-1 = 6.85$	$5.85+2-1 = 6.85$	5.941	27.96	0.245
C	7.85	$7.85+2-1 = 8.85$	$7.85+2-1 = 8.85$	4.713	35.25	0.251

It can be verified through the relationship below:

$$Length\ ratio = \frac{C\ slot\ length}{A\ slot\ length} = \frac{8.85}{6.35} = 1.39$$

$$Inverse\ of\ frequency\ ratio = \frac{A\ reject\ frequency}{C\ reject\ frequency} = \frac{6.356}{4.713} = 1.35$$

$Length\ ratio \approx Inverse\ of\ frequency\ ratio$ , proportionality is almost true.

Based on the a fore mentioned discussion, and since the length of each slot represents an independent resonator with a length approximately equal to  $\frac{1}{4}$  of the wavelength, changing the length of one of them will lead to the appearance of another resonant frequency (Reject Frequency) proportional to the change in the slot length after the change. From this, we conclude that a slight change in the length of one of the slots will lead to the emergence of a resonant frequency close to the basic resonant frequency and can be considered an increase in the frequency band of the total resonant frequency.

Figure (4.7) shows the frequency response of the filter when the side sections have unequal lengths of 5.35 mm and 5.85 mm. It can be seen that the two expected resonance frequencies corresponding to the two lengths are so close to each other, and a wide reject band has been achieved. The -10 dB bandwidth is 0.75 GHz, and the transmission coefficient goes down to lower than -18 dB.

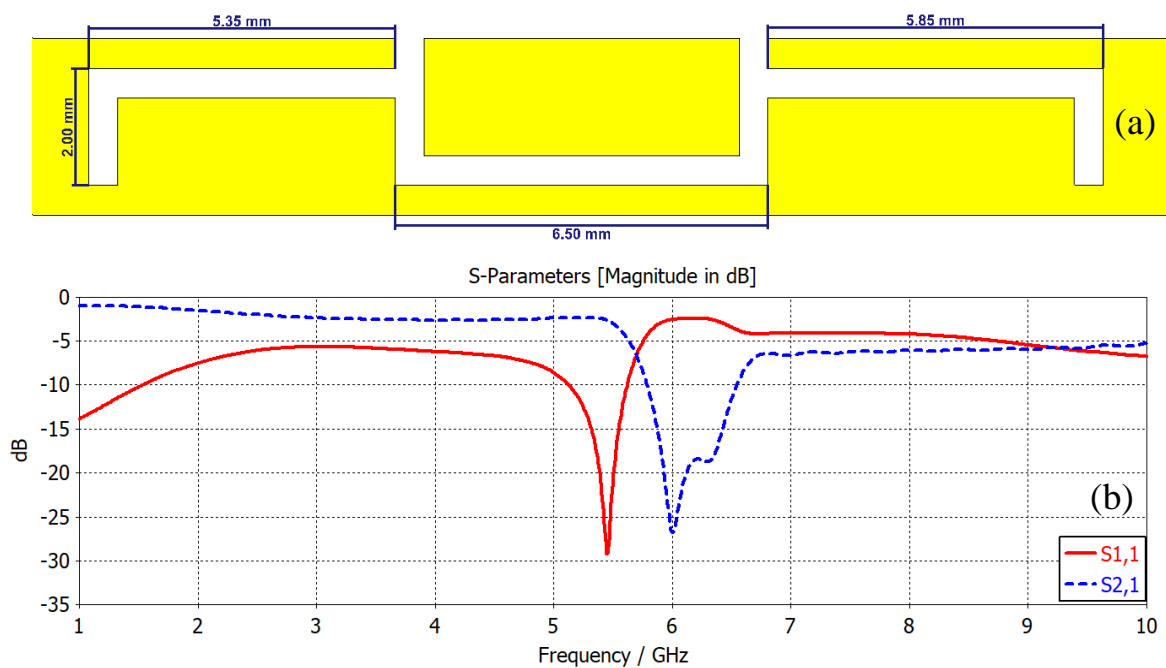


**Figure (4.7)** (a)-meandered slot filter has unequal lengths, (b)- frequency response of the filter

To get advantage of this feature in designing a filter whose bandwidth can be changed, a PIN diode can be placed in the position indicated in Fig. (4.8.a). When the PIN diode is in the OFF state, the filter works in its basic form by design, as the PIN diode will essentially not affect the filter. When the PIN diode is converted to the ON state, it will cancel the effect of the 2 mm vertical part of the slot, and thus the total slot length will change and turn from an L shape to a horizontal slot. This will lead to a change in the frequency response

of the filter that is manifested in an increase in the bandwidth as shown in Fig (4.8.b).

Figure (4.8) also explains the mechanism of action of the filter designed at a 5.8 GHz resonance frequency and commonly used in Wi-Fi applications, which necessitated that the length of the horizontal slit is 6 mm for both sides. An equivalent circuit of the RS-BAP51L PIN diode was added to the filter in the region indicated in Fig. (4.8.a). The results showed a bandwidth equal to 0.54 GHz when the diode is in the OFF state, while the bandwidth is 0.76 GHz when the diode is switched to the ON state. Table (4.3) shows all details for each case.

The relation between the length of each slot and the effective wavelength in the above results is that;

slot length =  $\left(\frac{1}{4}\right)$  effective wavelength “ $\lambda_e$ ”.

This shows that a slot is behaving like an open-ended quarter-wavelength transmission line resonator. Thus, the notch frequency (band-reject frequency), and the width of the reject-band can be chosen by setting the slot length to the proper value employing the following relations.

$$\text{Slot length } L_s = \frac{C}{4 f_r \sqrt{\epsilon_e}} = \frac{\lambda_r}{4 \sqrt{\epsilon_e}} = \frac{\lambda_e}{4} . \quad \left( \lambda_r = \frac{C}{f_r} , \lambda_e = \frac{\lambda_r}{\sqrt{\epsilon_e}} \right)$$

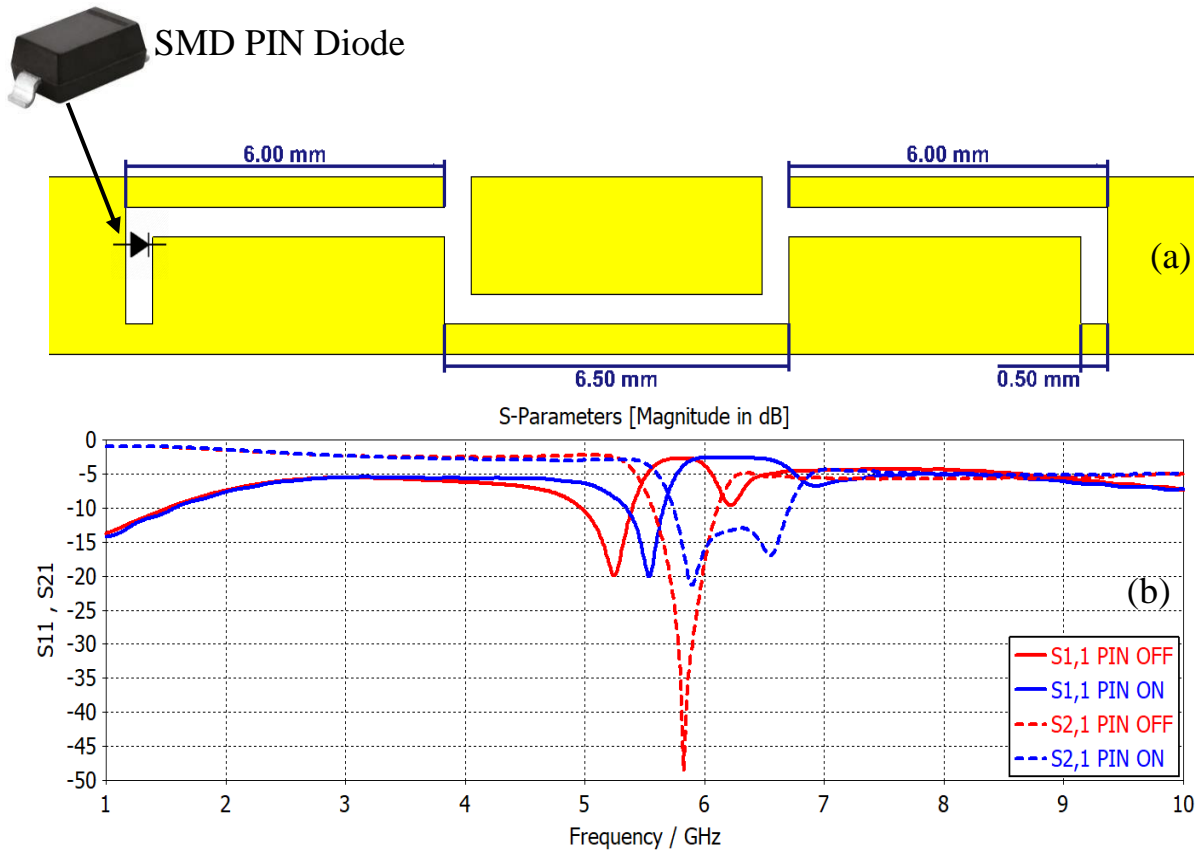


**Figure (4.8)** (a)- The proposed filter geometry showing the PIN diode, (b)- frequency response for both states (ON and OFF) of the diode

**Table (4.3)** The Filter Characteristics When the PIN Diode is in “ON” and “OFF” States. Length of the Center Slot  $\approx 10$  mm

PIN State	Left slot				Right slot				$\frac{F_1}{F_2}$	$\frac{R \text{ slot length}}{L \text{ slot length}}$
	Length (mm)	$F_1$ (GHz)	$\lambda_{e1}$ (mm)	$\frac{Slot \ length}{\lambda_e}$	Length (mm)	$F_2$ (GHz)	$\lambda_{e2}$	$\frac{Slot \ length}{\lambda_e}$		
OFF	$6+2-1=7$	5.82	28.5	0.245	$6+2-1=7$	5.82	28.5	0.245	1	$7/7=1$
ON	6	6.2	26.8	0.223	$6+2-1=7$	5.95	27.9	0.261	1.04	$7/6=1.1$

#### 4.4 Analysis of The Meandered Slot Reconfigurable Band-Reject Filter

The proposed design of the meandered slot filter can also be used as a reconfigurable filter with two or more options according to the number of switches used. The meandered filter design as shown in Fig. (4.9.a), was simulated and the obtained frequency response is shown in Fig. (4.9.b). The response shows a band-reject property at the frequency of 5.8 GHz when the length of the legs is 6 mm. This frequency is used in the Wi-Fi band.

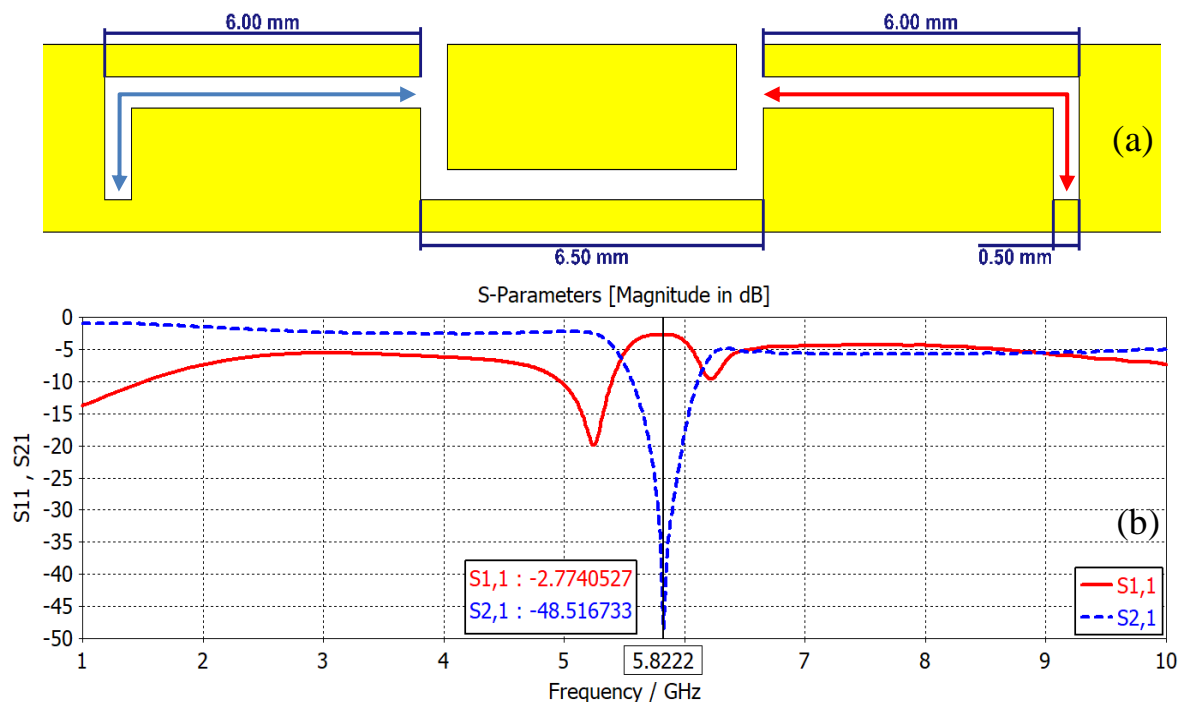


**Figure (4.9)** (a)- Filter geometry in normal mode, (b)- frequency response

When adding a connecting switch “short circuit” at the point indicated in Fig. (4.10.a), the left opening in the slot will be closed and the length of the left leg will change from 6 mm up to approximately 17 mm. This change in length will lead to the appearance of another resonant frequency, as can be noticed from the frequency response shown in Fig. (4.10.b). The new

frequency is 2.46 GHz, which is lower than the former one (5.8 GHz), as the new length is larger.

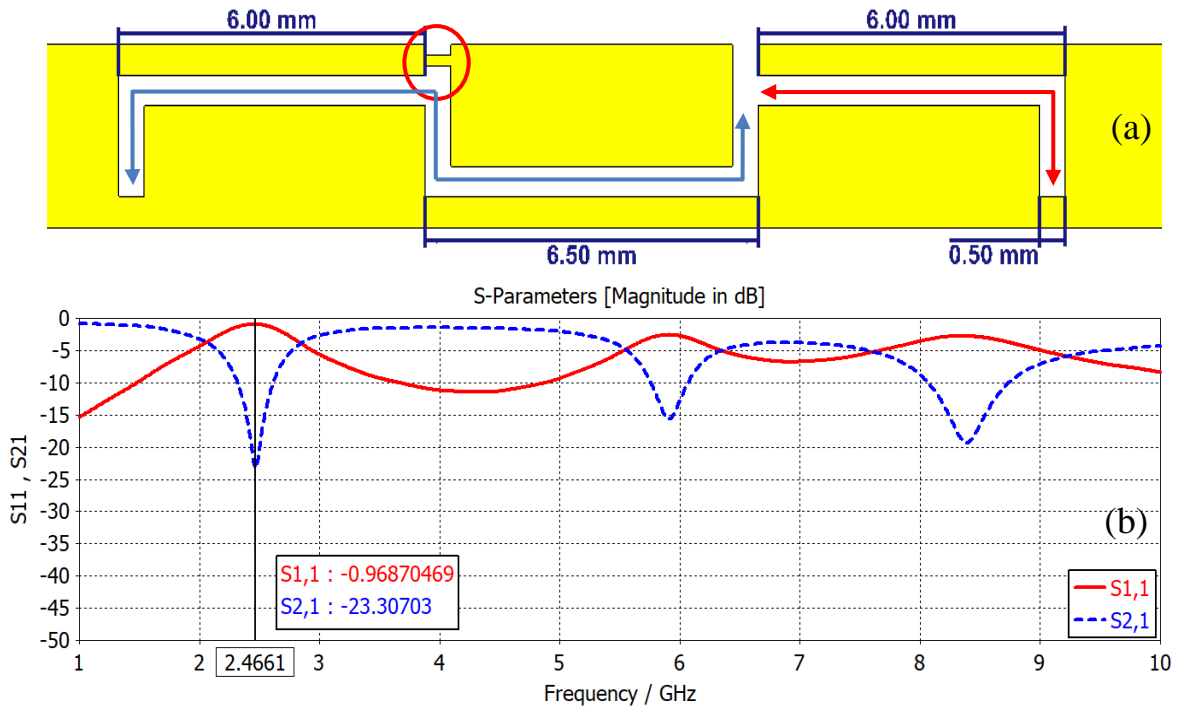


**Figure (4.10)** (a)- Filter geometry when adding short on the left side at the marked point, (b)- frequency response

The various parameters of results are compared in Table (4.4).

As can be seen in Fig. (4.10), there are various portions of the slot as indicated by the red and blue arrows. These portions of the slot resonated at various frequencies corresponding to the lengths. In the design (4.10) (Fig. (4.10.a)), the total length of the left slot (indicated by the blue arrow) is approximately 17.5 mm. Comparing the lengths yield:

$$\text{Length ratio} = \frac{(4.10a) \text{ left slot length}}{(4.9a) \text{ left slot length}} = \frac{17.5}{7.00} = 2.5$$

$$\text{Inverse of frequency ratio} = \frac{(4.9a) \text{ reject frequency}}{(4.10a) \text{ reject frequency}} = \frac{5.8}{2.4} = 2.41$$

This ratio is almost equal to the inverse ratio of the corresponding frequencies.

Thus, it can be concluded that the frequency ratio is the inverse of the length ratio.

The other design state is that for closing the two slits as in the design shown in Fig. (4.11.a). The two parts of the slot are merged and become a single slot of a length of approximately 22 mm and thus resulting in one notch frequency at 7.97 GHz.

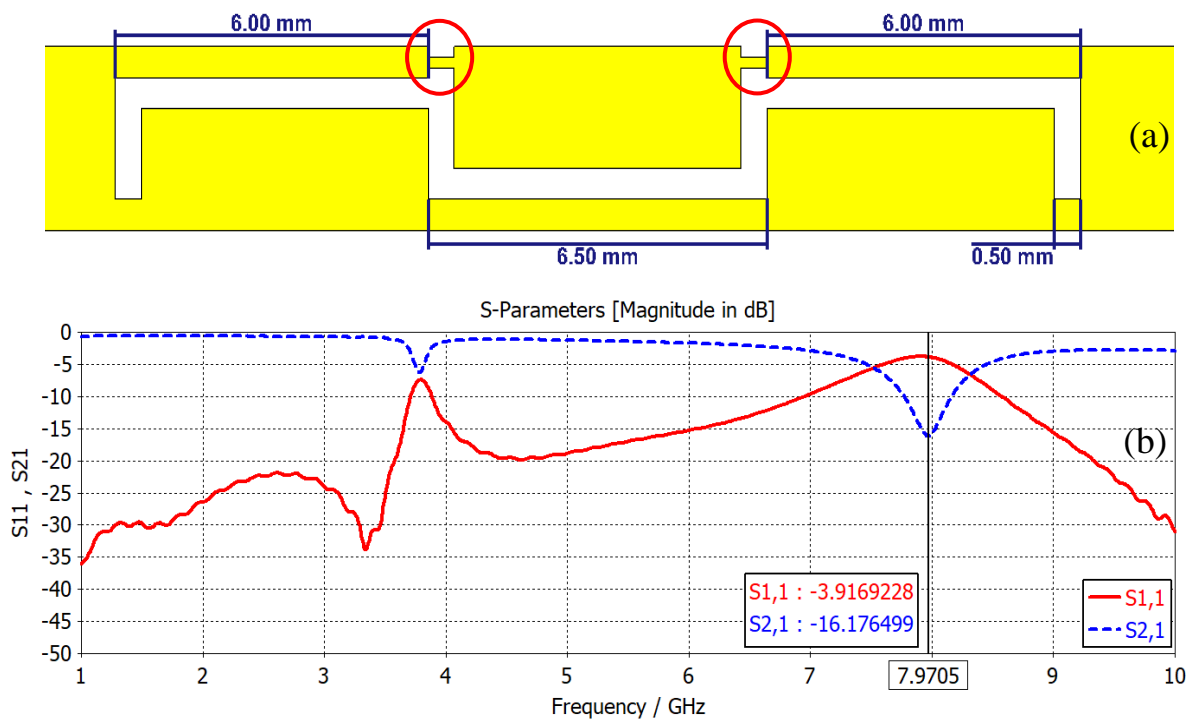


**Figure (4.11)** (a)- Filter geometry when adding shorts on both sides at the marked points, (b)- frequency response

7.97 GHz (X-Band) or  $\lambda_e \approx 21 \text{ mm}$ . Thus, the total length of the slot is:  
 $(2*4) + (2*6) + 6.5 - 1 = 25.5 \text{ mm}$ , or  $1.21 \lambda_e$

<b>Table (4.4)</b> The Filter Characteristics for the Three States Shown in Fig. 4. (9,10, and 11), The center slot length $\approx 10$ mm											
Design Figure	Left slot (mm)	Right slot (mm)	F1 GHz	$S_{11}$ dB	$S_{21}$ dB	F2 GHz	$S_{11}$ dB	$S_{21}$ dB	F3 GHz	$S_{11}$ dB	$S_{21}$ dB
4.9a	$6+2-1=7$	$6+2-1=7$	5.8	-2.7	-48	-	-	-	-	-	-
4.10a	$2+6+2+6.5+2-1=17.5$	$6+2-1=7$	2.4	-0.9	-23	5.9	-2.6	-15	8.4	-2.8	-19
4.11a	$(4*2)+(2*6)+6.5-1=21.7$		-	-	-	7.9	-3.9	-15	-	-	-

Thus, the filter can be reconfigured to work in the following three states:

1. When there are two openings in the slot, the filter shows a band-reject property (large  $S_{11}$  value and small  $S_{21}$  value) at 5.8 GHz.
2. When closing the left opening of the slot (indicated by the red circle in Fig. 4.10a), the filter shows the state of the band-reject for three frequencies, the (2.4, 5.9, and 8.4) GHz, two of which are used in the Wi-Fi range.
3. For the case of closing the two openings of the slot, the filter shows a large  $S_{11}$  value and a small  $S_{21}$  value at a frequency of 7.97 GHz.

Figures (4.9), (4.10), and (4.11) show the frequency responses of the three cases, while Table 4.4 shows the values of  $S_{11}$ , and  $S_{21}$  as well as the resonance frequencies for each of the three cases.

#### 4.4.1 Changing the Position of the Opening in the Slot

For the purpose of studying the effect of the left opening, 8 positions for the opening were investigated using CST simulations. The position was changed by a step of 1 mm towards the left. Samples of the obtained frequency responses are shown in the figures below. The results indicate that the resonance frequency decreases as the opening is moved to the left.

Only three cases are shown here. The first case is shown in Fig. (4.12.a), and has band-rejection at frequencies of (2.6, 6.4, and 9.3) GHz. Due to the presence of two slots of different lengths, each of which has its own resonant frequency, that is governed by (slit length equals a quarter of the effective wavelength  $\frac{1}{4} \lambda_e$ ).

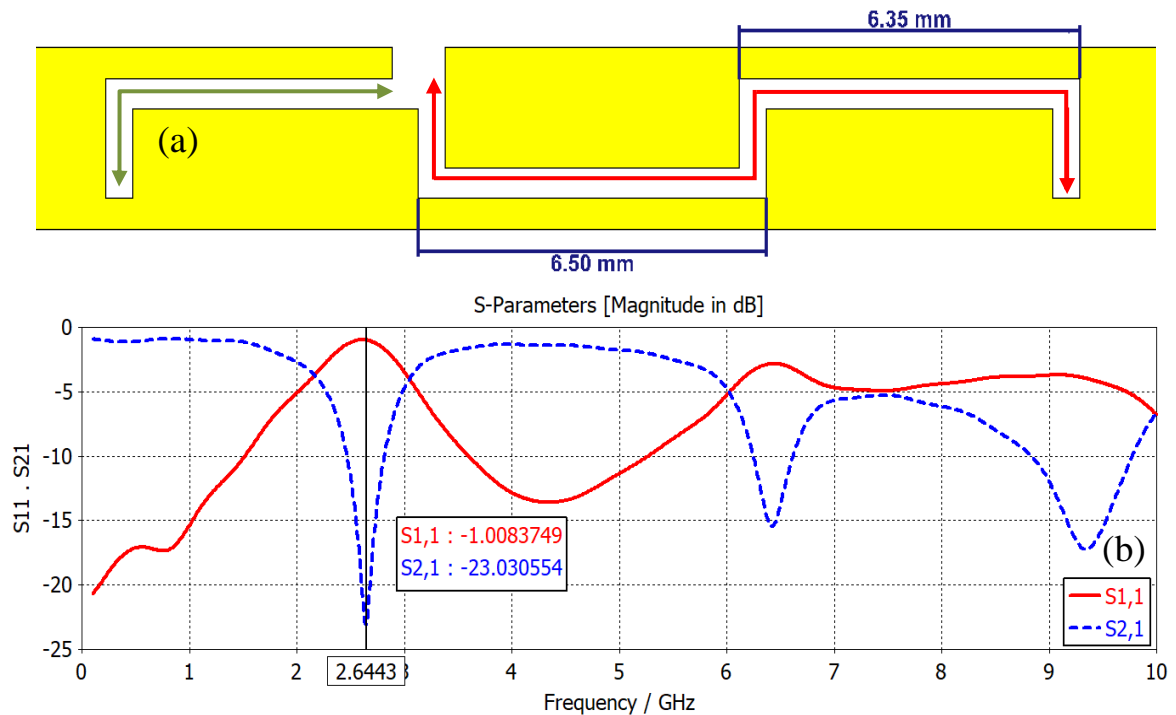


**Figure (4.12)** (a)- The geometry of the filter in the first case, (b)- frequency response

The model shown in Fig. (4.13.a) represents the second case, where the position of the slot was moved by 2 mm to the left. This means increasing the length of the right slit and decreasing the length of the left slit and thus one of the resonant frequencies will increase while the other will decrease. The third case is illustrated in Fig. (4.14.a), where the two slots have lengths is approximately 20 mm. Therefore, the frequency response has one reject-band at 2.08 GHz, which corresponds to the long slot. The other band does not appear as it is 20 GHz, which is outside the shown frequency range.

Table (4.5) shows the various parameters of the designed filters, for the three cases shown in Figures (4.12.a), (4.13.a), and (4.14.a).

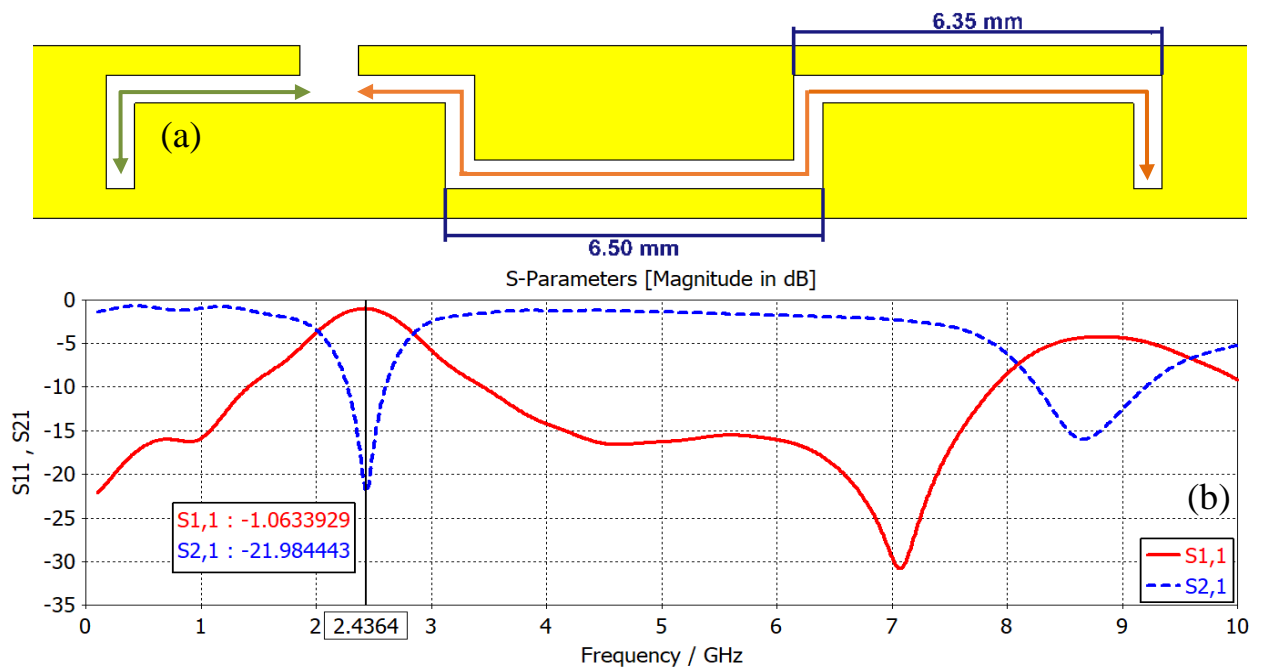


**Figure (4.13)** (a)- The geometry of the filter in the third case, (b)- frequency response

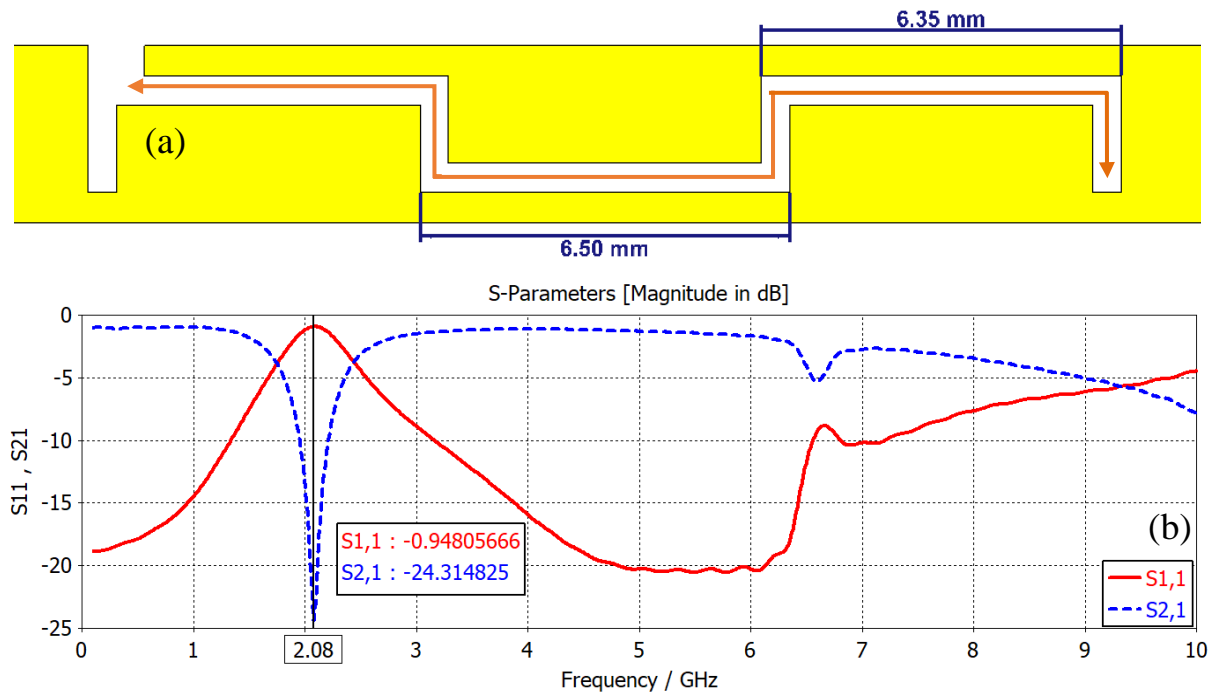


**Figure (4.14)** (a)- The geometry of the filter in the third case, (b)- frequency response

Table (4.5) The Filter Characteristics with Changing the Location of the Slot Opening								
Design Figure	Left slot (mm)	Right slot (mm)	$\frac{F1_{GHz}}{\lambda_{e1mm}}$	$\frac{F2_{GHz}}{\lambda_{e2mm}}$	$\frac{F3_{GHz}}{\lambda_{e3mm}}$	$\frac{Slot\ length}{\lambda_e}$		
4.12a	2+5.3-1 =6.35	(3*2)+12.85-2 =16.85	$\frac{2.6}{64}$	$\frac{6.4}{26}$	9.3(3 <sup>rd</sup> )	$\frac{16.8}{64} = 0.26$	$\frac{6.3}{26} = 0.24$	—
4.13a	3+2=5	(4*2)+12.85-2 =18.8	$\frac{2.4}{69}$	8.6(3 <sup>rd</sup> )	—	$\frac{18.8}{69} = 0.27$	—	—
4.14a	1.5	(3*2)+12.85+5-2 =22.3	$\frac{2.1}{79}$	6.6(3 <sup>rd</sup> )	—	$\frac{22.3}{79} = 0.28$	—	—

#### 4.4.2 An Alternative Way to Increase the Bandwidth

For the purpose of investigating ways to increase the bandwidth, using slots, the unequal length is presented here. The proposed design is shown in Fig. (4.15.b), which is a modified version of that shown in Fig. (4.15.a), The two “L-shape slots “have a small difference in length, that is 0.5 mm in this design. These two lengths correspond to two frequencies that are close in value, and the effect is a merged response that has a wider bandwidth as shown in Fig. (4.15.c).

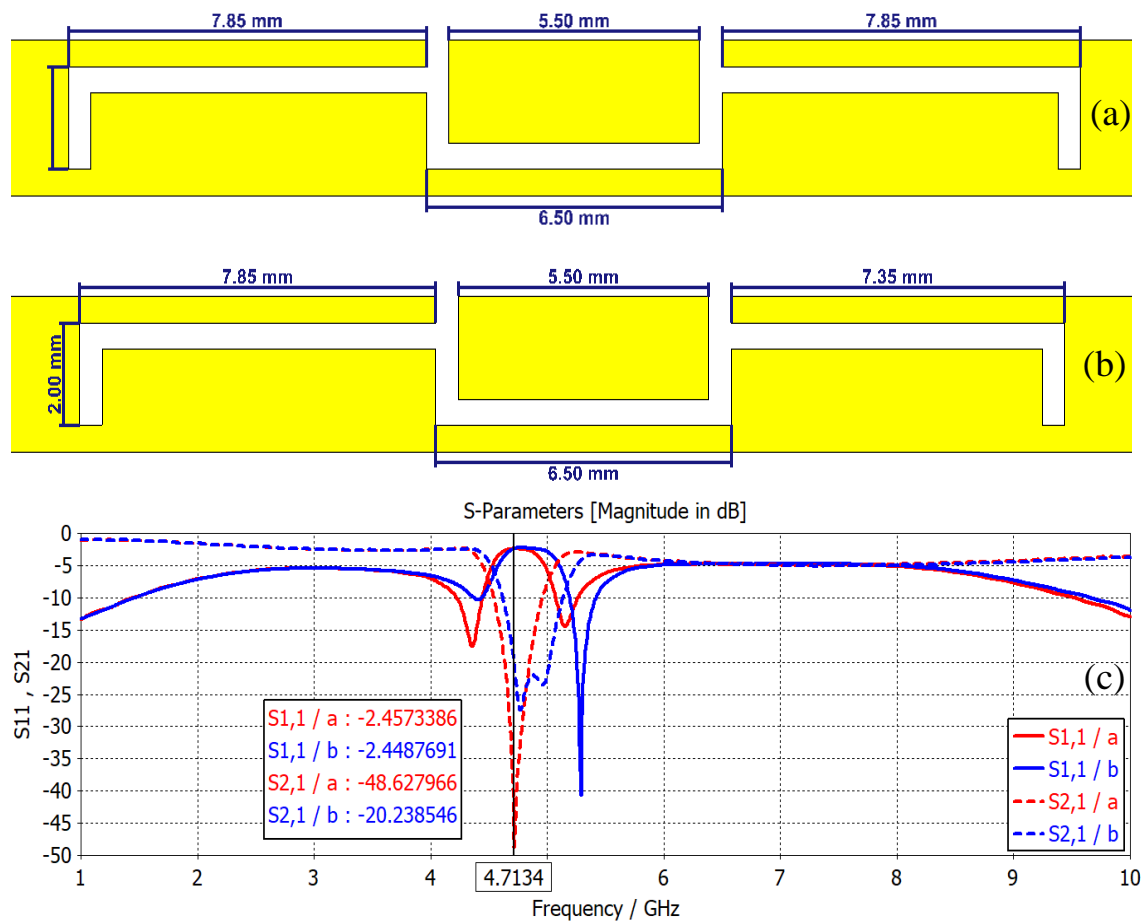


**Figure (4.15)** (a)- Filter with equal slots, (b)- Filter with unequal slots, (c)- Frequency responses of both cases

The other proposed idea is to add other vertical slots, that have various resonance frequencies in order to increase the bandwidth without affecting the depth of the transmission coefficient. Fig. (4.16.a) shows an added vertical slot of length 2 mm, while Fig. (4.16.b) shows two added slots of similar vertical length. A third slot was also added as can be seen in Fig. (4.16.c), and the obtained results for the three cases are compared in Fig. (4.16.d). Table (4.6) shows the various parameters of the three designed filters. The -10dB bandwidth slightly increased from 0.42 GHz to 0.49 GHz, or from (8.91%) to (10.76%) relative bandwidth (-10 dB bandwidth/center frequency), by employing two vertical slots on each side. By adding another slot on each side, the bandwidth increased to 0.56 GHz, then to 0.60 GHz at the third addition.

<b>Table (4.6)</b> The Characteristics of the Filter by Changing the Number of Vertical Slots					
Design	No. of vertical slots on each side	Frequency (GHz)	Minimum $S_{21}$ (dB)	-10dB BW (GHz)	% BW
Fig. 4.15. a	1	4.71	-48.6	0.42	8.91
Fig. 4.16. a	2	4.55	-43.9	0.49	10.76
Fig. 4.16. b	3	4.48	-39.1	0.56	12.5
Fig. 4.16. c	4	4.47	-36.1	0.60	13.1

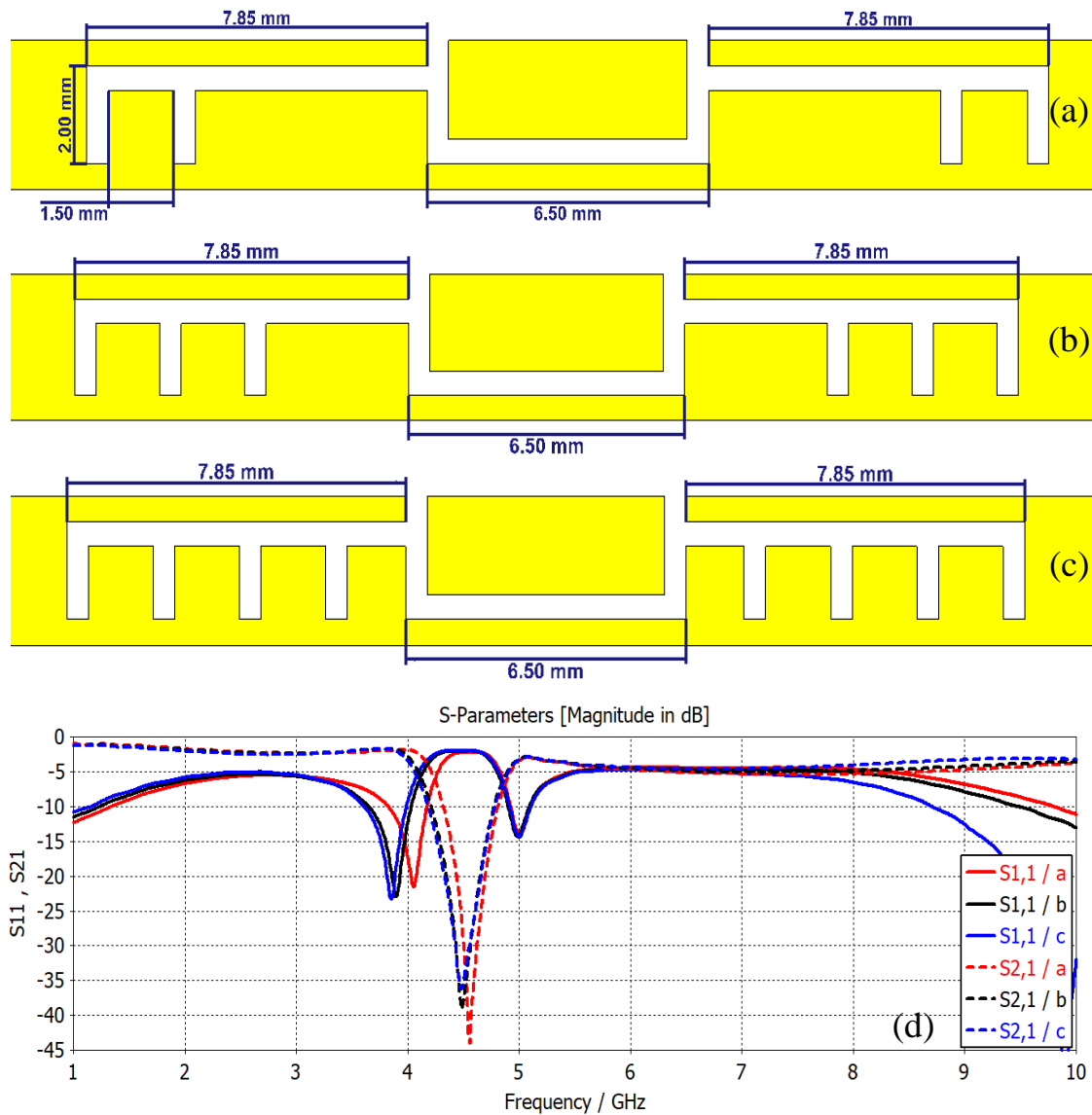


**Figure (4.16)** (a, b and c)-The geometry of the filter with the addition of vertical slits, (d)- Frequency response of the three cases

In another way to increase the bandwidth, three slots were placed on one side while the other side has one slot as shown in Fig. (4.17.a). For the purpose of comparison. Fig. (4.17.b) shows the frequency response of the three-slot filter, when the slots are placed on one side, compared to the frequency response of the case when the three slots are placed on both sides. Because of the slot length difference two very close resonant frequencies appear, and their responses merge together to yield some increase in the bandwidth.

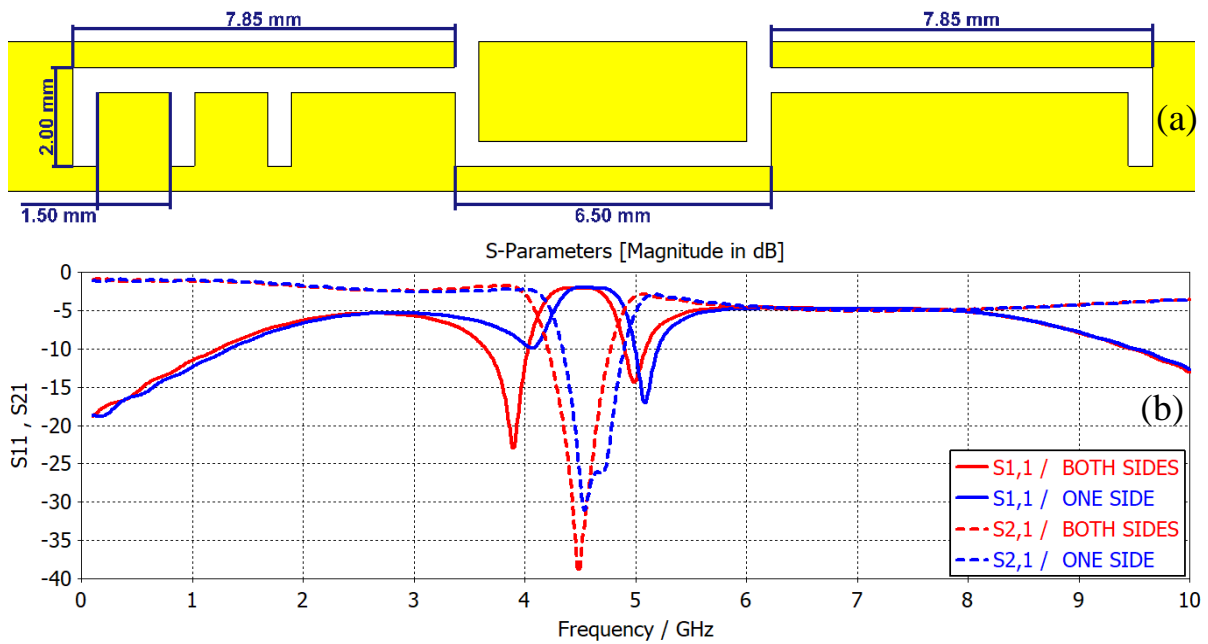


**Figure (4.17)** (a)- Filter geometry where slots are placed on the left side while the right side has one slot (b)- obtained results for one side and both sides slots

# CHAPTER FIVE

## CONCLUSIONS AND FUTURE WORK

### 5.1 Conclusions

In this dissertation, it was demonstrated that the U-shaped filter can be developed to have two options; an all-pass and a band-reject by adding a suitable element that acts as a switch in a suitable location in the filter structures. Other ideas for filters that can control the bandwidth and use more than one ringing frequency as an option were presented.

The contributions of the study in this dissertation can be summarized as follows:

1. The U-shaped slot etched on the microstrip line offers band-reject filter properties. The filter has a very compact size, of length equals quarter of the effective wavelength at the stopband frequency due to the folding of the slot. The width of the filter is no more than that of the microstripline itself. The characteristics of the U-slot filter, such as the resonance frequency and bandwidth, are influenced by the slot length, slot width, and the separation between the two legs of the slot.
2. The width of the reject-band and the transmission coefficient depend on the width of the slot. As the U-slot is embedded into the microstrip line, then this can restrict the width of the filter. Therefore, using a thicker substrate will lead to a broader microstrip line. Wider microstrip line offers more flexibility in choosing the slot width, which favorable in the fabrication process.
3. The loss tangent of the substrate affects the insertion loss at the passband, or the transmission coefficient. A low loss substrate will be needed to enhance the transmission coefficient across the reject-band

and reduce the insertion loss across the pass-band. For better performance better than FR4 substrate (loss tangent 0.025) will be needed.

4. The simulations and measurements presented show that a U-shaped slot filter can be reconfigured from band-reject to all-pass by switching one PIN diode.
5. Examination of the distribution of the electric field around the U-slots gives a good insight into understanding the operation of the filter. Moreover, the change between the two states of the operation can be better understood. This understanding has helped in the process of improving the filter properties, as well as developing the filter to be reconfigurable.
6. The testing of the fabricated prototypes showed good agreement with the results of the simulations, thus verifying the proposed idea and good operation of the designs.
7. According to its symmetrical design, the meandred slot filter presented in Chapter 4 achieves very small  $S_{21}$  and can be considered as two filters with the same resonance frequency. On this basis, any change in the length of one of the side slots will lead to the appearance of two different frequencies with a higher value  $S_{21}$ .
8. The proposed designs can be used in a variety of applications requiring small size and reconfigurability.

## 5.2 Future Work

The current work can be further extended considering the following issues:

1. Employing the other type of the microstrip line, namely the coplanar waveguide which is known to have wider line width. Therefore, there will be more room to implement other slot-based filters.
2. Using more than one PIN diode to achieve more options in the reconfiguration process, and the influence of their positions.
3. Aiming to increase the transmission coefficient of the filter, other types of substrates with lower values of the loss tangent can be used.
4. Investigation of the radiated field from the filter for both of the band-reject and all-pass states.

## REFERENCES

- [1] K. Chang, "RF and Microwave Wireless Systems", John Wiley & Sons, Inc, 2000.
- [2] M. Steer, "Microwave and RF Design, Transmission Lines", Vol. 2 (3<sup>rd</sup> Edition), NC State University, 2019. doi: <https://doi.org/10.5149/9781469656939> Steer.
- [3] R. J. Cameron, Ch.M. Kudsia, R.R. Mansour, "Microwave Filters for Communication Systems", Wiley – Interscience, 2007.
- [4] E. da Silva "High Frequency and Microwave Engineering", Butterworth– Heinemann, 2001.
- [5] Yuxiang Tu, Yasir I. A. Al-Yasir, Naser O. Parchin, Ahmed M. Abdulkhaleq, and Raed A. Abd-Alhameed, "A Survey on Reconfigurable Microstrip Filter–Antenna Integration: Recent Developments and Challenges", *Electronics* 2020, 9, 1249; doi:10.3390/electronics9081249.
- [6] J. Hong and M. J. Lancaster, *Microstrip Filters for RF / Microwave*, vol. 7. 2001.
- [7] A. Boutejdar, A. Elsherbini, A. Balalem, J. Machac, and A. Omar, "Design of new DGS hairpin microstrip bandpass filter using coupling matrix method," *Prog. Electromagn. Res. Symp.*, no. January, pp. 261–265, 2007.
- [8] R. S. Kshetrimayum, S. Kallapudi, and S. S. Karthikeyan, "Stop Band Characteristics for Periodic Patterns of CSRRs in the Ground Plane," *Int. J. Microw. Opt. Technol.*, vol. 2, no. 3, pp. 210–215, 2007.
- [9] B. Jitha, P. C. Bybi, C. K. Aanandan, "Microstrip Band Rejection Filter Using Open Loop Resonator," *Microw. Opt.*, vol. 48, no. 12, pp. 2611–2615, 2008.
- [10] S. Fallahzadeh and M. Tayarani, "A compact microstrip bandstop filter," *Prog. Electromagn. Res. Lett.*, vol. 11, pp. 167–172, 2009.
- [11] W. Tang and J. Hong, "Varactor-Tuned Dual-Mode Bandpass Filters," p. 2010, 2010.
- [12] I. Llamas-Garro and Z. Brito-Brito, "Reconfigurable Microwave Filters," *Microw. Millim. Wave Technol. from Photonic Bandgap Devices to Antenna Appl.*, no. April 2014, 2010.
- [13] M. Naghshvarian-Jahromi and M. Tayarani, "Defected ground structure band-stop filter by semicomplementary split-ring resonators," *IET*

- Microwaves, *Antennas Propag.*, vol. 5, no. 11, pp. 1386–1391, 2011.
- [14] L. BalaSenthilMurugan, S. A. A. Raja, S. D. Chakravarthy, and N. Kanniyappan, “Design and implementation of a microstrip band-stop filter for microwave applications,” *Procedia Eng.*, vol. 38, pp. 1346–1351, 2012.
- [15] L. Gao, S. W. Cai, X. Y. Zhang, and Q. Xue, “Dual-band bandstop filter using open and short stub-loaded resonators,” *2012 Int. Conf. Microw. Millim. Wave Technol. ICMMT 2012 - Proc.*, vol. 4, no. May, pp. 1544–1546, 2012.
- [16] T. P. Li, G. M. Wang, K. Lu, H. X. Xu, Z. H. Liao, and B. F. Zong, “Novel bandpass filter based on CSRR using Koch fractal curve,” *Prog. Electromagn. Res. Lett.*, vol. 28, no. August 2011, pp. 121–128, 2012.
- [17] K. H. Sayidmarie and T. A. Najm, “Performance Evaluation of Band-Notch Techniques for Printed Dual Band Monopole Antennas,” *Int. J. Electromagn. Appl.*, vol. 3, no. 4, pp. 70–80, 2013.
- [18] B. H. Ahmad and K. N. Minhad, “A Review on Reconfigurable Low Pass Bandstop Filter Based on Technology, Method and Design,” *Int. J. Electron. Comput. Sci. Eng.*, vol. 2, no. 1, pp. 395–404, 2013.
- [19] S. Ramya and I. S. Rao, “Design of compact ultra-wideband microstrip bandstop filter using split-ring resonator,” *2015 Int. Conf. Commun. Signal Process. ICCSP 2015*, pp. 105–108, 2015.
- [20] W. Y. Sam and Z. Zakaria, “A review on reconfigurable integrated filter and antenna,” *Prog. Electromagn. Res. B*, vol. 63, no. 1, pp. 263–273, 2015.
- [21] M. Esmaeili and J. Bomemaim, “Microstrip bandstop filters using L-And T-Shaped resonators,” *Asia-Pacific Microw. Conf. Proceedings, APMC*, vol. 1, pp. 5–7, 2016.
- [22] A. Boutejdar and S. D. Bennani, “Design and fabrication of tri-stopband bandstop filters using cascaded and multi-armed methods,” *Adv. Electromagn.*, vol. 6, no. 3, pp. 18–24, 2017.
- [23] B. Belkadi, Z. Mahdjoub, and M. L. Seddiki, “Design and analysis of dual-band rejection microwave filter employing SRR,” *2017 5th Int. Conf. Electr. Eng. - Boumerdes, ICEE-B 2017*, vol. 2017-Janua, pp. 1–7, 2017.
- [24] L. S. Yahya, K. H. Sayidmarie, F. Elmegri, and R. A. Abd-Alhameed, “Arc-shaped monopole antennas with reduced coupling for WLAN and WIMAX applications,” *2017 Internet Technol. Appl. ITA 2017 - Proc.*

- 7th Int. Conf., pp. 218–223, 2017.
- [25] Y. Wu, Y. Chen, L. Yao, W. Wang, and Y. Liu, “An independently reconfigurable dual-mode dual-band substrate integrated waveguide filter,” *PLoS One*, vol. 12, no. 6, pp. 1–13, 2017.
- [26] M. S. Khan, A. Iftikhar, A. D. Capobianco, R. M. Shubair, and B. Ijaz, “Pattern and frequency reconfiguration of patch antenna using PIN diodes,” *Microw. Opt. Technol. Lett.*, vol. 59, no. 9, pp. 2180–2185, 2017.
- [27] B. Sahu, S. Singh, M. K. Meshram, and S. P. Singh, “Study of compact microstrip lowpass filter with improved performance using defected ground structure,” *Int. J. RF Microw. Comput. Eng.*, vol. 28, no. 4, pp. 1–11, 2018.
- [28] F. C. Chen, R. S. Li, and J. P. Chen, “A tunable dual-band bandpass-to-bandstop filter using p-i-n diodes and varactors,” *IEEE Access*, vol. 6, pp. 46058–46065, 2018.
- [29] Y. Li, S. Luo, and W. Yu, “A compact tunable triple stop-band filter based on different defected microstrip structures,” *Appl. Comput. Electromagn. Soc. J.*, vol. 33, no. 7, pp. 752–757, 2018.
- [30] E. G. Ouf, A. S. Mohra, E. A.-F. Abdallah, and H. Elhennawy, “A Reconfigurable UWB Bandpass Filters with Embedded Multi-Mode Resonators,” *Open J. Antennas Propag.*, vol. 06, no. 03, pp. 43–59, 2018.
- [31] R. Bhat, A. W. Bhat, A. I. Khan, and A. Rasoolbhat, “A structural overview of microwave filters,” *Vol.(10)*, no. 3, pp. 112–118, 2018.
- [32] Y. I. A. Al-Yasir, N. O. Parchin, R. A. Abd-Alhameed, A. M. Abdulkhaleq, and J. M. Noras, “Recent progress in the design of 4G/5G reconfigurable filters,” *Electron.*, vol. 8, no. 1, 2019.
- [33] Y. Kusama and R. Isozaki, “Compact and broadband microstrip bandstop filters with single rectangular stubs,” *Appl. Sci.*, vol. 9, no. 2, 2019.
- [34] H. T. Ziboon and J. K. Ali, “Fractal Geometry: An Attractive Choice for Miniaturized Planar Microwave Filter Design,” *Fractal Anal.*, 2019.
- [35] C. F. Chen, “Design of a Microstrip Three-State Switchable and Fully Tunable Bandpass Filter with an Extra-Wide Frequency Tuning Range,” *IEEE Access*, vol. 8, pp. 66438–66447, 2020.
- [36] M. A. Al-Atrakchii, K. H. Sayidmarie, and R. A. Abd-Alhameed, “Compact Bandstop Microstrip Line Filter Using U-Shaped Slot,” *IETE J. Res.*, vol. 0, no. 0, pp. 1–8, 2020.
- [37] C. Asci, A. Sadeqi, W. Wang, H. Rezaei Nejad, and S. Sonkusale,

- “Design and implementation of magnetically–tunable quad–band filter utilizing split–ring resonators at microwave frequencies,” *Sci. Rep.*, vol. 10, no. 1, pp. 1–8, 2020.
- [38] Z. Zhibin and B. Lei, “Frequency-reconfigurable wideband bandstop filter using varactor-based dual-slotted defected ground structure,” *IEICE Electron. Express*, vol. 18, no. 10, pp. 1–6, 2021.
- [39] A. Gupta, M. Chauhan, A. Rajput, and B. Mukherjee, “Wideband bandstop filter using L-shaped and Quad mode resonator for C and X band application,” *Electromagnetics*, vol. 40, no. 3, pp. 177–185, 2020.
- [40] L. C. R and D. Kannadassan, “Coupled microstrip slot resonators for bandstop filters: theory and design,” *J. Electromagn. Waves Appl.*, vol. 35, no. 7, pp. 833–847, 2021.
- [41] D. K. Jhariya and A. Mohan, “Compact ultrawideband filter with reconfigurable band notch characteristics,” *Int. J. Electron. Lett.*, vol. 00, no. 00, pp. 1–11, 2022.
- [42] J. Choma, “Scattering Parameters: Concept, Theory, and Applications,” *Lecture*, no. November 2002, 2009.  
[https://www.ieee.li/pdf/essay/scattering\\_parameters\\_concept\\_theory\\_applications.pdf](https://www.ieee.li/pdf/essay/scattering_parameters_concept_theory_applications.pdf)
- [43] J. Hong and M. J. Lancaster, *Microstrip Filters for RF / Microwave*, vol. 7. 2001.
- [44] Samuel Y.Liao, “*Microwave Devices and Circuits*”, Pearson Education, 1990.
- [45] D. M. Pozar, “*Microwave Engineering*”, Forth Edition, John Wiley & Sons, 2012.
- [46] A. Balanis, “*Antenna Theory Analysis, and Design*”, vol. 4, no. 1. 2016.
- [47] P. Pramanick and P. Bhartia, “*Modern RF and Microwave Filter Design*”. 2016.
- [48] R. Phromlounsri, N. Thammawongsa, K. Somsuk, and P. Arunvipas, “Design of compact microstrip stepped-impedance resonator bandpass filters,” *Procedia Eng.*, vol. 8, pp. 30–35, 2011.
- [49] S. Srisathit, S. Patisang, R. Phromlounsri, S. Bunnjaweht, S. Kosulvit, and M. Chongcheawchamnan, “High isolation and compact size microstrip hairpin diplexer,” *IEEE Microw. Wirel. Components Lett.*, vol. 15, no. 2, pp. 101–103, 2005.
- [50] D. S. La, X. Guan, S. M. Chen, Y. Y. Li, and J. W. Guo, “Wideband

- band-pass filter design using coupled line cross-shaped resonator,” *Electron.*, vol. 9, no. 12, pp. 1–10, 2020.
- [51] M. Y. A. Shahine, M. Hussein, Y. Nasser, and K. Y. Kabalan, “A Varactor-based Tunable Microstrip Band Pass Filter,” *Prague, Czech Republic.*, vol. 9, no. 12, pp. 1–4, 2015.
- [52] A. Navya, G. Immadi, and M. V. Narayana, “Flexible ku/k band frequency reconfigurable bandpass filter,” *AIMS Electron. Electr. Eng.*, vol. 6, no. 1, pp. 16–28, 2022.
- [53] J. Dong, Y. Zhu, Z. Liu, and M. Wang, “Liquid metal-based devices: Material properties, fabrication, and functionalities,” *Nanomaterials*, vol. 11, no. 12, 2021.
- [54] E. Park, M. Lee, and S. Lim, “Switchable bandpass/bandstop filter using liquid metal alloy as fluidic switch,” *Sensors (Switzerland)*, vol. 19, no. 5, 2019.
- [55] Kurmendra and R. Kumar, “A review on RF micro-electro-mechanical-systems (MEMS) switch for radio frequency applications,” *Microsyst. Technol.*, vol. 27, no. 7, pp. 2525–2542, 2021.
- [56] W. H. Broer, J. (Jasper) Knoester, and Ipskamp Drukkers), *The Casimir force and micro-electromechanical systems at submicron-scale separations*, no. November. 2014.
- [57] A. H. M. Z. Alam, M. R. Islam, S. Khan, S. Farhana, N. N. A. B. Nik Noor Atikah, and N. Aziz, “RF bandpass tunable filter using RF MEMS,” *Proc. Int. Conf. Comput. Commun. Eng. 2008, ICCCE08 Glob. Links Hum. Dev.*, no. June, pp. 609–612, 2008.
- [58] Y. I. Abdulraheem, G. A. Oguntala, A. S. Abdullah, H. J. Mohammed, R. A. Ali, R. A. Abd-Alhameed, and J. M. Noras, “Design of Frequency Reconfigurable Multiband Compact Antenna using Two PIN Diodes for WLAN/WiMAX Applications,” *IET Microwaves, Antennas & Propagation*, Vol. 11, No. 8, PP. 1098-1105, 2017.
- [59] BAP51-L Silicone PIN Diode Data Sheet for Philips, last seen at <https://datasheetspdf.com/pdf/671685/NXPSemiconductors/BAP51L/1>
- [60] Y-H. Chun, J-S. Hong, P. Bao, T. J. Jackson, and M. J. Lancaster,” *BST Varactor Tuned Bandstop Filter with Slotted Ground Structure*”, *IEEE MTT-S International Microwave Symposium digest*, July 2008.

- [61] N. A. Shairi, B. H. Ahmad, and P. W. Wong,” Bandstop To Allpass Reconfigurable Filter Technique in SPDT Switch Design”, Progress In Electromagnetics Research C, Vol. 39, pp.265-277, 2013.
- [62] A. A. Zolkefli, N. A. Shairi, B. H. Ahmad, A. Othman, N. Hassim, Z.Zakaria, I. M. Ibrahim, H. A. Majid,” Switchable bandstop to allpass filter using cascaded transmission line SIW resonators in K-band”, Bulletin of Electrical Engineering and Informatics Vol. 10, No. 5, Oct. 2021, pp. 2617-2626.
- [63] Y. M. Hasan, A. S. Abdullah,” Compact Low-Cost Reconfigurable Microwave Bandpass Filter Using Stub-Loaded Multiple Mode Resonator for WiMAX, 5G and WLAN”, Basrah Journal for Engineering Sciences, Vol. 22, No. 1, 2021, pp.78-85.
- [64] A. T. Silva, C. F. Dias, E. R. Lima, G. Fraidenraich, and L. M. Almeida,” A New Reconfigurable Filter Based on a Single Electromagnetic Bandgap Honey Comb Geometry Cell”, Electronics 2021, 10, 2390. <https://doi.org/10.3390/electronics10192390>.

## المستخلص

مع التوسع الهائل في استخدام أجهزة الاتصالات، تتنافس الشركات على تقديم الأفضل لمستخدميها، حيث أن صغر حجم الجهاز وخفة وزنه والأداء العالي بالسعر المقبول تُعد أهم أهداف هذه الشركات. تُعد مرحلة المرشح من أهم المراحل داخل الأجهزة، وقد ركزت العديد من الدراسات على تصغير الحجم والوزن من خلال تقليل عدد المرشحات بتصميم مرشح يمكن تغيير خصائصه إلكترونياً، أي جعله قابلاً للتغيير.

في هذه الدراسة، تم استخدام مرشح منع الامرار الذي يحتوي على شق بشكل الحرف U باللغة الإنكليزية محفور على خط نقل دقيق (microstrip line) والعمل على تطويره وجعله قابلاً للعمل بين خيارى منع الامرار والامرار التام، أو لتغيير عرض حزمة الامرار من خلال استخدام PIN داوود يعمل كمفتاح يوضع بمنطقة محددة من المرشح ليؤدي الدور المناط به، كما تمت دراسة شكل توزيع المجال الكهربائي حول الشق ذي شكل حرف U في فهم ودراسة كيفية عمل هذا التصميم من المرشحات لغرض التطوير وتحسين الأداء.

تم الفحص المختبري للنماذج الأولية المصنعة للمرشح باستخدام محلل الشبكات ( Vector Network Analyzer) وأظهرت النتائج توافقاً جيداً مع نتائج المحاكاة المستحصل عليها باستخدام برامجيات CST مما يؤيد الفكرة المقترحة وسلامة التصميم.

كما تم تقديم مقترح آخر وهو التحكم بعرض حزمة ترددات المرشح، و استخدام أكثر من تردد لمنع الامرار للمرشح، حيث تم تحويل المرشح ذي شكل الحرف U ليكون بشكل آخر اطلق عليه تسمية المرشح ذي الشق المتعرج (meandred slot) وتمت دراسة خواصه وآلية عمله ومواصفاته. أظهرت نتائج المحاكاة أن هذا المرشح يمتاز بحزمة ترددات أعرض فضلاً عن المزيد من المرونة في عملية التحكم. يمكن الاستفادة من المرشحات التي تم اقتراحها ودراستها في مجموعة كبيرة من الاستخدامات التي تتطلب صغر الحجم وإمكانية سهولة للتحكم بالمواصفات.

### إقرار المشرف

أشهد بأن الرسالة الموسومة "تصميم وتحليل مرشحات قابلة لتغيير التردد" والمقدمة من قبل الطالب (أرقم محمد شريف سعيد) تحت إشرافي في قسم هندسة الاتصالات / كلية هندسة الإلكترونيات / جامعة نينوى، كجزء من متطلبات نيل شهادة ماجستير علوم في إختصاص هندسة الإتصالات.

التوقيع:

الاسم: أ.د. خليل حسن سيد مرعي

التاريخ: 2022/ /

### إقرار المقوم اللغوي

أشهد بأنه قد تمت مراجعة هذه الرسالة من الناحية اللغوية وتصحيح ماورد فيها من أخطاء لغوية وتعبيرية وبذلك أصبحت الرسالة مؤهلة للمناقشة بقدر تعلق الأمر بسلامة الأسلوب أو صحة التعبير.

التوقيع:

الاسم:

التاريخ: 2022/ /

### إقرار رئيس لجنة الدراسات العليا

بناءً على التوصيات المقدمة من قبل المشرف والمقوم اللغوي أشرح هذه الرسالة للمناقشة.

التوقيع:

الاسم:

التاريخ: 2022/ /

### إقرار رئيس القسم

بناءً على التوصيات المقدمة من قبل المشرف والمقوم اللغوي ورئيس لجنة الدراسات العليا أشرح هذه الرسالة للمناقشة.

التوقيع:

الاسم:

التاريخ: 2022 / /

## إقرار لجنة المناقشة

نشهد بأننا أعضاء لجنة التقويم والمناقشة قد اطلعنا على هذه الرسالة الموسومة (تصميم وتحليل مرشحات قابلة لتغيير التردد) وناقشنا الطالب (أرقم محمد شريف سعيد) في محتوياتها وفيما له علاقة بها بتاريخ / / 2022 وقد وجدناه جديراً بنيل شهادة الماجستير-علوم في اختصاص هندسة الاتصالات.

التوقيع:  
عضو اللجنة:  
التاريخ: / / 2022

التوقيع:  
رئيس اللجنة:  
التاريخ: / / 2022

التوقيع:  
عضو اللجنة(المشرف): أ.د. خليل حسن سيد مرعي  
التاريخ: / / 2022

التوقيع:  
عضو اللجنة:  
التاريخ: / / 2022

## قرار مجلس الكلية

إجتمع مجلس كلية هندسة الإلكترونيات بجلسته المنعقدة بتاريخ: / / 2022 وقرر المجلس منح الطالب شهادة الماجستير علوم في اختصاص هندسة الإتصالات.

رئيس مجلس الكلية:  
التاريخ: / / 2022

مقرر المجلس:  
التاريخ: / / 2022



جامعة نينوى  
كلية هندسة الإلكترونيات  
قسم هندسة الإتصالات

## تصميم وتحليل مرشحات قابلة لتغيير التردد

رسالة تقدم بها  
أرقم محمد شريف سعيد

إلى  
مجلس كلية هندسة الإلكترونيات  
جامعة نينوى  
كجزء من متطلبات نيل شهادة الماجستير  
في  
هندسة الإتصالات

بإشراف

الأستاذ الدكتور خليل حسن سيد مرعي